JOURNAL OF THE AERONAUTICAL SCIENCES

VOLUME 13 MARCH, 1946 NUMBER 3

Some Elementary Details of Ramming Intake and Propulsive Jets for Airplanes

SANFORD A. MOSS* AND W. R. FOOTE†

General Electric Company

(Publication of this paper, substantially in its present form, had nearly been accomplished in July, 1941, when military considerations held it up because of beginning of actual jet propulsion in the United States. However, the matters presented are not connected with any actual development and relate only to mathematical items that might have been stated at any time since Newton.)

Introduction

THE OPERATION of any usual airplane requires that an appreciable quantity of air be taken on board the plane from the atmosphere and that this air later be discharged. The air may be used for combustion in the engine, for cooling of the engine or other parts, for a propulsive jet, or for some other purpose. Frequently, the intake of air is by means of a suitably located ram whose diffuser increases the static pressure of the air in a supercharger or engine inlet or provides pressure to force air through a cooling duct. At discharge, air or exhaust gases may be directed rearwardly and so exert a propelling force on the airplane. The limit of this is an airplane driven by propulsive jets rather than by a propeller.

The intake of air exerts a retarding force on the airplane, a theoretical value of which may be found by the application of Newton's laws of motion. A theoretical value of the propelling force of a jet may be found in a similar fashion. These forces exist whenever air is taken on board the plane and air or exhaust gases are discharged from it, regardless of the use on the airplane. It is the purpose of this article to give theoretical values of the forces, powers, and energies for these cases and to discuss them briefly for an airplane flying at constant altitude without acceleration.

Nomenclature

F_1 = drag due to inlet ram, lbs.-force
F_2 = propelling force due to jet propulsion, lbs.-force
F = $F_2 - F_1$, net thrust force
w_1 = Flow of air taken on airplane, lbs.-mass per sec.
w_2 = Flow of exhaust gases expelled from airplane, lbs.-mass per sec.
V = airplane velocity, ft. per sec.
V_2 = theoretical nozzle velocity of jet with respect to the airplane, ft. per sec.
g = dimensionless proportionality factor, equal to the standard absolute value of the acceleration of gravity
P_1 = power required for intake, ft.lbs. per sec.
P_2 = power produced by jet propulsion, ft.lbs. per sec.
P = $P_2 - P_1$.
E_1 = energy acquired per lb. of air because of ramming intake, ft.lbs. per lb.-mass
E_2 = energy to propel airplane per lb. of exhaust gases, ft.-lbs. per lb.-mass
E = $E_2 - E_1$ = net energy used to propel airplane, ft.lbs. per lb.-mass
E_3 = kinetic energy lost because of absolute velocity of exhaust gases, ft.lbs. per lb.-mass
E_p = mechanical energy added per lb.-mass of air
η = E/E_p
c_p = specific heat at constant pressure
T_0 = static temperature of the atmosphere, degrees R
ρ = density, lb.-mass per cu.ft.
J = mechanical equivalent of heat
Q = flow, cu.ft. per sec.
A = area, sq.ft.
p_0 = external ambient pressure
p_1 = pressure after ram diffuser

Newton's Law Relations at Intake

In order to get air on board an airplane it usually is necessary to accelerate it from the atmosphere up to the airplane velocity, a steady-state flow of air being produced. Consider a mass dW_1 of air being taken on board in time dt. This air must have its momentum changed from zero to airplane velocity. By the application of Newton's second law of motion, the impulse is

Received August 20, 1945.

* Consulting Engineer, Aircraft Gas Turbine Engineering Division.

† Engineer, Air Conditioning Division.

equal to the change in momentum, or

$$F_1 dt = (dW_1/g)(V - O) \quad (1)$$

Here F_1 is the force necessary to accelerate the mass of air. It is also the retarding force on the airplane due to taking the air on board. There may be substituted in Eq. (1) the steady-state relation $w_1 = dW_1/dt$, whereupon

$$F_1 = (w_1/g)V \quad (2)$$

The power used is

$$P_1 = F_1 V = (w_1/g)V^2 \quad (3)$$

The energy received by each pound-mass of air, in foot-pounds, is

$$E_1 = V^2/g \quad (4)$$

In the derivation of the preceding equations nothing whatever was said as to the location on the airplane where the air was to be taken on board or through what size or shape intake this was to be accomplished. All that was said was that a certain quantity of air is accelerated up to the airplane velocity. It follows that power of the amount given in Eq. (3) is a primary item regardless of how or where the air is taken on board. Hence, power of this amount is a reasonable datum against which the power used by an actual intake may be compared.

These Newton law relations sidestep the details of the way the various pressures produce the forces, and this is elaborated upon in the Appendix.

Ramming Intake

A ramming intake is an opening that faces in the forward direction. The purpose of this arrangement is to obtain a pressure beyond the intake higher than the static pressure of the atmosphere by making use of the relative motion to convert velocity into pressure. Since the Newton's law relations apply regardless of where or how air is taken on board, it follows that they must apply to this case of a ramming intake. Thus, there is no theoretical reason why a ramming intake should require any more power than any other intake. Since an increased pressure is produced, there is every reason why such an intake should be used.

Eq. (4) stated that air taken on board receives energy of amount V^2/g ft.lbs. per lb. of air. This assumes that the air is brought completely to rest relative to the airplane. When so brought to rest, the air has a velocity V with respect to the original atmosphere, so each pound of air has a kinetic energy $V^2/2g$. This is just half of the energy, V^2/g, that the air receives at intake. The other half, $V^2/2g$, is potential energy that the air receives, shown as rise in temperature and pressure.

The mathematical fact, Eq. (4), that the air receives both kinetic and potential energy at intake, and receives these in equal amounts, may be shown physically as well. The air just previous to intake has a velocity V with respect to the airplane. When the air is finally on the airplane, this relative velocity is practically eliminated. Assume for the moment that this reduction of relative velocity takes place in a diffusing passage. Then, as the relative velocity is reduced, the pressure is increased. If the relative velocity is brought to a negligible value, then the air has acquired a potential energy of amount $V^2/2g$, and this energy will be in the form of increased temperature and pressure. At the same time that the relative velocity is being reduced, the absolute velocity of the air with respect to the atmosphere is being increased. Thus, simultaneously with the acquisition of the potential energy, $V^2/2g$, the air acquires a kinetic energy of the amount $V^2/2g$.

The form in which the potential energy of amount $V^2/2g$ appears needs further explanation. Assume for the moment that an uncompressed fluid is taken on board any moving vehicle. An illustration of this is a moving boat taking water on board. If the intake and diffuser has no friction or shock losses, then it is known from Bernoulli's equation that the potential energy $V^2/2g$ would appear as a pressure rise

$$p_1 - p_0 = \rho V^2/2g \quad (5)$$

when the water is brought completely to rest with respect to the boat. If there are friction and shock losses at intake and diffuser, all or part of the energy $V^2/2g$ is dissipated as heat, and the temperature of the water is raised. In this case the pressure rise is only a fraction of the value $\rho V^2/2g$. In the limit there is no pressure rise because of diffusion, and the energy $V^2/2g$ appears wholly as heat.

The intake of air onto an airplane at constant altitude without acceleration differs somewhat from this, since the air is compressible. If energy $V^2/2g$ is added to a perfect gas, the temperature of the gas is raised an amount

$$T_1 - T_0 = V^2/2gJc_p \quad (6)$$

and this temperature rise takes place regardless of any pressure changes. If the intake and diffuser have no friction or shock losses, then the isentropic pressure rise should be produced. By equating the isentropic work of compression to $V^2/2g$, the final pressure is

$$p_1 = p_0[1 + (V^2/2gJc_pT_0)]^{k/k-1} \quad (7)$$

In case there are friction and shock losses, the final pressure will be less than the above value. However, the temperature rise will be the same, since this is determined by the amount of the potential energy added to the gas. This is the same whether there is a perfect diffuser, loss of all of the velocity by shock, or anything between.

For the range of airplane speeds sometimes encountered, the pressure rise may be found approximately by assuming the air to be uncompressed. Thus, for an airplane velocity of 400 m.p.h. at sea level, the pressure

rise for a frictionless and shockless intake, calculated for N.A.C.A. standard atmosphere for a compressed fluid, is 6.19 in. Hg, while the pressure rise for an uncompressed fluid is 5.78 in. Hg, a difference of 6.7 per cent. Since this difference is not great, an uncompressed fluid will be assumed throughout the rest of this paper. If it is desired to evaluate the effect of compressibility, Eq. (7) may be put in the form

$$p_1 - p_0 = c\rho V^2/2g \tag{8}$$

where the factor c could be found by combining Eqs. (7) and (8).

Since the pressure rise $\rho V^2/2g$ or its isentropic equivalent is produced on the average by a frictionless and shockless intake, it seems reasonable to use this value as the ideal with which the pressure rise produced by actual intake may be compared. This is probably the greatest pressure rise that can be produced by a simple ramming intake. It is, of course, possible to place an intake directly behind a propeller and in this way to utilize to advantage some of the irregular velocity and pressure disturbances created by the propeller. However, except for an inlet influenced by the slipstream, from the propeller, it seems reasonable that the pressure rise, $\rho V^2/2g$, is the greatest that can be produced with a ram with negligible final duct velocities with respect to the plane. This is justified further by known pressure and velocity distributions about airfoils. It is well known that the total pressure about an airfoil is the static pressure of the atmosphere plus the velocity head, $\rho V^2/2g$, where V is the plane velocity with respect to the atmosphere. Such a total pressure is often found everywhere around an airfoil except on the top side near the rear. Here a lower pressure may be found, since the flow is undoubtedly influenced by the boundary layer. Thus, no case of a static pressure rise greater than $\rho V^2/2g$ is known to be produced by simple ram.

It has sometimes been stated that the forward stagnation point at the leading edge of the wing section is the optimum location for a ramming intake, since at this point the velocity head has been converted into pressure. This assumption has gone so far as to suppose that there could be flow with velocity V into an intake, starting with the static pressure that would have existed when there was no flow into the intake. This is greater than the ambient pressure by $\rho V^2/2g$. Then, after a perfect ram, there would be a static pressure of $\rho V^2/g$. However, the stagnation point is the place on the forward edge of the wing where the flow divides to pass on either side. There is no flow at this point, and the static pressure is increased by the amount $\rho V^2/2g$. This is identical with the action of an impact tube. At an intake there is flow of the air, so that, if an intake is located where the stagnation point would otherwise be, it follows that the stagnation point must change its location. Therefore, it is a question as to whether or not the stagnation point as a location for an intake has any special advantage over any other point on a wing. However, there is need for further ram research.

It has been shown that a pressure rise of $\rho V^2/2g$ is theoretically possible, but that this may be reduced by friction or shock. These factors depend upon the flow area and shape of the intake, as well as upon the location. If the intake is at the nose of a wing section or fuselage or at a forward scoop projecting some distance from the airplane, the area necessary to get a flow Q on board is

$$A = Q/V \tag{9}$$

where V is the airplane velocity. If the air is to be used for combustion, the flow Q is determined principally by the motor characteristics, so that in this case the flow Q is fixed chiefly by conditions beyond the intake. By means of Eq. (9) an area may be found so that the air has a relative velocity V with respect to the airplane at intake. Since this relative velocity is to be reduced and a pressure rise produced, in accordance with Bernoulli's equation, the passageway should be, theoretically, a diffusing one. However, it is a matter for experiment to determine whether the area given by Eq. (9) is best and whether a diffusing passageway does produce the maximum pressure rise. Flow conditions at an intake are such that some other area or form may be found to be preferable, although in no case would a pressure rise greater than $\rho V^2/2g$ be expected. Furthermore, with the actual flow Q fixed by an engine displacement or by nozzle area of a jet propulsion gas turbine, the area required for a given V and Q as given by Eq. (9) will not, in general, match the actual area of the ramming intake. If the actual area is too great, some of the flow heading for the ramming intake will not enter it but will branch off at the edges. If the ramming intake area is too small for a given V and Q, other losses will occur which are not here investigated, these probably needing research.

Consideration must be given not only to pressure rise but also to retarding forces on the plane. It has been shown that the Newton's law force at intake is $w_1 V/g$. It seems reasonable to expect that any intake will affect the flow of air around a plane and change the drag. The amount of this change depends on the location and form of the intake. It is not apparent whether the drag is increased or reduced, and it is impractical to try to evaluate the change theoretically. The Newton's law retarding force on an airplane because of an intake is $w_1 V/g$, but the total effect of this retarding force, including the change in the airplane drag, remains undetermined. It is a matter for experiment to determine the optimum location and form for a ramming intake so that the total force holding the airplane back is a minimum and so that as large a pressure rise as possible is obtained. A similar situation exists at discharge of cooling air, exhaust, or a propulsive jet. The Newton's law forces for intake and discharge are imposed on an airplane, which, without the openings

for the intake and discharge, has a certain drag. The changes in the airplane drag due to the presence of the openings may be called "intake interference drag" and "discharge interference drag."

Finally, any intake that supplies air for combustion should be in a region of steady flow. If the intake should be in a region of pulsating flow and there is a compressor beyond, the pulsations may be magnified and produce an undesirable effect.

Newton's Law Relations at Discharge

The theoretical forces produced by a rearward discharge of air or exhaust gases from an airplane may be found in a manner similar to that with which the forces at intake were found. Suppose that a mass of gases w_2 is discharged rearwardly with a velocity relative to the airplane of V_2. These gases can have no knowledge as to whether the airplane is at rest or in a condition of steady motion. They merely have their velocity relative to the airplane changed from a negligible value up to the velocity V_2. Thus, as in Eq. (2), the force acting on the gases to accelerate them from an original negligible velocity with respect to the plane up to the velocity V_2 is

$$F_2 = w_2 V_2/g \tag{10}$$

If the gases are discharged rearwardly this force acts on the airplane in a forward direction and, hence, helps to propel it. The propulsive power used in this way is

$$P_2 = F_2 V = w_2 V_2 V/g \tag{11}$$

The propulsive energy from each pound-mass of gas discharged is

$$E_2 = V_2 V/g \tag{12}$$

Propulsive Jets

Thus a rearward discharge exerts a propulsive force on an airplane. Such a discharge may be the engine exhaust gases, the engine cooling air, a propulsion jet, or a discharge for any other reason. The theoretical forces, powers, and energies arising from consideration of only the discharge have been given. It should be noted that the propulsive force involves the jet speed relative to the airplane but does not involve the airplane speed. For this reason a propulsion jet is sometimes considered as a constant thrust device.

A propulsive jet undoubtedly affects the parasitic drag on the airplane, as is the case of ramming intake, but the amount of this change cannot be predicted by simple theory. It has been suggested that the jet could be placed so that it would help clear away the boundary layer on the top rear part of a wing, and in this way improve the performance of the wing, or that a low pressure region could be found so that the jet velocity would be greater than that obtained by an expansion to the static pressure of the atmosphere. It is a matter for experiment to determine whether there is any way to discharge a jet with a velocity V_2, determined by expansion to atmospheric pressure, without extra drag due to the jet or with no extra drag and a greater velocity. Until such knowledge is available it seems best to assume the theoretical values given above.

The fact that the propulsive energy per pound-mass of gas discharged is given by the expression $V_2 V/g$ may be given a physical interpretation by means of the mathematical identity

$$\frac{V_2 V}{g} = \frac{V^2}{2g} + \frac{V_2^2}{2g} - \frac{(V_2 - V)^2}{2g} \tag{13}$$

The quantity $V^2/2g$ is the kinetic energy of the gases while they are yet on the airplane in a duct with negligible velocity. In order to discharge them from the airplane it is necessary to give them a velocity relative to it, which is obtained by a conversion of a pressure produced on the airplane, into relative velocity. That is, previous to discharge, the gases must have a pressure greater than the static pressure of the atmosphere. This pressure represents potential energy $V_2^2/2g$, converted into kinetic energy by the jet nozzle, and the gases have this in addition to the kinetic energy, $V^2/2g$. These two items are directly comparable to conditions at an intake where the air acquires both kinetic energy and pressure. However, at discharge a third item is involved. The relative velocity of the gases at discharge generally differs from the airplane velocity, so that the jet has an absolute velocity in space, $(V_2 - V)$, with respect to the atmosphere. Since this velocity is eventually dissipated by friction, it represents kinetic energy $(V_2 - V)^2/2g$, which is entirely wasted. To obtain the energy used to propel the airplane it is necessary to subtract this loss from the kinetic and potential energies the gases have just previous to discharge, as is done in Eq. (13).

Propulsive Jet with Intake Force Deduction

Consideration has been given to the forces, powers, and energies of discharge. If the gases were originally on board the airplane, as in the case of a rocket, this would be the complete procedure. However, often, air has to be taken on board the airplane from the atmosphere. To find a true measure of the effectiveness of a propulsive jet, it is necessary to subtract the retarding force and the power at intake from the jet propulsive force and power at discharge. Thus the net propulsive force is

$$F = F_2 - F_1 = (w_1/g)[(w_2 V_2/w_1) - V] \tag{14}$$

This equation completely sidesteps the pressures on the various walls that serve to produce F, and these are deduced in detail in the appendix. The net power used to drive the airplane is

$$P = P_2 - P_1 = (w_1 V/g)[(w_2 V_2/w_1) - V] \tag{15}$$

The net energy used by the airplane per pound-mass of air taken on board is

$$E = E_2 - E_1 = (V/g)[(w_2V_2/w_1) - V] \quad (16)$$

These equations apply to any backward discharge from an airplane. In the case of a radiator or cooling duct, the discharge flow would be equal to the intake flow, $w_2 = w_1$, and the above equations are somewhat simplified. In the case of air taken on board to be used for combustion in a power plant, the discharge flow would be greater than the intake by the amount of fuel added. For the case of a nozzle discharging a jet of exhaust gases, it may be assumed that V_2 is an ideal velocity and that the actual relative velocity is less than this by a nozzle velocity coefficient or other loss factor w_1/w_2, which is a reasonable value. Then, for discharge of cooling air, exhaust, or a propulsive jet, Eqs. (14) and (16) will be written

$$F = F_2 - F_1 = (w/g)(V_2 - V) \quad (17)$$

and

$$E = E_2 - E_1 = (V/g)(V_2 - V) \quad (18)$$

It is interesting to note that the net propulsive force and energy given by Eqs. (17) and (18) depend on the velocity difference $(V_2 - V)$. This is the final absolute velocity of the gases. If $V_2 = V$, the jet is stationary with respect to the atmosphere so that the propulsive force of the jet is equal to the retarding force due to intake. If the propulsive force is to be greater than the force at intake, it follows that the jet velocity relative to the airplane must be greater than the airplane velocity. This produces an absolute velocity giving the kinetic energy loss

$$E_3 = (V_2 - V)^2/2g \quad (19)$$

Thus, for a jet to produce a propulsive force at discharge greater than the retarding force at intake, there is an inevitable loss in the kinetic energy of the jet. It should be noted that the relative velocity at discharge may be less than the airplane velocity. In this case there is a propulsive force at the discharge, given by Eq. (10), but the retarding force at intake is greater than the jet force at discharge so that the net effect on the airplane is a retarding force as given in Eq. (17).

To produce a jet an energy input is necessary, which is given by

$$E_p = (1/2g)(V_2^2 - V^2) \quad (20)$$

This quantity E_p is the potential energy added to the gases while on the airplane. It has already been shown that previous to jet discharge the gases on the airplane are at a pressure above that of the atmosphere and that this pressure energy is given by $V_2^2/2g$. Likewise, in the discussion of ramming intake it was shown that the air acquired pressure energy, $V^2/2g$, by means of the ramming intake. Hence, the difference $(V_2^2 - V^2)/2g$ is the potential energy added to the air while it is on the airplane. Nothing is said here as to how this energy is added.

There has now been discussed the propulsive energy E, the kinetic energy loss E_3, and the net potential energy added to the gases on the airplane, E_p. The kinetic energy loss is the only loss. Hence

$$E + E_3 = E_p \quad (21)$$

This relation may be verified by the substitution of Eqs. (18), (19), and (20). Since the input is E_p and the output is the propulsive energy E, the ideal efficiency is given as

$$\eta = E/E_p = (2V/V_2)/[1 + (V/V_2)] \quad (22)$$

It can be seen that η is a function of the ratio V/V_2 and is so plotted in Fig. 1. This shows the reduction in efficiency when the airplane speed is less than the jet speed, although this condition is necessary if the propulsive force at discharge is to be greater than the retarding force at intake.

So far, the jet speed has been related to the airplane speed, but it remains to find the best value of the airplane speed. To do this it will be assumed that a constant amount of potential energy is added to each pound of air as it goes through the airplane. Thus, in Eq. (20) it is assumed that E_p is held constant. Then

$$V_2 = \sqrt{2gE_p + V^2} \quad (23)$$

and the efficiency η can be found in terms of the airplane speed.

$$\eta = 2V[\sqrt{2gE_p + V^2} - V]/2gE_p \quad (24)$$

This equation could be plotted, but this is not here included. The best airplane speed can now be found by setting the derivative $d\eta/dV$ to zero. Thus

$$\frac{d\eta}{dV} = \frac{\left[\sqrt{2gE_p + V^2} - V\right]^2}{gE_p\sqrt{2gE_p + V^2}} = 0 \quad (25)$$

or

$$2gE_p + V^2 = V^2 \quad (26)$$

This equation can be satisfied only if E_p is zero or V is infinite. If E_p is zero, there is no net propulsive effect on the airplane. It follows that, theoretically, the best speed for an airplane with jet propulsion is infinite. Such a speed is, of course, impossible, but the analysis shows that for good propulsive efficiency the airplane speed must be high.

The thrust that is obtained by jet propulsion is given in Eq. (17),

$$F = (w/g)(V_2 - V) \quad (17)$$

If Eq. (20) is substituted in this, there results

$$F = (w/g)\left[\sqrt{2gE_p + V^2} - V\right] \quad (27)$$

The thrust when the airplane is at rest is found to be

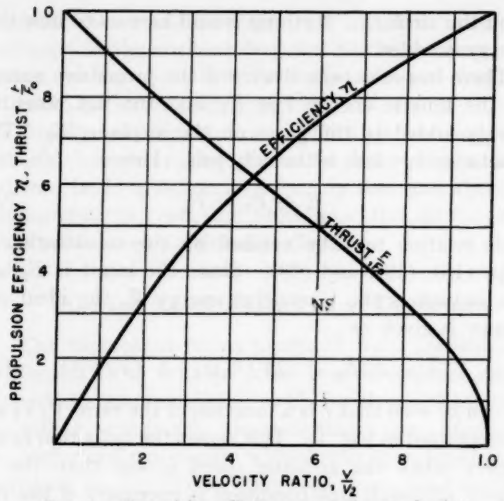

FIG. 1. Propulsion efficiency and thrust of a jet.

$$\eta = \frac{2(V/V_2)}{1 + (V/V_2)}$$

$$\frac{F}{F_0} = \sqrt{\frac{1 - (V/V_2)}{1 + (V/V_2)}}$$

V = plane velocity
V_2 = jet velocity relative to plane
F_0 = jet thrust at take-off
F = jet thrust at velocity, V

In deriving the expression for F/F_0 it is assumed that a constant amount of energy $E_p = (1/2g)(V_2^2 - V^2)$ is added to each pound of air passing through.

$$F_0 = (w/g)\sqrt{2gE_p} \tag{28}$$

Note that the quantity $\sqrt{2gE_p}$ is the jet velocity when the airplane is at rest. It is convenient to use this quantity when considering the thrust produced when the airplane is moving. Thus

$$\frac{F}{F_0} = \sqrt{1 + \frac{V^2}{2gE_p}} - \frac{V}{\sqrt{2gE_p}} = \sqrt{\frac{1 - (V/V_2)}{1 + (V/V_2)}} \tag{24}$$

This equation is plotted in Fig. 1. It can be seen that the thrust is a maximum when the airplane is at rest—in other words, at take-off. This is a fortunate circumstance, since it is at take-off that the maximum thrust is needed. This occurs if the airplane takes on air as rapidly at take-off as it does later. This is probably not the case, but the thrust produced for each pound of air going through the airplane is a maximum at take-off.

Before concluding the discussion of jet propulsion, it is in order to compare the performance of jet propulsion with that of propeller propulsion. It is well known that to produce a thrust a propeller must create a stream of air going backward with a velocity greater than the forward speed of the airplane, thus giving rise to a kinetic energy loss. This loss is similar to the kinetic energy loss with jet propulsion. There is, however, one difference between the two. A propeller generally stirs up a large amount of air and adds but little energy to each pound of it. Hence it is suitable for low velocity travel. A propulsive jet of high velocity can be produced, and such a jet is suitable for high velocity travel.

Finally, it should be noted that no consideration has been given to the effect of a propeller slipstream on an intake and discharge, such as occurs in the N.A.C.A. cowling or other openings.

The authors gratefully acknowledge the assistance given in writing this paper by Dale D. Streid, Charles T. Oergel, and Dr. Chester W. Smith.

BIBLIOGRAPHY

Buckingham, Edgar, *Jet Propulsion for Airplanes*, N.A.C.A. T.R. No. 159, 1923.

Jacobs, Eastman N., and Shoemaker, James M., *Tests on Thrust Augmentators for Jet Propulsion*, N.A.C.A. T.N. No. 431, 1932.

Higley, Frank H., *Wind-Tunnel Tests of Carburetor Intake Rams*, N.A.C.A. T.N. No. 631, 1938.

APPENDIX—PRESSURES ON WALLS OF A VESSEL WHICH PROVIDE THE JET MOMENTUM FORCES

(Added in 1945 with the collaboration of C. W. Smith)

Consider a vessel moving without acceleration, or stationary. This may be a jet-propelled airplane at constant altitude, a chamber for measuring nozzle reaction, a bend in a pipe carrying flowing fluid, or any similar vessel. An axial direction is defined, for convenience, parallel and opposite in direction to a principal jet leaving the vessel through an opening. There is supposed a variable internal pressure p, and an external ambient pressure p_0 on all external walls, and the discharge of a fluid jet with the same final pressure p_0, through an area A_2 with a velocity V_2. There may be any number of other inlet and outlet openings, and the area A to be considered is the total projected area of all fluid openings in planes perpendicular to the axial direction.

A major use of the equations herein is the measurement of nozzle velocity by weighing nozzle reaction. In this case the fluid inlet area is in a plane parallel to the axial direction and so is taken as zero. Another use is computation of force on a pipe elbow; another is effect of air taken on and discharged from an airplane flying without acceleration at constant altitude (perhaps with propulsion jet and an augmenter) and with V_2 less than sonic velocity or with a nozzle expanding portion suited to supersonic V_2. The general purpose of this appendix is to show the parts played by the fluid

pressures on the vessel walls. These are sidestepped in the previously given and usual treatment of the problem based on theory of conservation of momentum of the flowing fluid. (The senior author remarks that during 40 years of work with nozzle reaction, etc., there has not been the clear picture shown by the analysis herein.) Fig. 2 gives a diagram for the particular case of inlet and outlet flow parallel to the axis.

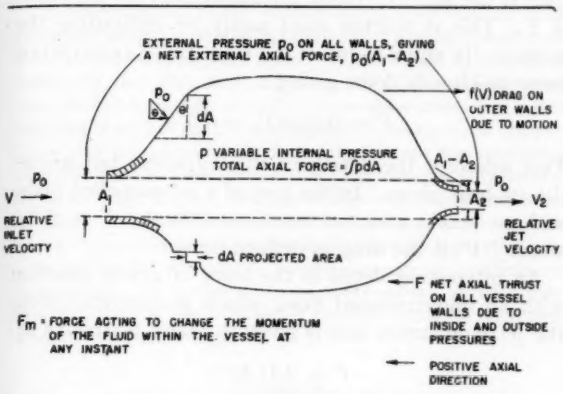
EXTERNAL PRESSURE p_0 ON ALL WALLS, GIVING A NET EXTERNAL AXIAL FORCE, $p_0(A_1-A_2)$
p_0
dA
f(V) DRAG ON OUTER WALLS DUE TO MOTION
p VARIABLE INTERNAL PRESSURE
TOTAL AXIAL FORCE = $\int p dA$
A_1-A_2
p_0
V
A_1
A_2
V_2
RELATIVE INLET VELOCITY
RELATIVE JET VELOCITY
dA PROJECTED AREA
F NET AXIAL THRUST ON ALL VESSEL WALLS DUE TO INSIDE AND OUTSIDE PRESSURES
F_m = FORCE ACTING TO CHANGE THE MOMENTUM OF THE FLUID WITHIN THE VESSEL AT ANY INSTANT
POSITIVE AXIAL DIRECTION

FIG. 2. Diagram in a plane parallel to the axial direction.

NOMENCLATURE FOR APPENDIX

$\int p\,dA$	=	internal pressure axial force, equal and opposite for vessel and fluid
w	=	flow (lb.-mass per sec.)
p_0	=	external ambient pressure (constant)
p	=	internal pressure (variable)
A_1	=	sum of all inlet areas projected on planes perpendicular to the axis
A_2	=	exit areas projected on planes perpendicular to the axis
A	=	projected area in general, in a plane perpendicular to axial direction
V	=	inlet velocity
V_2	=	exit velocity
F_m	=	net force acting on fluid
F	=	net force acting on walls
g	=	dimensionless factor equal to acceleration of gravity
$f(V)$	=	drag on outer walls (which do not include A_1 and A_2) due to vessel motion

The vessel walls inside and out are equivalent to a number of steps on each of which is the pressure p or p_0, so that the axial force is $p\,dA$ or $p_0\,dA$. There could be resolved, in the axial direction, pressures on a wall at any angle, which would give the same result. This is because a pressure p_0 on an inclined wall area ds gives an axial force $p_0\,ds\cos\theta$. But an inclined wall area ds gives a projected area $dA = ds\cos\theta$. Hence the axial force is $p_0\,dA$ or $p\,dA$.

Instantaneous force equations will be written for two independent bodies: first, the vessel itself; second, the body of fluid within the vessel. There is a common internal force acting equally and oppositely on vessel and body of fluid due to the variable internal pressure p, which is given by $\int p\,dA$.

In a jet-propelled plane the vessel that is considered is the passage system through which the fluid passes from inlet to outlet. It has various wall areas on which this pressure p is exerted. In the case of a plane with ramming intake and diffuser, there is a positive force on the diffuser walls. In a jet-propelled plane the passage walls include the air compressor chamber and the combustion chamber, where there may be comparatively high pressures. Finally, there is the jet discharge nozzle within which the pressure gradually decreases to the ambient value p_0. The net difference between the high pressure on the inner wall area and the gradually decreasing pressure on the nozzle walls is the major force propelling a jet plane. This is visualized most easily by thinking of a vessel used for nozzle reaction. Here the nozzle hole is a gap in the wall, so there is a thrust force due to the corresponding area at the opposite side of the vessel, as well as decreased pressure near the discharge nozzle. (All of the internal space in the plane, other than the complete passage between inlet and discharge jets, constitutes a completely closed vessel whose interior is filled with air at the ambient pressure p_0. There is no net axial force from the pressure within such a closed vessel.)

In addition to the equal and opposite interior pressure on vessel and body of fluid, there are exterior forces due to the openings in the vessel walls. For a vessel for measurement of nozzle reaction, or a 90° elbow, there is one opening in a plane perpendicular to the axial direction, where the jet is discharged. The inlet opening is zero in a plane perpendicular to the axial direction. For an airplane with ram inlet, or a jet-propelled plane, there are inlet and outlet openings in planes perpendicular to the axial direction. If there were no such openings in the vessel, the net force on the outer walls due to the ambient pressure p_0 would be zero. For a jet propulsive apparatus on block test, there is a large inlet opening and a smaller opening for the jet discharge, as shown diagrammatically in Fig. 2, so that there is a net external force pushing the vessel in the axial direction,

$$p_0(A_1 - A_2)$$

This is a real part of the force on the vessel, whose existence often is forgotten. For the case of a vessel for measuring nozzle reaction, A_1 is zero, and the force is $-p_0A_2$. This is the force on the vessel due to the pressure on all of the external walls but with no wall at the nozzle opening. For the case of an airplane with cooling air entering and leaving, A_2 may be larger than A_1 because of the lower velocity, and so $p_0(A_1 - A_2)$ may be a retarding force. In any case the effective vessel surface on which the external pressure acts is the difference between the entrance and exit areas A_1 and A_2. It is to be noted that we assume the areas A_1 and A_2 to be completely filled by continuous flow of fluid, with the velocities V and V_2. Otherwise complications arise not here investigated. No method is here proposed for accomplishing this exact filling at all speeds and all altitudes.

For a jet propulsive apparatus on block test the ambient pressure gives the above axial force on the difference of inlet and jet openings. When the jet-propelled plane is in motion, there is a retarding drag force $f(V)$. This is defined as being the resistance introduced by motion.

So much for the pressure forces on the external vessel walls due to the inlet and outlet openings. There also are forces on the fluid passing through the vessel due to the ambient pressure of the inlet and outlet fluid streams

$$-p_0A_1 + p_0A_2$$

or

$$-p_0(A_1 - A_2)$$

This is exactly equal and opposite to the force on the external vessel walls due to the inlet and outlet openings.

So the gross forces F and F_m on the vessel walls and on the fluid within the vessel have the numerically equal but opposite terms, with absolute magnitudes of

$$\int p\,dA \text{ and } p_0(A_1 - A_2)$$

that is,

$$F = \int p\,dA + p_0(A_1 - A_2)$$

and

$$F_m = -F$$

The force F on the vessel walls is the real force that pushes it and should have further analysis. One part, $p_0(A_1 - A_2)$, is the ambient pressure, p_0, acting on that part of the external walls not neutralized by an equal wall area on the opposite side because of an opening.

Inside of most of the vessels being considered, there is for the most part a high pressure p, except near the nozzle opening. Here the pressure on the nozzle walls is gradually reduced to the ambient value while fluid is being accelerated. The pressure p on the corresponding opposite wall gives an internal pushing force. The total force is the sum expressed mathematically by the value of F. This is written most easily by computing the numerically equal value of F_m from the Newton's law forces as already done, giving

$$F = (w/g)(V_2 - V)$$

This sidesteps the details in this appendix but misses the analysis given. In the case of a jet-propelled plane without acceleration, at constant altitude, $F = f(V)$, where $f(V)$ is the drag as defined herein.

An interesting detail is the force of nozzle reaction with an uncompressed fluid, which is computed from the jet momentum and is given in many textbooks as

$$F = 2A(\Delta p)$$

That is, the force is the pressure difference on twice the unbalanced area, because of the decreased internal pressure on the internal walls near the nozzle opening. It is to be repeated that in all of the matter in this paper relating to a jet-propelled plane, we assume constant altitude and no acceleration and inlet and outlet openings are assumed to be *filled* with fluid at the ambient pressures p_0. This postulates exactly the proper areas and a proper nozzle, with expanding portion if there is supersonic velocity.

Changes of Address

To facilitate the prompt receipt of copies of the JOURNAL OF THE AERONAUTICAL SCIENCES, members and subscribers are requested to give the Institute 30 days' notice of any change of address.

Notices should be sent directly to:

Institute of the Aeronautical Sciences, Inc.
2 East 64th Street, New York 21, New York

Stability of Semimonocoque Wing Structures*

HENRY L. LANGHAAR†

Consolidated Vultee Aircraft Corporation

ABSTRACT

The Consolidated Vultee Aircraft Corporation recently built and tested several cambered box beams that were structural models of stressed-skin airplane wings. It was found, as a result of these tests, that plate-stringer column-fixity factors of the specimens ranged from 1.00 to 3.00. These observations are rather revealing in view of the frequent arguments among stress analysts concerning the correct fixity factor to be used for calculating allowable plate-stringer loads. It is therefore especially satisfying to find that the test data are in harmony with a simple approximate theory of elastic stability of wing structures. This theory exposes the possibility of occasionally exerting control over fixity factors for purposes of weight economy or bulkhead rearrangement. It further suggests modifications of wing construction, such as the substitution of shallow ribs for bulkheads in highly cambered wings.

SYMBOLS

L = bulkhead spacing
B = peripheral interspar distance
t = skin thickness
t_e = area of a representative unit width of the plate-stringer cross section. (The area t_e may be called "equivalent thickness" because it is the thickness of a homogeneous shell with the same weight and area as the given plate-stringer panel)
ρ = radius of gyration of an element of the plate-stringer cross section with reference to its centroidal axis
z = ordinate of the centerline of the plate-stringer cross section measured from the neutral plane of the wing
$z_{max.}$ = the maximum value of z
$\bar{z}$ = a mean value of z, defined by Eq. (14)
x, y = peripheral and spanwise coordinates (see Fig. 1)
$\xi = \pi x/B$, $\eta = \pi y/L$, $\zeta = z/B$ (dimensionless coordinates)
R = radius of curvature of a cross section of the compression panel at the point x
$\kappa = B/\pi R$, a dimensionless measure of the curvature
C = the panel fixity constant
m = the number of half waves in a cross section of the buckled panel
λ = the ratio of the elastic modulus of a bulkhead chord member to the effective modulus of the plate-stringer combination
ν = Poisson's ratio
J = torsional rigidity of a bulkhead chord member
$a_n^{(m)}$ = coefficients in the Fourier analysis, Eq. (21)
A, A_1, A_2, K = dimensionless constants defined by Eq. (10)

Received April 16, 1945.

* A part of a program of investigation of the stability of semimonocoque wing structures that was initiated and directed by Mr. Roy A. Miller, of the Consolidated Vultee Aircraft Corporation. The theoretical side of the project was originally submitted to the Engineering Experiment Station of the University of Illinois, but Prof. N. M. Newmark, who directed the study at Illinois, was forced to discontinue this work because of more pressing duties. Nevertheless, the author is indebted to Professor Newmark for ideas that have been followed in the present theory.

† Structural Research Engineer.

INTRODUCTION

THE COMPRESSION SURFACE of a semimonocoque wing is structurally analogous to a set of parallel columns that acquire compression loads by the bending of the wing. Accordingly, a column fixity factor C is commonly employed for determining allowable stringer stresses. There is, however, a tendency by some engineers to discredit the use of a fixity coefficient C for short-column calculations—a bias that seems to stem from the idea that the reduced column length L' has a more fundamental significance than the constant C. This, of course, is not the case if one adheres to the usual definition $L' = L/\sqrt{C}$ or to the general Euler column formula with a reduced modulus. The main reason for preferring C rather than L' in the present study is that the former constant is dimensionless.

There are several effects that cause the constant C to differ from unity. First, there is the possibility that the bulkheads are so light that they participate in the buckling. This condition inherently contributes a negative increment to C. However, for the present study, the phenomenon of linear bulkhead deflection is excluded. There then appear to be only two effects that can influence stability. These are the restraints furnished by the skin and by the bulkhead connections.

The restraining effect of the skin consists essentially of two parts, membrane action and flexural action. The former action is known to be peculiar to curved shells; it consequently has significance only for cambered wings. Likewise, the flexural stiffness of the skin and the torsional stiffness of the bulkhead chord members are ordinarily negligible for flat compression panels. However, these factors should not be disregarded in the theory of stability of a cambered wing, for without them the mode of buckling becomes indeterminate. This circumstance arises because the flexural stiffness of the skin and the torsional stiffness of the bulkhead chord members do have significance for modes of buckling which present several waves in a cross section of a panel.

In order to formulate the stability problem that is suggested by the above remarks, the view is adopted that the compression surface of a wing is an orthotropic shell. The significant plate-stringer dimensions are then the skin thickness t, the radius of gyration ρ, and the thickness t_e of an equivalent homogeneous shell. Attention is confined to a single, cylindrical, compression panel that is constrained so that the normal and transverse components of the elastic displacement vec-

tor vanish at the ends (i.e., at the bulkheads), while only the normal component vanishes at the longitudinal edges (i.e., at the wing spars). Rotational restraints of uniform bulkhead chord members are considered to act at the ends of the panel.

Potential Energy of a Buckled Panel

The cylindrical compression panel under consideration is schematically shown in Fig. 1. The type of edge support that is considered has been discussed in the preceding paragraph. Peripheral and axial coordinates (x, y) are set up as shown in the figure. The bulkhead spacing L and the peripheral interspar distance B are indicated by the bulkhead locations $y = 0$, $y = L$ and the spar locations $x = 0$, $x = B$.

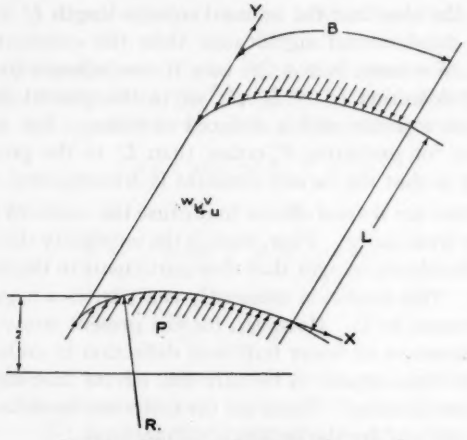

FIG. 1. Diagram of compression panel.

The axial load P is considered to be proportional to the ordinate z, measured from a fixed plane. The maximum value of P may be represented in the form

$$P_{max.} = C\pi^2 E t_e \rho^2 / L^2 \tag{1}$$

in which $t_e\rho^2$ is the moment of inertia of a unit width of the plate-stringer cross section and E is Young's modulus. Since this relation formally agrees with the Euler column formula, the constant C denotes the fixity factor that is conventionally used when margins of safety are based upon the most highly stressed stringer.

The physical idea behind the following mathematical investigation is the energy theory of elastic stability, which characterizes the buckling point of an elastic system by an equality between the work of the external forces and the increment of strain energy in a small buckling deformation. A virtual deformation is defined by the transverse, axial, and normal components (u, v, w) of a vector displacement function (Fig. 1). It is assumed in the sequel that the elastic restoring forces exerted by the stringers preclude axial displacements v other than the second-order displacements attending bending of the stringers. With this assumption, the various components of potential energy are evaluated.

(A) *Virtual Work of the External Forces*

By geometry, the axial contraction of a stringer is

$$e = {}^1/_2 \int_0^L (\partial w/\partial y)^2 \, dy$$

and, consequently, the virtual work of the compression load is

$$W = {}^1/_2 \int_0^B P dx \int_0^L (\partial w/\partial y)^2 \, dy \tag{2}$$

It is convenient to employ, instead of the coordinates (x, y), the dimensionless coordinates

$$\xi = \pi x/B, \quad \eta = \pi y/L \tag{3}$$

With these variables, Eqs. (1) and (2) yield

$$W = \frac{C\pi^2 B E t_e \rho^2}{2L^3} \int_0^\pi \int_0^\pi \frac{z}{z_{max.}} w_\eta^2 \, d\xi \, d\eta \tag{4}$$

in which the subscript η denotes a partial derivative.

(B) *Energy of the Stringers*

The strain energy of bending of the stringers, as determined by elementary beam theory, is

$$U_1 = {}^1/_2 E t_e \rho^2 \int_0^B \int_0^L w_{yy}^2 \, dx \, dy$$

With the introduction of the variables (ξ, η), this expression becomes

$$U_1 = \frac{\pi^2 B E t_e \rho^2}{2L^3} \int_0^\pi \int_0^\pi w_{\eta\eta}^2 \, d\xi \, d\eta \tag{5}$$

(C) *Energy of Flexure of the Skin*

The strain energy of bending of the skin is developed in the general theory of elastic plates.[1] Specifically,

$$U_2 = \frac{Et^3}{24(1-\nu^2)} \int_0^B \int_0^L \times [w_{xx}^2 + 2\nu w_{xx} w_{yy} + 2(1-\nu) w_{xy}^2] \, dx \, dy$$

The term w_{yy}^2 is here discarded because it is contained in the expression for the energy of the stringers (Eq. 5). In terms of the variables (ξ, η), the above equation becomes

$$U_2 = \frac{\pi^2 E t^3 L}{24(1-\nu^2)B^3} \int_0^\pi \int_0^\pi \left[w_{\xi\xi}^2 + 2\nu \left(\frac{B^2}{L^2}\right) w_{\xi\xi} w_{\eta\eta} + 2(1-\nu) \left(\frac{B^2}{L^2}\right) w_{\xi\eta}^2 \right] d\xi \, d\eta \tag{6}$$

(D) *Membrane Energy of the Skin*

Since $v = 0$, the membrane strain components are

$$\epsilon_x = \frac{\pi}{B} u_\xi + \frac{w}{R}, \quad \epsilon_y = 0, \quad \gamma = \frac{\pi}{L} u_\eta$$

in which R is the radius of curvature of the panel cross

section at the point ξ. The fundamental membrane-energy expression,

$$U_3 = \frac{Et}{2(1-\nu^2)}\int_0^L\int_0^B \times [\epsilon_x^2 + \epsilon_y^2 + 2\nu\epsilon_x\epsilon_y + {}^1/_2(1-\nu)\gamma^2]\,dx\,dy$$

then reduces to

$$U_3 = \frac{EtL}{2(1-\nu^2)B}\int_0\int_0^\pi\left[\left(u_\xi + \frac{Bw}{\pi R}\right)^2 + {}^1/_2(1-\nu)\left(\frac{B^2}{L^2}\right)u_\eta^2\right]d\xi\,d\eta \quad (7)$$

(E) *Energy of the Bulkhead Chord Members*

In general, the restraining effect of a bulkhead is divided between two consecutive compression panels, and therefore the strain energy of only one bulkhead chord should be assigned to a panel. The twist per unit length of the bulkhead chord at $y = 0$ is $w_{xy}\ (x, 0)$.

Hence, if J denotes the torsional stiffness of the chord member, the strain energy is

$$U_4 = {}^1/_2GJ\int_0^B w_{xy}^2(x, 0)\,dx$$

or

$$U_4 = (\pi^3GJ/2BL^2)\int_0^\pi w_{\xi\eta}^2(\xi, 0)\,d\xi \quad (8)$$

(F) *General Equation of Buckling*

With Eqs. (4) to (8), the buckling criterion ($W = U_1 + U_2 + U_3 + U_4$) yields

$$C\int_0^\pi\int_0^\pi \frac{z}{z_{max.}}w_\eta^2\,d\xi\,d\eta = \int_0^\pi\int_0^\pi w_{\eta\eta}^2\,d\xi\,d\eta + A\int_0^\pi\int_0^\pi [(u_\xi + \kappa w)^2 + Ku_\eta^2]\,d\xi\,d\eta + A_1\int_0^\pi\int_0^\pi\left(w_{\xi\xi}^2 + \frac{4\nu K}{1-\nu}w_{\xi\xi}w_{\eta\eta} + 4Kw_{\xi\eta}^2\right)d\xi\,d\eta + \frac{\pi}{2}\lambda A_2\int_0^\pi w_{\xi\eta}^2(\xi, 0)\,d\xi \quad (9)$$

where, for conciseness, the following dimensionless nomenclature is employed

$$\left.\begin{aligned} A &= L^4t/\pi^2B^2\rho^2I_e(1-\nu^2)\\ A_1 &= \pi^2At^2/12B^2\\ A_2 &= LJ/B^2\rho^2I_e(1+\nu)\\ \lambda &= \text{ratio of Young's modulus for a bulkhead chord to the effective modulus of the plate-stringer combination.}\\ \kappa &= B/(\pi R)\\ K &= 0.5\,(1-\nu)B^2/L^2 \end{aligned}\right\} \quad (10)$$

It may be noted that Young's modulus cancels out of Eq. (9), except for the factor λ, and it is therefore to be expected that this equation remains valid for the short-column range, provided that λ is calculated with a reduced modulus.

The forced boundary conditions that attend Eq. (9) are

$$\left.\begin{aligned} w(\xi, 0) &= w(\xi, \pi) = w(0, \eta) = w(\pi, \eta) = 0\\ u(\xi, 0) &= u(\xi, \pi) = 0 \end{aligned}\right\} \quad (11)$$

In addition, there are the natural boundary conditions

$$u_\xi(0, \eta) = u_\xi(\pi, \eta) = 0 \quad (12)$$

which arise from the assumption that the spar flanges have negligible lateral stiffness. These relations are simply derived from the stress-strain relation,

$$\sigma_x = [E/(1-\nu^2)](\epsilon_x + \nu\epsilon_y) = 0$$

With the initial assumption, $v = 0$, this reduces to $\epsilon_x = 0$. In view of Eq. (11), the vanishing of ϵ_x is equivalent to Eq. (12).

The effect of lateral stiffness of the spar flanges may be incorporated in the theory as a perturbation by adding the strain energy of spar bending to the other components of potential energy while retaining Eq. (12). However, this refinement is usually insignificant.

Approximate Mathematical Theory

The minimum value of the constant C that is consistent with Eqs. (9), (11), and (12) will be sought with the aid of the assumption that, in the process of buckling, the panel acquires a sinusoidal wave form with a single longitudinal loop but several chordwise loops. Mathematically, this assumption is expressed

$$w = w_0 \sin m\xi \sin \eta \quad (13)$$

A thorough discussion of the validity of this assumption cannot be given. However, it is pertinent to remark that, if the skin stiffness and the rotational end restraints are disregarded and if the load distribution P is uniform, then the problem admits a rigorous treatment without the use of assumption (13). This leads to the conclusion that the fixity constant C is an eigenvalue of the Sturm-Liouville differential equation

$$\phi'' - K\phi + [AK\kappa^2/(C-1)]\phi = 0$$

with the boundary conditions $\phi(0) = \phi(\pi) = 0$. The essential feature of the secondary restraints is that they furnish criteria for selecting a particular one of these eigenvalues. The corresponding eigenfunction ϕ is proportional to the normal deflection function w with a factor that depends upon κ. In the case of circular camber (κ = const.) the ϕ functions are seen to be circular functions, and it follows that Eq. (13) is theoretically correct for this case.

With the introduction of Eq. (13), the left side of Eq. (9) may be evaluated as follows:

$$\int_0^\pi\int_0^\pi \frac{z}{z_{max.}}w_\eta^2\,d\xi\,d\eta = \frac{\pi w_0^2}{2z_{max.}}\int_0^\pi z\sin^2 m\xi\,d\xi$$

Now, by the mean-value theorem for integrals, there

exists a constant $\bar{z}$ in the range $z_{min.} < \bar{z} < z_{max.}$, such that

$$\bar{z} = (2/\pi)\int_0^\pi z \sin^2 m\xi \, d\xi \tag{14}$$

Hence,

$$\int_0^\pi \int_0^\pi \frac{z}{z_{max.}} w_\eta^2 \, d\xi \, d\eta = \frac{\pi^2 w_0^2 \bar{z}}{4 z_{max.}} \tag{15}$$

The other integrals in Eq. (9) which depend only upon w may be immediately evaluated. Thus, Eq. (9) is reduced to

$$C\left(\frac{\bar{z}}{z_{max.}}\right) = 1 + \frac{4A}{\pi^2 w_0^2}\int_0^\pi \int_0^\pi [(u_\xi + \kappa w)^2 + K u_\eta^2] \, d\xi \, d\eta + A_1\left[m^4 + \left(\frac{4K}{1-\nu}\right)m^2\right] + \lambda A_2 m^2 \tag{16}$$

It is now not difficult to choose the function $u(\xi, \eta)$ to minimize the integral

$$Q = \int_0^\pi \int_0^\pi [(u_\xi + \kappa w)^2 + K u_\eta^2] \, d\xi \, d\eta \tag{17}$$

For this integral, Euler's equation of the calculus of variations is

$$u_{\xi\xi} + K u_{\eta\eta} = -(\partial/\partial\xi)(\kappa w) \tag{18}$$

A solution of Eq. (18) which satisfies the boundary conditions (11) and (12) is representable in the form

$$u = f(\xi) \sin \eta \tag{19}$$

This form automatically satisfies the boundary conditions (11), and it reduces Eq. (18) to the ordinary differential equation

$$f'' - Kf = -w_0(d/d\xi)(\kappa \sin m\xi) \tag{20}$$

Since the function $\kappa \sin m\xi$ is determined by the geometry of the airfoil, it may be represented by a Fourier analysis of the type

$$\kappa \sin m\xi = \sum_{n=1}^{\infty} a_n^{(m)} \sin n\xi \tag{21}$$

Eq. (20) then becomes

$$f'' - Kf = -w_0 \sum_{n=1}^{\infty} n a_n^{(m)} \cos n\xi \tag{22}$$

By Eq. (12), the boundary conditions associated with this equation are

$$f'(0) = f'(\pi) = 0 \tag{23}$$

The solution of Eqs. (22) and (23) is

$$f(\xi) = w_0 \sum_{n=1}^{\infty} [n a_n^{(m)}/(K + n^2)] \cos n\xi \tag{24}$$

Eqs. (13), (17), (19), (21), and (24) now furnish the following evaluation of the integral Q:

$$Q = (\pi^2 w_0^2/4) \sum_{n=1}^{\infty} K (a_n^{(m)})^2/(K + n^2) \tag{25}$$

Hence, Eq. (16) is reduced to

$$C\frac{\bar{z}}{z_{max.}} = 1 + A\sum_{n=1}^{\infty} \frac{(a_n^{(m)})^2}{1 + (n^2/K)} + A_1 m^4 + \left[\left(\frac{4K}{1-\nu}\right)A_1 + \lambda A_2\right]m^2 \tag{26}$$

This is an explicit formula for the fixity that is developed by a wing structure that contains no supporting elements for the compression panels other than longitudinal spars and rigid-acting bulkheads.

Application of the Theory

A number of numerical methods are available for evaluating the constant $\bar{z}$ and the Fourier coefficients $a_n^{(m)}$ which are required for the utilization of Eq. (26). An elementary procedure that is usually expeditious is illustrated below by an example.

Values of ordinates z that locate centroids of elemental plate-stringer areas with respect to the principal axis of inertia of the wing cross section are usually given in formal wing stress analyses. This tabulation defines, at discrete points, a functional relation between the dimensionless coordinates $\xi = \pi x/B$ and $\zeta = z/B$. A fourth-degree polynomial usually represents this function with sufficient accuracy. Thus, from given wing data, the following relation has been derived by forming a table of divided differences and by applying Newton's interpolation formula:[2]

$$\zeta = -0.00111\xi^4 + 0.0172\xi^3 - 0.0970\xi^2 + 0.173\xi + 0.0685 \tag{27}$$

The same relation could have been derived directly—though with greater labor—by assuming that a fourth-degree approximation

$$\zeta = c_0\xi^4 + c_1\xi^3 + c_2\xi^2 + c_3\xi + 0.0685$$

is admissible, and then solving four linear equations that result by selecting four representative points from the given geometric data.

Differentiation of Eq. (27) yields the following results:

$$\left.\begin{aligned} \pi\zeta' &= -0.0139\xi^3 + 0.162\xi^2 - 0.610\xi + 0.545 \\ \pi\zeta'' &= -0.0417\xi^2 + 0.3245\xi - 0.610 \end{aligned}\right\} \tag{28}$$

With the following formula of geometry, these equations determine the curvature of the airfoil profile:

$$\kappa = B/\pi R = -\pi\zeta''/(1 + \pi^2\zeta'^2)^{3/2} \tag{29}$$

Since the effect of the denominator in this expression is not large, it may be expected that κ is roughly proportional to ζ''. A plot of Eq. (29) reveals that a reasonable approximation is

$$\kappa = -0.85\pi\zeta'' = 0.0355\xi^2 - 0.276\xi + 0.520 \tag{30}$$

Now, by the theory of Fourier series, the coefficients $a_n^{(m)}$ of Eq. (21) are represented by the integrals

$$a_n^{(m)} = (2/\pi)\int_0^\pi \kappa \sin m\xi \sin n\xi \, d\xi \qquad (31)$$

Hence, by Eq. (30),

$$a_n^{(m)} = 0.0226\int_0^\pi \xi^2 \sin m\xi \sin n\xi \, d\xi - 0.176\int_0^\pi \xi \sin m\xi \sin n\xi \, d\xi + \begin{cases} 0.519, & m = n \\ 0, & m \neq n \end{cases} \qquad (32)$$

Also, by virtue of Eqs. (14) and (27),

$$\bar{\zeta} = \bar{z}/B = -0.00071\int_0^\pi \xi^4 \sin^2 m\xi \, d\xi + 0.0109\int_0^\pi \xi^3 \sin^2 m\xi \, d\xi - 0.0617\int_0^\pi \xi^2 \sin^2 m\xi \, d\xi + 0.110\int_0^\pi \xi \sin^2 m\xi \, d\xi + 0.0685 \qquad (33)$$

Since the integrals of Eqs. (32) and (33) are generally useful, they are evaluated below:

$$\left.\begin{aligned} &\int_0^\pi \xi^2 \sin m\xi \sin n\xi \, d\xi = (-1)^{m+n}\pi\{(m-n)^{-2} - (m+n)^{-2}\}, \; m \neq n \\ &\int_0^\pi \xi \sin m\xi \sin n\xi \, d\xi = \tfrac{1}{2}\{1 - (-1)^{m+n}\} \times \{(m+n)^{-2} - (m-n)^{-2}\}, \; m \neq n \\ &\int_0^\pi \xi^4 \sin^2 m\xi \, d\xi = \frac{\pi^5}{10} - \frac{\pi^3}{2m^2} + \frac{3\pi}{4m^4} \\ &\int_0^\pi \xi^3 \sin^2 m\xi \, d\xi = \frac{\pi^4}{8} - \frac{3\pi^2}{8m^2} \\ &\int_0^\pi \xi^2 \sin^2 m\xi \, d\xi = \frac{\pi^3}{6} - \frac{\pi}{4m^2} \\ &\int_0^\pi \xi \sin^2 m\xi \, d\xi = \pi^2/4 \end{aligned}\right\} \qquad (34)$$

With these results, Eqs. (32) and (33) yield

$$\left.\begin{aligned} a_n^{(m)} &= 0.0710\,[(m-n)^{-2} - (m+n)^{-2}], \quad m \neq n, \; (-1)^{m+n} = +1 \\ a_n^{(m)} &= 0.105\,[(m-n)^{-2} - (m+n)^{-2}], \quad m \neq n, \; (-1)^{m+n} = -1 \\ a_m^{(m)} &= 0.202 - (0.0177/m^2) \end{aligned}\right\} \qquad (35)$$

$$\frac{\bar{z}}{z_{max.}} = \frac{\bar{\zeta}}{\zeta_{max.}} = 0.800 + \frac{0.116}{m^2} - \frac{0.0102}{m^4} \qquad (36)$$

The foregoing results were obtained from data for a typical wing, for which the pertinent constants (Eq. 10) corresponding to a station near the root are

$$A = 10.83, \; A_1 = 1.17 \times 10^{-5}, \; A_2 = 1.28 \times 10^{-5}, \; K = 4.54$$

With these constants, it is determined by Eq. (35) that the values of the expression

$$\sum_{n=1}^{\infty} (a_n^{(m)})^2/[1 + (n^2/K)]$$

corresponding respectively to $m = 1, 2, 3, 4, 5, 6, 7$ are 0.033, 0.0315, 0.0213, 0.0144, 0.0099, 0.0072, and 0.0053. Likewise, by Eq. (36), the respective values of $z_{max.}/\bar{z}$ are 1.10, 1.22, 1.25, 1.25, 1.25, 1.25, and 1.25. Hence, denoting the value of C corresponding to m-lobe buckling by C_m, one obtains, by Eq. (26), $C_1 = 1.49$, $C_2 = 1.64$, $C_3 = 1.54$, $C_4 = 1.46$, $C_5 = 1.41$, $C_6 = 1.38$, and

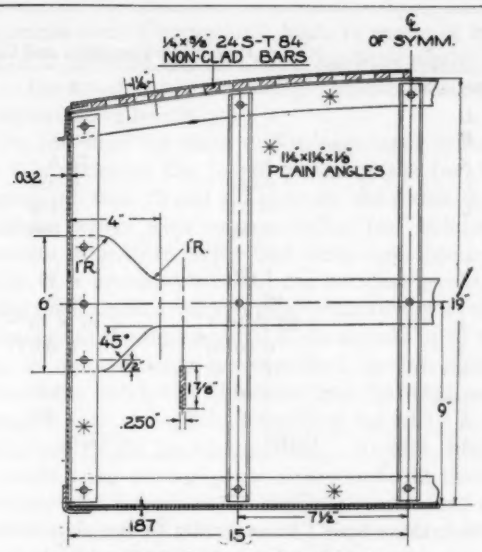

FIG. 2. Typical cross section of test beam.

$C_7 = 1.38$. Beyond C_7, the numbers of this sequence obviously increase. Thus, the design value for the fixity is $C = 1.38$ in this example.

TEST RESULTS

Five beams with cross sections like that shown in Fig. 2 have been tested. The stringers were $^1/_4$ by $^5/_8$ in. 24S-T84 unclad bars spaced at $1^1/_4$ in., and the skins were 0.051-gage or 0.080-gage 24S-T86 Alclad sheets. The bulkhead chord members were $^1/_8$ by $1^1/_4$ by $1^1/_4$ in. plain 24S-T Alclad angles, with two intermediate supports as shown in Fig. 2. All specimens had constant radii of curvature on their upper surfaces.

The specimens were tested by applying bending couples at the ends. Injurious end effects were prevented by local reinforcements extending over two bays. In each case, the unreinforced test section extended over five bays. The loading mechanism was operated by means of a calibrated system of hydraulic rams with pressure-gage attachments. The measured loads determined the bending moments, and, since pure flexure was

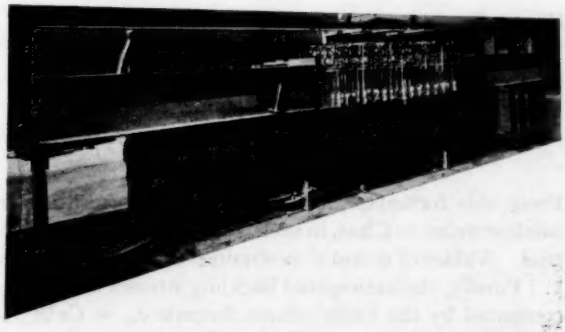

FIG. 3. Buckling of semimonocoque wing structures.

TABLE 1
Descriptive Constants and Calculated Characteristics of Test Beams

Beam No.	1	2	3	4	5
L	8	8	8	12	12
B	30	30.1	31.4	31.4	31.4
R	∞	73.5	30	30	30
t	0.050	0.051	0.051	0.051	0.080
t_s	0.173	0.172	0.173	0.167	0.196
ρ	0.089	0.089	0.089	0.0915	0.0974
κ	0	0.131	0.333	0.333	0.333
K	4.92	4.96	5.40	2.40	2.40
A	18.5	18.6	17.2	85.5	101.0
A_1	4.20×10^{-5}	4.40×10^{-5}	3.70×10^{-5}	1.85×10^{-4}	5.39×10^{-4}
A_2	0.00730	0.00717	0.00665	0.00976	0.00735
m	1	3	5	5	5
$z_{max.}/\bar{z}$	1.00	1.05	1.14	1.13	1.13
C	1.01	1.25	1.78	2.57	3.04
σ_{cr}	13,000	16,100	22,800	15,500	20,800

applied, these bore a known ratio to the plate-stringer stresses. In some cases the stresses were checked with electric strain gage equipment. On all beams, deflections were thoroughly mapped with dial gages. Fig. 3 is a photograph of a typical test setup.

Dimensions of the specimens are shown in Table 1. Aside from differences indicated by these dimensions, the specimens were identical. The following material constants were adopted for all specimens:

$$E = 10.5 \times 10^6 \text{ lbs. per sq.in.}$$
$$\nu = 0.30, \quad \lambda = 1.00$$

The torsional rigidity J of a bulkhead chord member is obtained from the well-known torsion formula for open sections: $3J = A_b t_b^2$. For the $^1/_8$ by $1^1/_4$ by $1^1/_4$ in. angle sections used in the box beams, the area A_b is 0.280 sq.in., and, consequently, $J = 0.00146$.

The constants A, A_1, A_2, K, and κ given in Table 1 were computed by the formulas of Eq. (10). The ordinates z were measured from the centroidal axes of the beam cross sections, and the quantities $\bar{z}$ were obtained by numerical integration of Eq. (14). Since all beams had circular camber, the Fourier analysis (Eq. (21)) degenerates, in each case, to

$$a_n^{(m)} = \begin{cases} \kappa \text{ if } m = n \\ 0 \text{ if } m \neq n \end{cases}$$

Hence, Eq. (26) becomes

$$C\left(\frac{\bar{z}}{z_{max.}}\right) = 1 + \frac{A\kappa^2}{1 + (m^2/K)} + A_1 m^4 + \left(\frac{4KA_1}{1-\nu} + A_2\right)m^2 \quad (37)$$

From this formula, the integer m that furnishes the smallest value to C has, in each case, been determined by trial. Values of m and C so obtained are given in Table 1. Finally, the anticipated buckling stresses have been computed by the Euler column formula $\sigma_{cr} = C\pi^2 E \times (\rho/L)^2$.

It may be observed that the effects of the bulkhead uprights have been neglected in the calculations of Table 1. For Beam 1 these effects are certainly negligible, and for Beam 2 they are null because the nodes in the twisted bulkhead chord occur at the uprights. For Beams 3, 4, and 5, the effects can be no greater than those attending an increase of m from 5 to 6, since, with $m = 6$, there is no bending of the uprights. Hence, for the first four beams, the perturbation of C due to the uprights is not more than 1 per cent, while for Beam 5 it is known only that it is less than 9 per cent.

To substantiate the foregoing theory, it would be simplest to compare the calculated buckling stresses (Table 1) with observed buckling stresses. However, because of unavoidable imperfections of materials and workmanship and because of natural deformations attending bending of the beams, ideal buckling did not occur. A picture of the true behavior of the specimens is given by stress-deflection curves (Fig. 4). These show deflections relative to the spars at or near the centers of the compression surfaces. Relative deflections were automatically determined by mounting the dial gages on chordwise brackets that rested on the spar flanges (Fig. 3). Thus the curves (Fig. 4) present

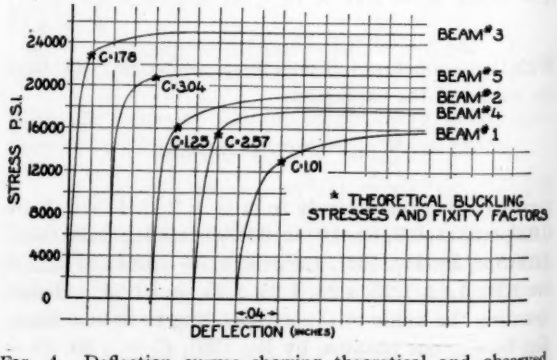

FIG. 4. Deflection curves showing theoretical and observed buckling stresses of test specimens.

a true representation of the chordwise arching or humping of the compression panels.

The deflection curves (Fig. 4) show definite knees, which presumably lie near the ideal buckling stresses. The calculated buckling stresses (Table 1) are indicated on the curves by stars, and the corresponding fixity factors are appended. It is seen that, in each case, the calculated buckling stress lies on the knee of the corresponding stress-deflection curve. This circumstance is a good confirmation of the present theory.

Conclusions

It is apparent from the test results illustrated in Fig. 4 that the conventional practice of utilizing an invariable specified fixity factor for all wing stress analyses admits significant refinements. The frequent specification $C = 1.5$ is certainly unsafe if the wing surface is nearly flat in the interspar region, whereas it is exceedingly conservative under other conditions.

Since the factor C determines reduced column lengths, its influence is smaller in the short column range than in the Euler range. However, with the advent of precipitation heat-treated aluminum alloys, column design curves have become much steeper, and fixity in the short-column range has consequently assumed greater importance than formerly.

The foregoing theory is presented as a rational approach to the "fixity problem." Within the range of the experiments, the theory has been well confirmed. Further tests are needed to verify the theory in cases of noncircular camber and to determine the effect of premature buckling of the skin. Although all of the test specimens carried appreciable loads in excess of buckling, it is probable that this effect has little significance when the stringers are thin-walled sections that cripple under excessive bending.

The fact that the fixity due to membrane action of the skin varies as the fourth power of the bulkhead spacing (cf. Eqs. 10 and 26) presents the possibility of designing wings with comparatively few bulkheads. However, in order to realize high fixity from membrane action, it is necessary to limit the buckling pattern to modes that exhibit a small number of chordwise waves—preferably to the fundamental mode defined by $m = 1$. This is most directly accomplished by introducing, between the bulkheads, chordwise ribs that exert small restraints against single-lobe buckling but which nevertheless control the buckling pattern. Results obtained by generalizing the foregoing theory indicate that exceedingly high fixities may sometimes be obtained with small weight cost by this device. However, test results for this type of construction are lacking at present. It should be observed that the theory, as presented, is not applicable for cases in which C exceeds four, since only single-loop buckling in the spanwise direction has been contemplated.

References

[1] Timoshenko, S. P., *Theory of Elastic Stability*, 1st Ed., p. 307, Eq. 199; McGraw-Hill Book Company, Inc., New York, 1936. [The strain energy expression for a curved shell (Eq. 255, p. 423, loc. cit.) is more accurate, but, for the present theory, the flat-plate equation is adequate.]

[2] Milne-Thompson, L. M., *The Calculus of Finite Differences*, 1st Ed., p. 3, Eq. 1; The Macmillan Company, London, 1933.

Reduction of the Adhesion of Ice to De-Icer Surfaces*

D. L. LOUGHBOROUGH† AND E. G. HAAS‡

The B. F. Goodrich Company

SUMMARY

Ice is removed from a De-Icer surface by mechanically applying concentrated stresses to the ice-rubber interface. It is obvious that a low value for the adhesive bond should be desirable, but it is conceivable that a zero value might not be practical. The shear strength of the bond to the De-Icer surface is as high as that between ice and any other solid; it increases linearly with decrease in temperature from a value of zero at 0 °C. to 150 lbs. per sq.in. or more at −25 °C. It is approximately 15 per cent higher to the surface of a rubber that has soaked in water and probably depends on surface smoothness only to the extent that a rough surface presents a greater area.

It has been found that silicone, either formed *in situ* by polymerization on the De-Icer surface or applied as ready-made polymer, improves the performance of De-Icers by lowering the adhesion of ice to the surface by as much as 90 per cent. These treatments have shown good results both in the laboratory and in flight tests. It is expected that, because of the toughness of the films formed by silicones, they will need to be applied only a few times during an icing season.

INTRODUCTION—PRESENT METHOD OF ICE REMOVAL

THE METHOD for the removal of ice from aircraft that has been used most extensively in this country is that involving the use of a pneumatically operated rubber boot known commercially as a De-Icer. The De-Icer consists of a rubber sheet, containing cells or tubes, stretched and mechanically attached at its outer margins to the leading-edge surface to be protected. The inflation and deflation of the cells cracks the ice so that it is carried away by the air stream. Fig. 1 is a schematic drawing of the basic three-tube De-Icer in the three inflation stages, while Fig. 2 shows an actual installation.

Though this device works well under most icing conditions, difficulty sometimes is encountered in completely removing ice, especially at low temperature where the ice adheres particularly tenaciously. For some time it has been felt that performance would be improved if the adhesion of ice to the surface could be lowered. The work toward this end reported here is only one phase of the research and development work that is being followed to improve the performance of this product.

Although the De-Icer is constructed of a pure gum natural rubber stock with fabric reinforcement where necessary, the surface usually is a neoprene cement coat. When the De-Icer surface is mentioned it is this thin neoprene surface which is meant.

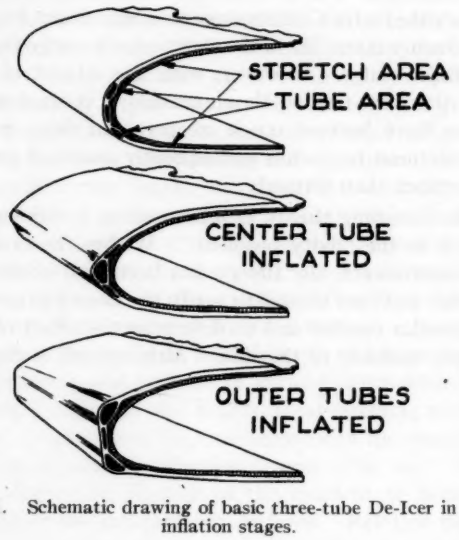

FIG. 1. Schematic drawing of basic three-tube De-Icer in three inflation stages.

FIG. 2. De-Icer installed on horizontal tail of an airplane.

Received August 13, 1945.

* We wish to acknowledge the assistance given by members of the research staff of the Dow-Corning Company and of the General Electric Company. Without their help the preparation of experimental lots of special samples would have been extremely difficult. We wish also to acknowledge the help of Dr. T. L. Gresham and Dr. T. M. Amacker of The B. F. Goodrich Research Laboratory for the preparation of special silanes.

† Research Supervisor.

‡ Senior Research Physicist.

Physical Principles Underlying Adhesion

A full understanding of the role that the adhesion of ice to rubber plays in De-Icer operation requires a consideration of some of the physical principles involved in the operation. A detailed discussion of these matters is complicated and outside the scope of this paper, but certain fundamental matters will be considered.

Applied Stress

On applying suitable stresses to a rubber sheet covered with ice the two components separate. The type of stress applied is not critical and is determined solely by mechanical convenience. In the De-Icer, forces in two different directions are used: (1) in the tube area (Fig. 1) the interface is distorted in a direction perpendicular to its plane; (2) in the stretch area (Fig. 1) the interface is distorted in a direction parallel to its plane.

The applied stress is magnified by the stress concentration to such an extent that the local force on the interface exceeds the bond strength. Analyses of these forces have been made and show that the multiplication of the stress is many fold. The bond can then be broken with a low load applied slowly. This is the important fact about De-Icer operation. A thin steel shell could be made to remove ice in the same way the rubber boot does, except extremely high forces would be required. The interface distorts until the concentrated force exceeds the adhesive force, and then the ice film cracks loose from the surface. The object of De-Icer design is to make the necessary applied load as low as possible. This can be done, as explained above, (a) by using a low modulus, elastic material so that high stress concentrations are possible, and (b) by lowering the adhesive force. It should be pointed out, however, that the latter scheme must not be carried too far, for, if the adhesive force were lowered to a zero value, it is doubtful that the ice cap could be removed. The stress applied by the De-Icer could not be transmitted to the ice to cause the breaking of the cap. It is desired, then, to reduce the adhesion to some low nonzero value.

Stress Concentration

The measurement of the adhesive force between two solids is complicated by the fact that stress on the interface is concentrated and locally exceeds the applied stress. When the materials are as different as ice and rubber, all values of adhesion must be questioned, since results from two slightly different experimental arrangements may easily differ by a factor of five. It is important for the evaluation of the true adhesion that the applied stress be constant over the interface or that the stress distribution be accurately known.

Methods of Measuring Adhesion

Each of the many methods which have been used to measure the adhesion between ice and various solids has an advantage for particular conditions. A centrifugal method developed by the Massachusetts Institute of Technology De-Icing Research Laboratory has been used to a large extent in this work. The apparatus (Fig. 3) consists of a horizontal plate that can be rotated at controlled speed. An ice button is frozen to a

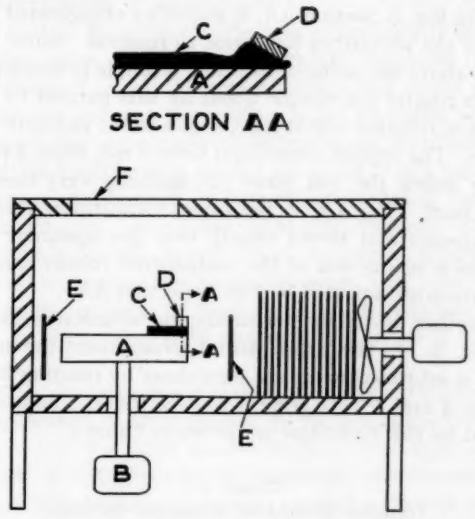

Fig. 3. Apparatus for measurement of ice adhesion by centrifugal method.

A. Rotating plate.
B. High-speed motor.
C. Sample.
D. Ice button.
E. Guard ring.
F. Window.

Section AA—Enlarged cross section of sample and ice button during measurement to adhesion.

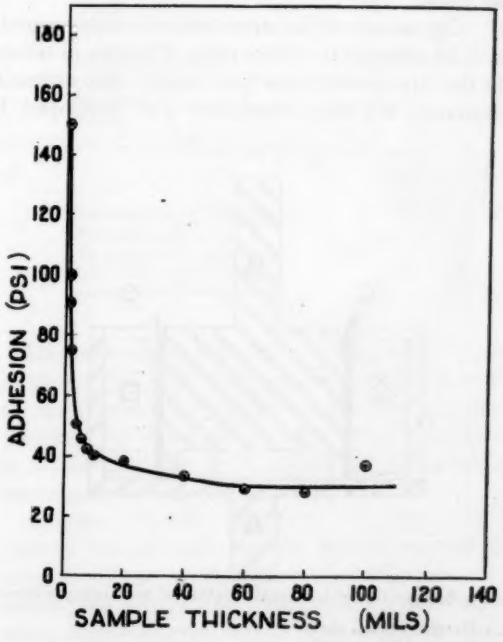

Fig. 4. Effect of thickness of sample on apparent adhesion of ice to pure gum rubber, −25°C.

rubber sample cemented to the disc, and the centrifugal force required to just free the button is measured. The motor B drives the plate A at the desired speed, measured by a stroboscope through the window F of the refrigerator. The speed is increased until the ice button D flies off the test sample C and strikes the guard ring E. In Fig. 3, Section AA, is shown an exaggerated detail of the ice button just prior to removal. Since the ice is above the plane of rotation, a couple is developed which rotates the sample about an axis parallel to the plane of rotation and at right angles to the radius of the plate. The applied centrifugal force is not, then, a pure shear unless the test piece (C) becomes very thin or very hard. Fig. 4 gives the values measured at various thicknesses and shows clearly that the apparent adhesion is a function of the undistorted rubber sample thickness as indicated by Fig. 3, Section AA.

Another device for measuring the adhesion is shown in Fig. 5. In this experimental arrangement the interface is subjected to almost pure shear by rotating brass shells A and B with respect to each other. Values secured by this technique are given in Table 1.

TABLE 1
Torsional Method of Measuring Adhesion
Mechanical Goods Rubber Stock

Temperature (°C.)	Adhesion Lbs. per Sq.In.
−10	80
−20	170
−30	200

Other methods of determining the adhesion based on totally different principles have been used. Two are given below.

(1) Calculation of the stress concentration around a piece of ice adhered to a large piece of rubber in tension (as in the stretch area) has been made. The necessary mathematics for this calculation was developed by Donnell.[1] By measuring the equilibrium area of contact between the two solids when a fixed elongation is applied to the rubber, it is possible to get an estimate of the adhesion. The experiment is too difficult to control for extensive use and has value primarily because it indicates the mechanism of De-Icer operation. No details will be given.

(2) By calculating the shear stresses between rubber and ice when the interface is deformed perpendicular to the interface, it is possible to secure an approximate value of the adhesive force.

In all of these methods the ice formed is of the hard glaze type. No method of easily forming other types is available in our laboratory at the present time. It is probable that rime or any other air-containing ice will show a lower value of the apparent adhesion only because of the reduced contact area.

Because the interfacial area is not accurately known, only a few results are given in absolute units. In most instances the values listed are comparative, and indicate either a per cent of the value for the untreated surface or a per cent of the value for a pure gum stock.

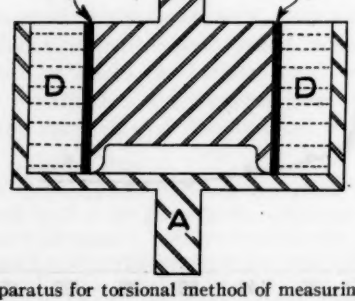

FIG. 5. Apparatus for torsional method of measuring adhesion.

A. External brass shell.
B. Internal brass shell.
C. Rubber.
D. Ice.

True Value of the Adhesion

From the first two tests it can be seen (Table 1, Fig. 4) that the adhesion of ice to rubber-like materials is about 170 lbs. per sq.in. at −25°C. In the second method discussed the difficulty of preparing samples is too great for routine testing. In general, the centrifugal device has been chosen, using test pieces about 0.05 to 0.1 in. thick. Although it was realized that the absolute adhesion was not correct, it was believed that the relative values for the different surfaces would be. Where some notion of the absolute value of the adhesion of ice to flexible material was desired, thin films were used as test samples.

That the true adhesion of ice to rubber is as high as that of ice to many other materials is shown in Table 2.

TABLE 2
Adhesion of Ice to Miscellaneous Materials
−25°C.—Centrifugal Method

Test Material	Shear Strength of Bond (Lbs. per Sq.In.)
Ice	250
Steel—polished	185
Copper—polished	124
24ST aluminum	220
Glass (96 per cent silica)	158
Microscope slide	122
Polyethylene	160
Rubber	170

From the above discussion it follows that the use of rubber in De-Icers is not dictated by the low adhesion but by the fact that low applied stresses can be used because of the stress concentration. The high value of the adhesion does indicate the possibility of considerable reduction, but, before discussing methods of

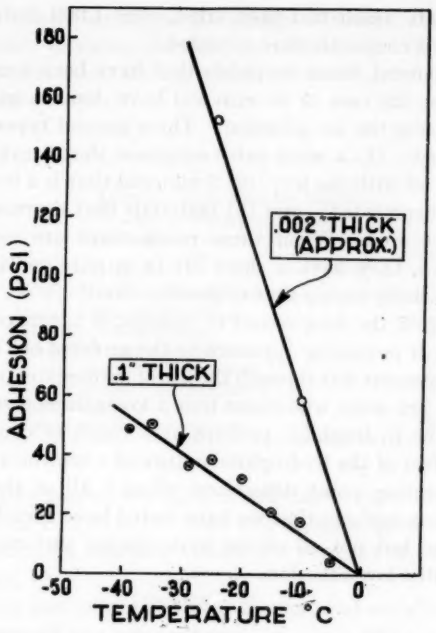

FIG. 6. Variation of adhesion with temperature (pure gum rubber).

achieving this, some understanding of the factors that affect the magnitude of the adhesion should be helpful.

Factors Affecting the Adhesion

Temperature.—The adhesion of ice to rubber and other materials changes linearly with the temperature as shown in Fig. 6. The slope of the curve for the thin sample is over four times as great as that for the thick sample. The distortion resulting from the 0.1-in. thick rubber sheet reduces the adhesion 76 per cent at all temperatures. The values for the thin sample approach more closely the true bond strength between ice and rubber.

The strong dependence of adhesion on temperature is not restricted to that between rubber and ice. As is shown in Table 3, the slopes are high for all materials but two. One of these is for the "adhesion" of ice to ice and forms an interesting and unexplained exception to the other materials. The other exception is silicone on rubber, which will be discussed later.

TABLE 3
Temperature Dependence of Adhesion

Test Material	Temperature Slope (Lbs. per Sq.In. per °C.)
Ice	0
Steel	−7.4
Copper	−5.0
Aluminum	−8.8
Glass (96 per cent silica)	−4.5
Polyethylene	−5.8
Rubber	−6.0
Silicone treated rubber	−0.4

This striking dependence on temperature (6 lbs. per sq.in. per °C.) is of interest to those studying the theory of adhesion. It is of even more importance for the understanding of the mechanical removal of ice at low temperature. It is under these conditions that a reduction in adhesion can be expected to give the greatest improvement in performance.

Surface Roughness.—The lack of sufficiently detailed information on molecular forces has prevented the development of any theory regarding the origin of the adhesion between two solids. It has generally been assumed that some materials adhere by the interlocking of surface irregularities, though the proof of this has never been secure because of lack of knowledge of the true contact area. In general, most workers imply that the adhesion largely results from molecular interaction. This is particularly probable when the adhesion is strongly temperature dependent in a temperature range in which neither solid greatly alters physical properties.

Two sets of data are presented in Table 4 to show the dependence of ice adhesion on surface conditions. In Part A of the table the rubber was cured against surfaces of different visually estimated roughnesses. In Part B the rubber was cured against a smooth surface and scored in the ways described.

TABLE 4
Surface Roughness

−30 °C.—Pure Gum Rubber

A

Surface Cured Against	Visual Smoothness Rating	Apparent Adhesion Per Cent of Highest Value
Fabric—rough	6	100
Holland cloth backed by fabric	5	50
Parchment paper	4	70
Holland cloth	3	60
Aluminum	2	65
Glass	1	25

−20 °C.—Neoprene Surface

B

Description of Sample	Adhesion (Per Cent of Value for the Original Surface)
Pricked with a pin	125
Covered with Santocel	164
Cut with razor blade	182
Roughened with emery	210

The increase in adhesion resulting from roughening of the surface could probably be completely attributed to the increase in contact area. This has not been proved. No matter what explanation is finally given, it is obvious that it is important to maintain the smoothness of De-Icer surfaces.

Moisture Content.—The data in Table 5 show the ratio of the adhesion value of dry to wet material for several different materials. In making the measurements, the material that had recently been soaked in water was considered to have a *wet* surface even though the surface was wiped dry.

TABLE 5
Effect of Moisture on Ice Adhesion
Soaked in Water at 70 °C. for 1 Hour

Rubber Stock	Ratio of Adhesion Value of Dry to Wet Material
Pure gum rubber	0.83
Rubber plus 60 parts Gastex	0.91
Neoprene compound	0.92
De-Icer surface	0.62
Mean of measurement on 10 different stocks	0.87

In De-Icer operation the adhesion is almost always to a wet surface. The water absorption of rubber is not primarily due to the rubber hydrocarbon but to the pigments, protein impurities, etc., which are present. Samples of gum rubber prepared from latices specially washed to remove moisture-absorbing ingredients were found to have only about half of the adhesion of a normal pure gum rubber stock.

Tables 1 through 5 have indicated the nature of ice adhesion. The desirability of finding a way to reduce it is obvious.

Surface Treatments.—The adhesion of ice to most elastomers from which De-Icers can be made is so nearly the same that little advantage could result from changing the elastomer. The only known exception to this generality is silicone "rubber," which shows promise especially for use as a surface coating on a rubber stock.

Present De-Icers have a coating of neoprene which protects the rubber from the sunlight and, because of its compounding ingredients, renders the surface conducting. Thus it is protected from electrical discharges. This surface cannot easily be altered unless the new material can also fulfill these functions. As an example Table 6 presents the adhesion of ice to a number of elastomers.

TABLE 6
Adhesion to Thin Films of Various Elastomers
−25 °C., 0.002 In. Thick—Centrifugal Method

Elastomer	Adhesion (Lbs. per Sq.In.)
Rubber	170
Hycar OR	150–160
GR-S	130
Thiokol FA	138
Koroseal[1]	120
Neoprene[2]	150
Polyethylene	160
Polystyrene[3]	115
Silicone rubber[4]	45

[1] Value determined by extrapolation. The value measured, −25 °C., is certainly too low, because the film is weak and adhesion of the film to metal (surface) is poor.
[2] For comparison purposes this may be considered as a De-Icer surface.
[3] Not an elastomer. Included here for general interest.
[4] Estimated from a determination made on a thick piece. Value on a 0.1-in. sample was 10 lbs. per sq.in. (See Fig. 6.)

A great number of surfaces and surface treatments have been tried by this and other laboratories in the past with little success. In a recent incomplete list of materials which had been tried, over 1,000 distinctly different chemicals were recorded.

In general, those materials that have been found to increase the ease of ice removal have done so without decreasing the ice adhesion. Three general types may be listed: (1) a weak salve or grease that breaks and comes off with the ice; (2) a material that is a freezing point depressant; and (3) materials that decrease the contact area. When these mechanisms are used in practice, they have a short life or require continuous replenishing during time of greatest need.

Despite the long record of failures, it appeared that the most promising approach to the problem of De-Icer improvement was through the use of surface treatments. There are some who claim that a low-adhesion surface must be hydrophilic, perhaps as a result of confusing the effect of the hydrophilic nature of a treatment with the freezing point depressant effect. All of the low-adhesion surfaces that we have tested have been hydrophobic, but not all of the hydrophobic surfaces have exhibited low adhesion.

SURFACE TREATMENT WITH SILANES AND SILICONES*

Of the number of materials tried, silicone, either polymerized from silanes applied to the test surface or applied directly as a silicone, proved most promising for use on De-Icers. Detailed investigation shows that they almost completely fulfill the requirements. The balance of this paper will be devoted to a discussion of the results with these materials.

Silanes

The silanes referred to in this work are organo-silicon halides analogous to the substituted methanes and having a general formula

$$R_n\mathrm{Si}\ \mathrm{Cl}_{4-n}$$

On exposure to a moist atmosphere they react rapidly with water-forming silicols. The silicols polymerize to silicones at a rate depending on the nature of the hydrocarbon radical. The dimethyl derivative polymerizes rapidly to an oil.

$$(CH_3)_2SiCl_2 + H_2O \rightarrow (CH_3)_2Si(OH)_2 + 2HCl$$

$$\rightarrow -O-\underset{\displaystyle CH_3}{\overset{\displaystyle CH_3}{\overset{|}{\underset{|}{Si}}}}-O-\underset{\displaystyle CH_3}{\overset{\displaystyle CH_3}{\overset{|}{\underset{|}{Si}}}}-O-\underset{\displaystyle CH_3}{\overset{\displaystyle CH_3}{\overset{|}{\underset{|}{Si}}}}-O + H_2O$$

The chemistry and properties of these materials have been described in the literature.[2–5]

* Materials of this nature and for this purpose are supplied commercially by The B. F. Goodrich Company. Their use for lowering of ice adhesion is now the subject matter of patent applications.

In Table 7 are given the results of some tests on the adhesion lowering resulting from treating rubber surfaces with liquid silanes, which, of course, polymerize to silicones.

TABLE 7
Adhesion Reduction by Silanes
−25°C.—De-Icer Surface

Silane (Applied as the Pure Liquid)	Adhesion (Per Cent of Untreated Surface)
Monomethyl trichlorsilane	12
Dimethyl dichlorsilane	20
Trimethyl monochlorsilane	23
Mostly diethyl dichlorsilane	2
Mostly dibutyl dichlorsilane	25
Mostly diphenyl dichlorsilane	25
Phenyl butyl dichlorsilane	17

In this type of testing it is difficult to control the experiment completely. Here and in subsequent tables, differences in adhesion values of 5 per cent are not significant.

Other methods of applying the material are also satisfactory.

TABLE 8
Method of Applying Silane
−25°C.—Silane

Treatment	Surface to Which Applied	Adhesion (Per Cent of Untreated Surface)
Vapor in a closed container 50 min.	Rubber	51
Vapor in a closed container 100 min.	...	30
Soaked in water 1 hour at 70°C., then exposed to vapor 90 min.	...	40
Equilibrium with room humidity, then exposed to vapor 90 min.	...	45
Hung over liquid—10 min.	De-Icer surface	18
Hung over liquid—60 min.	De-Icer surface	15
Treated with liquid	De-Icer surface	12
Treated with solutions	See Table 9	..

TABLE 9
Applying Silane from a Solution

A. Various Concentrations in CCl_4 on De-Icer Surface

Concentrations (Per Cent by Volume)	Adhesion (Per Cent of Untreated Surface)
4.5	31
9	33
17	22
28	16
33	23
50	18
100	12

B. Various Solvents

Solvent	30 Per Cent by Volume	50 Per Cent by Volume
Naphtha B	37	..
CCl_4	23	18
C_6H_{14}	42	21
$C_2H_4Cl_2$	33	15
C_6H_6	33	9
C_6H_5Cl	49	36

The adhesion is lowered by all methods of treatment, but the use of the pure liquid gives slightly better results. In most of our tests this method has been used exclusively.

A successful film must, in addition to lowering the adhesion, be reasonably permanent. Though the durability of the film will be considered in detail later, the data that follow will give the adhesion results after exposure to an ultraviolet light and then to a weatherometer.

The ultraviolet light is a Hanovia Chemical Company lamp, Type 7420, placed 15 in. from the sample in a partially closed space. The temperature rose about 15°C. above room temperature. The weatherometer is similar to that used in testing painted surfaces. The samples are suspended in a circle about a carbon arc light and rotated about the light every 15 min. Once during each rotation they are subjected to cold-water spray.

In Table 10 are collected the results achieved by using the pure silanes. The differences among these treatments show most significantly after aging under an ultraviolet light.

TABLE 10
Adhesion Reduction by Certain Silanes
Pure Liquids

Silane	Adhesion (Per Cent of Control) Initial	After 86 Hours Under Ultraviolet Light	After 86 Hours Under Ultraviolet Light and 20 Hours in Weatherometer
CH_3SiCl_3	12	>100	..
$(CH_3)_2SiCl_2$	16	41	62
$(CH_3)_3SiCl$	23	75	..

Silicones

Two possible disadvantages in polymerizing the silicones *in situ* are apparent: (1) the polymerization conditions are uncontrolled, and (2) the copious evolution of HCl may be hazardous to personnel and equipment unless special precautions are taken. It would be more convenient to make the silicones and apply them to the surface to be protected, provided the results were equally good. Which results are better may depend on how firmly the respective films are bound to the rubber surface. It is possible that the mode of attachment of the rubber to the film formed from the silanes is through a primary valence brought about by the reaction of the halogen in the silane with a hydrogen in the surface. Table 11 and Fig. 7 present the data on silicones and mixtures of silicones. The adhesion reduction is noticeably improved by lowering the CH_3-Si ratio to a value of 2 or less. The results do not depend on the silanes chosen but on the methyl silicon ratio. Similar results have been found for mixtures of silanes except that in this case copolymers of mono- and trimethyl silane are significantly poorer than other copolymers of the same CH_3/Si.

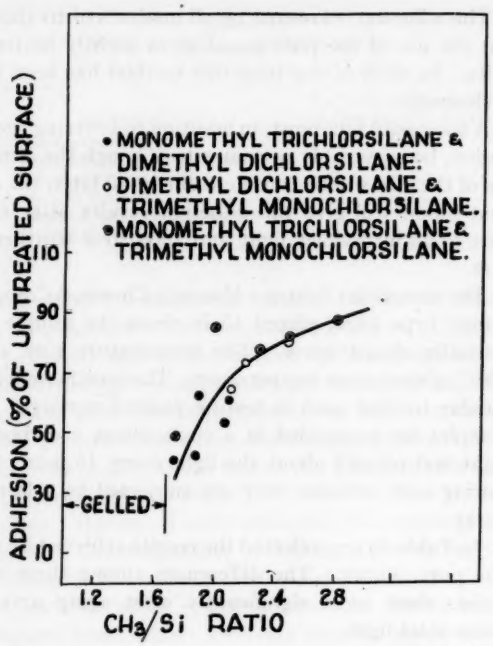

FIG. 7. Adhesion to De-Icer surface treated with silicones prepared from mixtures of methyl chlorsilanes, −25°C. Thickness of sample, 0.060 in.

TABLE 11
Silicones from Mixtures of Silanes

Monomers	CH_3/Si	Adhesion (Per Cent Untreated Surface) Unaged	86 Hours Under Ultraviolet Light	86 Hours in Ultraviolet Light and 20 Hours in Weatherometer
Mono- and dimethyl	1.75	6	40	50
	1.88	14	42	52
	1.90	13	62	54
Di- and trimethyl	2.08	8	52	65
	2.10	13	66	77
	2.20	16	73	77
	2.50	48	81	79
Mono- and trimethyl	1.67	17	48	73
	2.00	37	85	87
	2.30	40	77	67
	2.50	42	81	81
	2.80	31	87	71

The silicones can be applied in a number of ways, but a direct application is the most successful.

The effectiveness of the silicones for the purpose is remarkable, especially since other materials, such as polyethylene, which present an equally pure hydrocarbon surface, are poor for lowering ice adhesion. Further increasing the length of the aliphatic chain in the monomeric silane does not improve the ice-adhesion lowering. Some other feature of molecular structure must account for the unique value of this polymer. The explanation finally accepted must account for the low ice adhesion

FIG. 8. Laboratory test of ice removal from treated and untreated De-Icer surface. Three-tube De-Icer, −25°C. Ice thickness, 0.030 in. Methyl chlorsilane treatment. Treated surface on right.

in a way that does not require high water repellency, for it can easily be shown that there is poor correlation between these two properties.

Durability

That lowering the adhesion improves De-Icer performance is indicated in Fig. 8. A laboratory wing section was mounted in a refrigerator with the leading edge up. The area on the right was treated with Icex prior to coating the rubber with a 0.030-in. thick cover of glaze ice at −32°C. The De-Icer was inflated once, and all of the ice came off the treated area. In the photograph the black areas are free of ice; in the white areas the ice is free but is held in place by that which is tightly adhered and appears dark gray. This type of testing indicates promising materials but fails as a service test because it does not subject the surface to the severe abrasion met in service. To duplicate such action in the laboratory is difficult.

The films, when placed on De-Icers in service, must withstand ultraviolet light, exposure to impact of water drops, and repeated removal of ice caps. The duplication of these conditions in the laboratory is not strictly possible, but from certain of the tests described below some notion of the performance characteristics of the material can be gathered. Neither material has a measurable effect on the usually measured properties of rubber or De-Icer surface, such as modulus, tensile strength, elongation, flex life, etc.

TABLE 12
Durability to Solvents
Silane

	Per Cent of Surface with No Silane
Washed with benzene	4
Washed with acetone	19
Washed with butyl acetate	44
Washed with methyl ethyl ketone	33
Washed with soap and water	19
Soaked in water 1 hour at 70°C.	15
None	12

TABLE 13
Stability Under Ice-Forming Conditions
Silane
Repeat Values on Same Spot on Sample

	Adhesion (Per Cent of Control)		
	Rubber	Aluminum	Steel
1st button	17	19	16
2nd button	12	28	98
3rd button	15	74	..
4th button	21	..	..

The treatment is surprisingly stable to a range of solvents and is not dissolved or freed from the surface by water.

In De-Icer operation many ice caps are removed in succession. If the material is low in strength (like Vaseline), some of it will come off with each ice cap and consequently will appear satisfactory on one test but poorer on each successive test. The silane-treated rubber surface is satisfactory but a similar treatment on metal is not.

The preprepared silicones under some circumstances are more resistant to weathering conditions than surfaces treated with silanes to produce silicones *in situ*. Silicones can be produced to have almost any viscosity between that of water and that of a heavy grease or rubbery material. These latter materials are of special interest from the standpoint of durability. On initial application they reduce the "adhesion" greatly—like any grease. Actually, the material is removed by the ice cap. With successive ice-button removal the adhesion rises to a constant value. At this point the film is thin and strong, and, henceforth, no further silicone is removed by the ice. Data for one such grease are given in Table 14.

That this increase in adhesion was accompanied by removal of silicone was proved by adding a small portion of radioactive phosphorus to the silicone and following each adhesion test with a measurement of the activity of the treatment with a Geiger counter.

When a surface treated with a high-viscosity silicone is exposed to a high-velocity water spray (100 m.p.h.*) the adhesion rises to the same value as indicated in Table 14 and remains constant during many hours of exposure. This is shown in Table 15 in comparison with a silane treatment.

Since the De-Icer must stretch to operate the treatment must also elongate. Table 16 indicates that the silane-treated surface is satisfactory in this regard. The value after 2 weeks on the roof is the same whether the sample was flexed or not.

Table 17 shows some typical weathering data on various films under a number of conditions. The water-spray data were taken as follows. High-velocity water spray was thrown on the sample in the refrigerator. About 0.1 in. of ice per min. was built on the surface. By the inflatable De-Icer principle the ice caps were removed approximately every minute. The adhesion values were measured at the end of the times noted.

* The velocity cannot be directly compared to airplane speeds because the radius of the sample while being sprayed is smaller than the wing (2-in. diameter cylinder), and, hence, impact velocities are higher in the laboratory. Further, the drops are larger and liquid water content of the spray is higher than in natural fogs.

TABLE 14
Durability Under Ice-Forming Conditions
High Viscosity Silicone Grease
Repeated Values on the Same Spot on Sample

Number of Removals	Adhesion (Per Cent of Control)
1	3.6
2	4.0
3	5.0
4	7.2
5	7.8
6	10.4
7	14.0
8	15.6
9	17.0
10	17.2
11	13.4
12	19.2
13	19.8

TABLE 15
Durability of a Silicone Grease to Water Spray

Hours	Adhesion (Per Cent Untreated, Unexposed Surface)		
	Silane	Silicone Liquid	Silicone Grease
0			
1	17	22	6.0
2	80	..	..
3	71	..	..
4	87	85	..
8	..	..	..
16	..	..	..
24	..	..	15.0
48	..	..	28.0
72	..	..	56.0
96	..	..	81.0

TABLE 16
Effect of Stretching on Efficacy of Silane Treatment

Exposure	Adhesion (Per Cent of Untreated Surface)	
	Treated Stretched	Treated Unstretched
No exposure	23	19
Stretched 30 per cent in weatherometer 50 hours	58	55
Stretched 30 per cent on roof—2 weeks	41	28
Looped on roof—2 weeks	26	19
Flexed (200 cycles per min.) on roof—2 weeks	37	31

TABLE 17
Weathering Conditions on Various Films

Material	Adhesion (Lbs. per Sq.In.) Exposed to Room, Wks.				Exposed on Roof in California, Wks.				Exposed on Roof in Akron, Wks.		
	0	1	2	4	1	2	4	8	1	2	4
A silane	6	6	7	1	25	47	47	71	7	17	64
A silicone	2	4	4	7	8	24	26	37	14	22	33

Exposed 4 Hours to High-Velocity Water Spray After Akron Roof Exposure of Following Times in Weeks	Original	0	1 Wk.	2 Wks.	4 Wks.
A silane*	6	17	26	27	61
A silicone	2	40	34	40	32

This table and those previously given indicate that the adhesion lowering accomplished by these compounds is reduced (1) by exposure to ultraviolet light at about 90°F., (2) by exposure to ultraviolet light and high-velocity water spray, and (3) by exposure to summer weather. Further, it is not affected by exposure to normal room conditions. The serious damage done by the spray is nearly independent of the exposure to the ultraviolet light and has recently been shown to be equally detrimental when used at room temperature. Since the correlation between these laboratory conditions and those met in flight are not known, the laboratory tests can only be used in a comparative way.

In Fig. 9 is a photograph illustrating the ice-removal ability of the treatment after exposure to natural icing conditions as encountered on the summit of Mt. Washington. This photograph is one of a great number secured in our extensive test program on De-Icer design and surface treatments carried out on the summit of Mt. Washington where the temperature, wind velocity, and humidity are such as to give frequent icing conditions comparable to those encountered by low-speed airplanes in flight. The tests were made with cooperation of the Weather Bureau staff assigned to the Mt. Washington Observatory. The results of these tests prove that surfaces treated with silicone materials leave some 50 per cent less residual ice. A silane was effective for over 15 days of almost continual ice and high winds. Silicone oil had an equal life. A specially treated silicone grease was still effective after 1 month of exposure.

The results obtained in the laboratory have been confirmed in flight tests by comparing the operation of treated and untreated De-Icers on airplanes in service. In one case, ice was removed more quickly and clearly from the treated than from the untreated surface after being exposed to over a week of normal flying weather. In another case the material was applied on a rainy day and flown through a heavy rainstorm for a number of hours without any apparent damage to the effectiveness as shown when ice was encountered. In other flight tests the treated portion of the De-Icers completely removed the accumulated ice at the end of one cycle, while additional inflations were required to remove the ice from the untreated area.

FIG. 9. Ice removal from treated and untreated De-Icer surface on Mt. Washington. Icex VIa treatment. Five-tube De-Icer. Treated surface on right.

It is felt that further trials may prove that one application will last through a winter season. In any event repeated applications of the silane or silicone can easily be made.

REFERENCES

[1] Donnell, L. H., *Stress Concentrations Due to Elliptical Discontinuities in Plates Under Edge Forces*, Theodore von Kármán Anniversary Volume—Contributions to Applied Mechanics and Related Subjects by Friends of Theodore von Kármán on His Sixtieth Birthday, p. 293, 1941.

[2] Norton, F. J., General Electric Review, August, 1944.

[3] Hyde, J. F., and Delong, R. C., Journal of the American Chemical Society, Vol. 63, p. 1194, 1941.

[4] Rochow, E. G., and Gillian, W. F., Journal of the American Chemical Society, Vol. 63, p. 798, 1941.

[5] Bass, S. L., Hyde, J. F., Britton, E. C., and McGregor, R. R., Modern Plastics, Vol. 22, p. 124, 1944.

A Procedure for Determining the Critical Load for a Column of Varying Section

G. H. MARTIN*

Illinois Institute of Technology

SUMMARY

This manuscript presents an approximate method for determining the critical load for a pinned end column of varying cross section. Although there are various procedures available for obtaining a solution to the problem, the author believes that the application of the method suggested here is simpler in principle and that it requires relatively less calculation for the degree of accuracy obtained.

The following examples of pinned end columns have been solved in the paper:

(1) Columns of constant section.
(2) Symmetrical columns of varying section.
(3) Unsymmetrical columns of varying section.

INTRODUCTION

THE SLENDERNESS RATIO for a structural member that is subjected to axial compressive loads is defined as the ratio of L/k, where L is the length of the member and k is the least radius of gyration of its cross section. Members for which the value of L/k is greater than 160 may be called long columns. All columns referred to in this paper will be considered as long columns.

In Fig. 1 is shown a free end column subjected to an axial load P. The centerline of the column when in the deflected position is called the elastic curve, and the deflection of any point on this curve from the straight line AB is designated as y. The shape of the elastic curve is governed by the familiar differential equation

$$EI(d^2y/dx^2) = -M \qquad (1)$$

In Eq. (1), E is the modulus of elasticity of the material, I is the moment of inertia of the cross section, d^2y/dx^2 is the rate of change in the slope of the elastic curve, and M is the bending moment at any point on the elastic curve.

For the column shown in Fig. 1, the bending moment at a particular point on the elastic curve is Py. If this value for the bending moment is substituted for M in Eq. (1), we get

$$EI(d^2y/dx^2) = -Py \qquad (2)$$

The term critical load, as applied to an axially loaded column, is the load that will just cause buckling to begin. An extremely slight increase in the load above this value which causes a slight buckling, will increase the deflection greatly. The fiber stress will increase with the deflection, and, when it has passed the yield point of the material, the column will fail with no further increase of the load. The critical load, therefore, is taken as the ultimate load and is represented by P in Eq. (2).

If a column is considered as being composed of a number of sections and if the deflection curve is assumed to exist in the form of a straight line between sections, an expression may be obtained for the change in slope at any section.

Let Fig. 2 represent a portion of a deflection curve, and consider the length of the column to be divided into a number of equal segments of length d. The slope of this approximate deflection curve midway between sections a and b may be called y_a', then

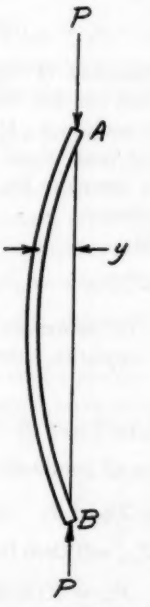

FIG. 1. Column subjected to an axial load.

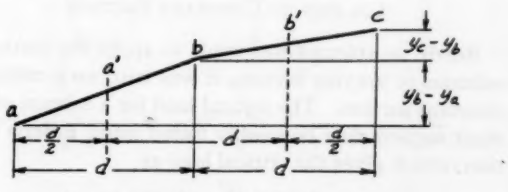

FIG. 2. Portion of a deflection curve.

Received January 15, 1945.

* Department of Mechanical Engineering.

$$y_a' = (y_b - y_a)/d$$

Similarly the slope of the approximate deflection curve midway between sections b and c may be called y_b', then

$$y_b' = (y_c - y_b)/d$$

These values for y_a' and y_b' may be considered as the average values of the slope of the actual deflection curve between sections a and b and sections b and c, respectively. The change in the average slope of the actual deflection curve as we move from section a' to section b' is

$$y_b' - y_a' = \frac{y_c - y_b}{d} - \frac{y_b - y_a}{d} = \frac{y_c - 2y_b + y_a}{d}$$

Also, $y'' = (d/dx)(y')$ and

$$\Delta y'/\Delta x = (y_b' - y_a')/d$$

where d is the distance between sections a' and b'. Substituting the value of $y_b' - y_a'$ into the last equation,

$$\Delta y'/\Delta x = (y_c - 2y_b + y_a)/d^2$$

This expression is an approximation to the average value of the second derivative which exists between sections a' and b'. Assuming this as the value for d^2y/dx^2 at b on the actual deflection curve, Eq. (2) becomes

$$EI[(2y_b - y_c - y_a)/d^2] = Py_b \qquad (3)$$

The right-hand member of Eq. (3) represents the bending moment, and the left member represents the resisting moment at section b. Under the critical load the resisting moment must equal the bending moment for equilibrium, and therefore Eq. (3) must hold for all sections along the column.

Rewriting Eq. (3),

$$(EI/y_bd^2)(2y_b - y_c - y_a) = P \qquad (4)$$

If we let P in Eq. (4) represent the critical load and since E and d are constants, then, for Eq. (4) to hold, the quantity

$$(I/y_b)(2y_b - y_c - y_a)$$

must be constant for all points along the column. Then

$$(I/y_b)(2y_b - y_c - y_a) = K \qquad (5)$$

The critical load, P_{cr}, will then be

$$P_{cr} = K(E/d^2)$$

Column of Constant Section

Before an attempt was made to apply the method to columns of varying section, it was tried on a column of constant section. The critical load for a column of constant section may be readily found using Euler's equation, which gives the critical load as

$$P_{cr} = 9.870EI/L^2$$

Certainly, if the method is valid, it should agree with the Euler result. Thus the column of constant section was treated as a first attempt in verifying the method.

The procedure for a column of constant section is the same as that which will be explained for a symmetrical column of varying section. It will subsequently be shown that the critical load is

$$P_{cr} = K_tE/(L/S)^2 \qquad (6)$$

A comparison of the values for P_{cr} as determined by Eq. (6) for several values of S,* with P_{cr} using Euler's equation, appears in Table 1.

Table 1
Comparison of P_{cr} with Exact Value

Euler Equation	$S = 4$	$S = 6$	$S = 16$
$P_{cr} = 9.870EI/L^2$	$K_tEI/(L/S)^2$		
$P_{cr} =$	$9.50EI/L^2$	$10.08EI/L^2$	$9.80EI/L^2$
Per cent error	3.75	2.13	0.80

Symmetrical Column of Varying Section

Knowing that the deflection curve for a symmetrical column is also symmetrical, we may consider just one-half of the column (see Fig. 3).

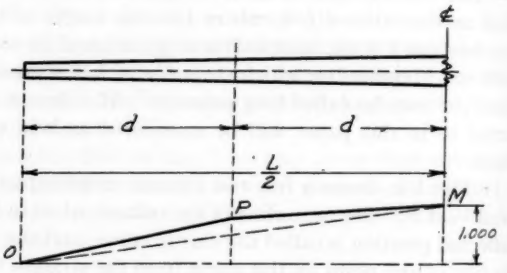

Fig. 3. Symmetrical column.

The procedure is as follows:

(1) Divide $L/2$ into a number of equal segments of length d.

(2) Assume the deflection at the center to be 1.000, and assume the deflection curve to be a straight line from 0 to M as indicated by the dotted line in the figure.

(3) Using Eq. (5) calculate K for each section except section 0, taking the deflections which correspond to the straight line $0M$. In applying the equation to a particular section, the value of the deflection at the section is the value to be used for y_b in the equation. The value of the deflection at the adjacent section to the right is to be used for y_c, and the value of the deflection at the adjacent section to the left is to be used for y_a in the equation. The value of K at section 0 is indeterminate, since the deflection at 0 is zero.

(4) Average the K's and let the value obtained be called K_{av}.

* S is the number of equal segments considered over the full length of the column.

(5) Apply Eq. (5) to the center section M and then to each section to the left of M in succession, solving for y_a in each case by using K_{av} as the value for K in Eq. (5). All along the column the value to be used for y_b at a particular section is to be the value previously found for y_a in the treatment of the immediate section to the right.

(6) When the equation has been applied to the section adjacent to 0, the value determined for y_a will be the deflection at point 0. Let the deflection at 0 be called y_0. Since the load is applied at the ends where the deflection is zero, y_0 must come out equal to zero. A positive value for y_0 would indicate that K_{av} is too small. A negative value for y_0 would indicate that K_{av} is too large. The value of y_0 is affected in this way by K because a small value for K produces a small amount of curvature in the deflection curve; likewise, a large value for K produces a large amount of curvature in the deflection curve. The use of K_{av} as explained in step (5) will yield a value for y_0 near zero. For this reason K_{av} is a good value to use for K to start with. If several values of K are chosen and y_0 is calculated for each, K may be plotted against y_0 on coordinate paper. A smooth curve drawn through several plotted points will indicate the value of K which will make y_0 equal zero (see Fig. 4).

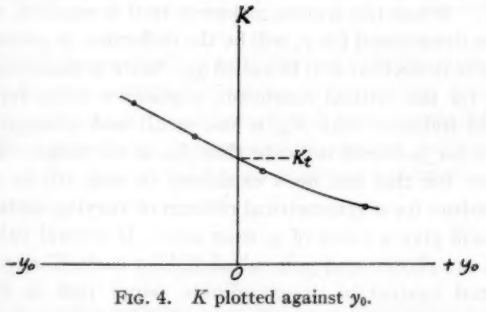

FIG. 4. K plotted against y_0.

Let K_t be the value of K corresponding to $y_0 = 0$. Then

$$P_{cr} = K_t E/(L/S)^2$$

where S is the number of segments in the full length of the column. The greater the number of segments used, the more accurate will be the value obtained for P_{cr}.

In Fig. 5 a symmetrical column with a constant moment of inertia I' along its middle is shown. I is the value of the moment of inertia at the ends. P_{cr} has been determined for this type of column by the method just described, assuming the cross section to be circular, for a value of a/L equal to 0.4 and for a value of I/I' equal to 0.6. The calculations appear in the Appendix.

The critical load has been calculated for this column using various numbers of segments. Fig. 6 shows how the value of P_{cr} approaches the exact value that has been determined by A. N. Dinnik[1] and which is described by Timoshenko.[2] The curve shows K_t plotted against S, the number of segments. The curve indicates that the greater the number of segments considered, the more accurate will be the value for the critical load.

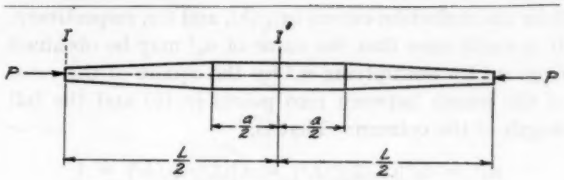

FIG. 5. Symmetrical column of varying section.

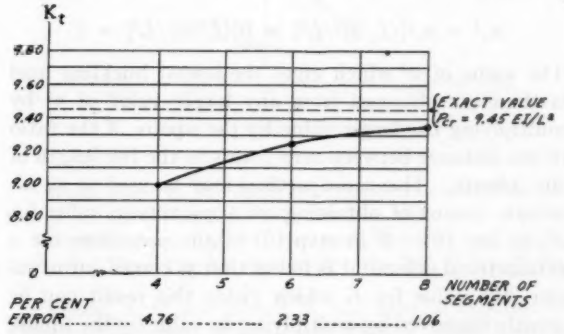

FIG. 6. Effect of increasing the number of segments in determining the critical load.

AN ALTERNATE METHOD FOR DETERMINING THE CONSTANT K_t

In the procedure just presented, it was explained that, if too large a value for K is tried, the result will be a deflection curve that crosses the x axis. It can readily be seen that the constant K_t in Eq. (6) is analogous to the constant n^2 in the Euler equation, which gives

$$P_{cr} = n^2\pi^2 EI/L^2$$

where n is 1, 2, or 3, etc., depending on the order of the buckling load.

The deflection curves for the first three buckling loads for a column of constant cross section with pinned ends are shown in Fig. 7. In Fig. 7 n has the value 1, 2, and

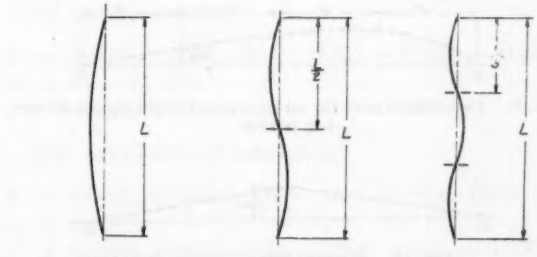

FIG. 7. Buckling loads for a pinned end column.

3 for the deflection curves (*a*), (*b*), and (*c*), respectively. It is easily seen that the value of n_a^2 may be obtained from n_b^2 by multiplying n_b^2 by the square of the ratio of the length between zero points in (*b*) and the full length of the column. That is,

$$n_a^2 = n_b^2[(L/2)^2/L^2] = 4[(L^2/4)/L^2] = 1$$

Similarly,

$$n_a^2 = n_c^2[(L/3)^2/L^2] = 9[(L^2/9)/L^2] = 1$$

The value of n^2 which gives the lowest buckling load is therefore obtained from any larger value of n^2 by multiplying the larger value by the square of the ratio of the distance between zero points to the full length of the column. This same method may be used as an alternate means of obtaining an approximate value for K_t in Eq. (6). If in step (6) of the procedure for a symmetrical column it is found that y_0 comes out negative, the value for K which yields this result can be greatly improved by multiplying its value by the square of the ratio of the distance between zero points and the full length of the column. This method for adjusting K may also be used when treating unsymmetrical columns. Such columns will now be discussed.

Unsymmetrical Column of Varying Section

In Fig. 8 a column of varying section which is unsymmetrical with respect to its centerline is shown. The procedure is similar to that for a column that is symmetrical, except that the deflection curve for the entire length of column must be considered. The procedure is as follows:

Fig. 8. Unsymmetrical column of varying section.

Fig. 9. Deflection curve for an unsymmetrical column of varying section.

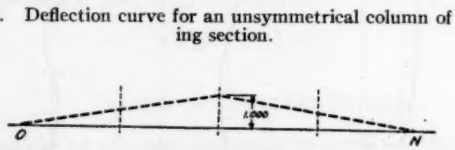

Fig. 10. Straight-line deflection curve.

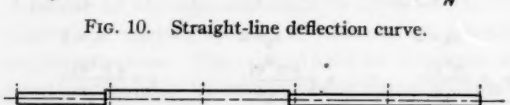

Fig. 11. Column with abrupt changes in section.

(1) Divide the length into a number of equal segments of length d (see Fig. 9).

(2) Let 0 designate the left end of the column and N the right end. If the deflection at N is taken as zero and the deflection at the section adjacent to N as 1.000, a deflection curve may be found which passes through these two points and also through point 0.

(3) The critical load is given by Eq. (6) which gives

$$P_{cr} = K_t E/(L/S)^2$$

The approximate magnitude of K_t may be found by assuming a straight-line deflection curve from each end to the center temporarily (see Fig. 10). Assume the deflection at the center to be 1.000; then the deflections at the other sections can readily be determined from the straight-line relationship. Apply Eq. (5) to each section except sections 0 and N to determine K for each section except these two.

(4) Average the values of K found in step (3) to obtain K_{av}.

(5) Apply Eq. (5) to the section adjacent to N using K_{av} as the value for K in the equation. Solve for y_a, taking y_b as 1.000 and y_c as zero (see Fig. 9).

(6) Eq. (5) may then be applied to each of the remaining sections to the left in succession, solving for y_a each time. The value used for y_b at a particular section is to be the value found for y_a in the treatment of the immediate section to the right.

(7) When the section adjacent to 0 is reached, the value determined for y_a will be the deflection at point 0. Let the deflection at 0 be called y_0. Since y_0 must equal zero for the critical condition, a positive value for y_0 would indicate that K_{av} is too small and a negative value for y_0 would indicate that K_{av} is too large. The reason for this has been explained in step (6) in the procedure for a symmetrical column of varying section. K_{av} will give a value of y_0 near zero. If several values of K are chosen and y_0 is calculated for each, K may be plotted against y_0 on coordinate paper just as it is shown in Fig. 4 for a symmetrical column. A smooth curve drawn through several plotted points will indicate the value of K which will make y_0 equal zero. Let K_t be the value of K corresponding to y_0 equal zero. Then,

$$P_{cr} = K_t E/(L/S)^2$$

Column with Abrupt Changes in Section

The column with abrupt changes in section may be treated in the same manner as the column with gradual change in section. A column with abrupt changes in section is shown in Fig. 11. In dividing the length of the column into segments of equal length, it is advisable to take segments of such a length that sections within proximity of each discontinuity of cross section shall be considered. The larger the number of sections considered, the greater will be the accuracy in determining the critical load.

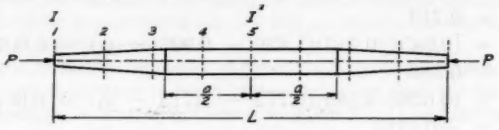

FIG. 12. Symmetrical column of varying section.

CONCLUSIONS

The procedure presented in this manuscript for columns of varying section has been shown to be simple and to yield accurate results. The maximum error in determining the critical load for a variety of cases of symmetrical columns considered was found to be only $1^{64}/_{100}$ per cent. This was the error when just four sections were considered over the half length of the column.

It has also been demonstrated that greater accuracy may be obtained in determining the critical load by considering more sections. The effect of the number of sections considered on the per cent error in the critical load for a column of constant section is shown in Table 2.

TABLE 2
Effect of Considering More Sections on the Accuracy of P_{cr}

No. of sections in $L/2$	2	3	5	8
Per cent error in P_{cr}	3.75	2.13	1.12	0.80

While the method has been applied to both symmetrical and unsymmetrical columns, in comparison to other existing methods it has been found to be especially expedient for solving unsymmetrical columns, in that less calculation is required for an equivalent degree of accuracy in the critical load.

ACKNOWLEDGMENT

The author wishes to express his appreciation to Dr. C. O. Harris for his suggesting the possibility of approaching the problem by such an approximate method and for his many suggestions that were helpful in formulating the procedure.

REFERENCES

[1] Dinnik, A. N., *Iswestia Gornogo Instituta*, Ekaterinaslav, 1914, and *Westnik Ingenerow*, Moscow, 1916.

[2] Timoshenko, S., *Theory of Elastic Stability*, 1st Ed., p. 137; McGraw-Hill Book Company, Inc., New York, 1936.

[3] Harris, C. O., *Suggestions for Columns of Varying Sections*, Journal of the Aeronautical Sciences, Vol. 9, pp. 97–99, 1942.

[4] Newmark, N. M., *Numerical Procedure for Computing Deflections, Moments, and Buckling Loads*, Transactions A.S.C.E., Vol. 108, pp. 1161–1234, 1943.

[5] Morley, Arthur, *Critical Loads for Ideal Long Columns*, Engineering, Vol. 97, pp. 566–568, 1914.

[6] Morley, Arthur, *Critical Loads for Long Tapering Struts*, Engineering, Vol. 104, pp. 295–298, 1917.

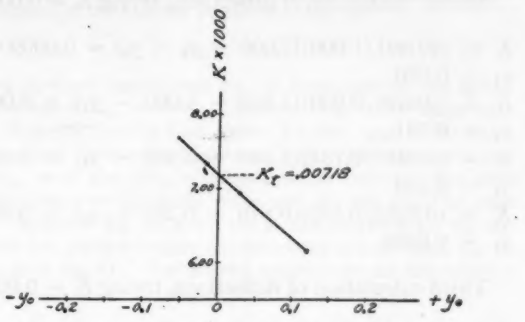

FIG. 13. K plotted against y_0.

[7] Westergaard, H. M., *Buckling of Elastic Structures*, Proceedings of the A.S.C.E., pp. 161–180, January, 1922.

[8] Drymael, Jean, *The Bent Strut with Variable Cross Section*, Journal of The Royal Aeronautical Society, Vol. 45, pp. 51–66, 1941.

[9] Eremin, A. A., and Gossard, M. L., *Numerical Procedure for Computing Deflections, Moments, and Buckling Loads*, Proceedings of the A.S.C.E., pp. 153–162, January, 1943.

[10] Boyd, J. E., *Tapered Struts: A Theoretical and Experimental Investigation*, Bulletin No. 25, The Ohio State University Engineering Experimental Station, September 15, 1923.

[11] Bairstow, L., and Stedman, E. W., *Critical Loads for Long Struts of Varying Sections*, Engineering, Vol. 98, pp. 403–404, 1914.

[12] Templeton, Hayden, *Approximate Solution for Tapered Pin Ended Struts*, Journal of The Royal Aeronautical Society, Vol. 48, pp. 6–11, 1944.

APPENDIX—COMPUTATIONS FOR DETERMINING THE CRITICAL LOAD FOR A SYMMETRICAL COLUMN OF VARYING SECTION

Circular section, $a/L = 0.4$ and $I/I' = 0.6$. Let D be the diameter of the cross section.

$D_1 = 0.880$ $\quad I_1 = 0.0294$
$D_2 = 0.930$ $\quad I_2 = 0.0363$
$D_3 = 0.980$ $\quad I_3 = 0.0451$
$D_4 = 1.000$ $\quad I_4 = 0.0491$
$D_5 = 1.000$ $\quad I_5 = 0.0491$

Assuming a straight-line deflection curve from section 1 to section 5, $y_1 = 0$, $y_2 = 0.250$, $y_3 = 0.500$, $y_4 = 0.750$, and $y_5 = 1.000$.

$K_5 = (0.0491/1.000)(2.000 - 0.750 - 0.750) = 0.0246$
$K_4 = K_3 = K_2 = 0$
$K_{av} = 0.0246/4 = 0.00615$

First calculation of deflections:

$K = (0.0491/1.000)(2.000 - y_4 - y_4) = 0.00615$
$y_4 = 0.938$
$K = (0.0491/0.938)(1.876 - 1.000 - y_3) = 0.00615$
$y_3 = 0.761$
$K = (0.0451/0.761)(1.522 - 0.938 - y_2) = 0.00615$
$y_2 = 0.480$
$K = (0.0363/0.480)(0.960 - 0.761 - y_1) = 0.00615$
$y_1 = 0.118$

Second calculation of deflections, trying $K = 0.00690$:

$$K = (0.0491/1.000)(2.000 - y_4 - y_4) = 0.00690$$
$$y_4 = 0.930$$
$$K = (0.0491/0.930)(1.860 - 1.000 - y_3) = 0.00690$$
$$y_3 = 0.731$$
$$K = (0.0451/0.731)(1.462 - 0.930 - y_2) = 0.00690$$
$$y_2 = 0.420$$
$$K = (0.0363/0.420)(0.840 - 0.731 - y_1) = 0.00690$$
$$y_1 = 0.0280$$

Third calculation of deflections, trying $K = 0.00725$:

$$K = (0.0491/1.000)(2.000 - y_4 - y_4) = 0.00725$$
$$y_4 = 0.925$$
$$K = (0.0491/0.925)(1.850 - 1.000 - y_3) = 0.00725$$
$$y_3 = 0.713$$
$$K = (0.0451/0.713)(1.426 - 0.925 - y_2) = 0.00725$$
$$y_2 = 0.386$$
$$K = (0.0363/0.386)(0.772 - 0.713 - y_1) = 0.00725$$
$$y_1 = -0.0181$$
$$P_{cr} = K_1 E/(L/S)^2$$
$$= 0.00718\, E/(L/8)^2, \text{ for } I' = 0.0491$$
$$= 0.00718\, EI'/0.0491(L/8)^2 = 9.35EI'/L^2, \text{ for any value of } I'$$

From Dinnik's equation, $P_{cr} = 9.45EI'/L^2$.
Per cent error:

$$[(9.45 - 9.35)/9.45]100 = 1.06$$

Letters to the Editor

Dear Sir:

A "beat" occurs when two simple harmonic motions, or two sine functions of any amplitudes but only slightly different frequencies, are added together. The result is a wave that is approximately sinusoidal, except that its amplitude and frequency vary periodically. It is well known how to find the beat frequency, ω_B, of the amplitude (and frequency) variation and the amplitudes of the two components from the composite curve. This letter shows that the frequencies of the components may also be found from the curve as follows: The frequency of the component with the larger amplitude, ω_1, is the same as the average frequency of the composite when measured over an integral number of beat cycles. The frequency ω_2 of the smaller component is $\omega_1 + \omega_B$ if the apparent frequency of the composite curve is larger at the portion of the beat cycle having a large amplitude than it is at the portion having a small amplitude (i.e., if the peaks are spaced closer together at the wide part of the beat than at the narrow part). ω_2 is $\omega_1 - \omega_B$ if the peaks are spaced farther apart at the wide part of the beat than at the narrow part.

Proof: To prove the stated properties, we study the synthesis of a beat, adding the two component sine waves:

$$x_1 = A_1 \cos \omega_1 t$$
$$x_2 = A_2 \cos (\omega_2 t + \theta_0)$$
$$x_B = x_1 + x_2$$

where A_1 is the larger amplitude and θ_0 is the phase lead of the smaller component relative to the larger at time $t = 0$. Fig. 1 gives the addition of the two sine waves in a vector diagram at an arbitrary instant. Each vector rotates counterclockwise with its own frequency, and its projection on the X axis is x. The larger vector A_1 is drawn from the origin. The two component vectors go around approximately together, changing their relative phase angle θ by only a few degrees in each revolution. Hence, the amplitude of the sum stays fairly constant, and in each cycle the composite motion closely resembles a sine wave.

The phase angle between the two components is

$$\theta = (\omega_2 t + \theta_0) - \omega_1 t = (\omega_2 - \omega_1)t + \theta_0 = \omega_B t + \theta_0$$

ω_B is the beat frequency and the frequency with which the two vectors come in phase.

Fig. 2 shows the variation of the resultant vector B relative to the larger component as θ changes with time. Fig. 3 gives the composite curve.

The "envelope" of the beat will be defined as the length of the vector B (Fig. 2) versus t. (This also happens to be the smoothest curve tangent to the composite curve.) We can find the amplitudes of the components by measuring $2B_{max.}$ and $2B_{min.}$ on the envelope. Then,

$$A_1 = (2B_{max.} + 2B_{min.})/4$$

and

$$A_2 = (2B_{max.} - 2B_{min.})/4$$

The frequency of the larger component may be found by measuring the frequency of the composite wave averaged over one cycle, from maximum to maximum of the beat, because the composite amplitude vector B never gets more than 90° out of phase with the larger component vector A_1, and B returns to the same phase relative to A_1 after each beat cycle (see Fig. 2). The frequency ω_1 is then the number of radians of rotation ($\omega_1 t_2 - \omega_1 t_1$) of the vectors divided by the corresponding length of time (see

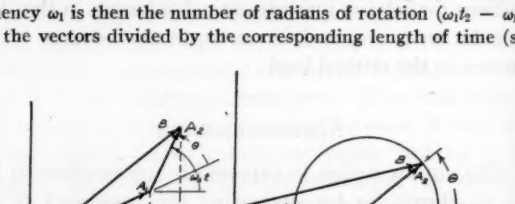

FIG. 1 (*left*). Vector addition of components A_1 and A_2 giving beat vector B. FIG. 2. (*right*). Variation of resultant vector B relative to the larger component A_1.

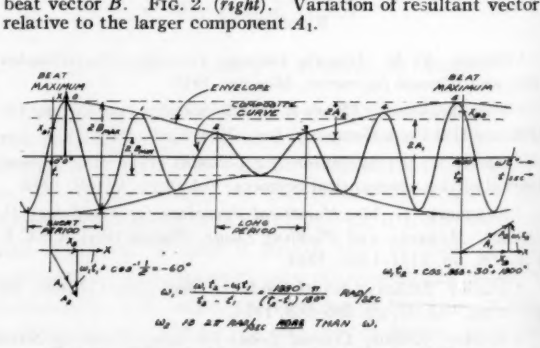
BEAT MAXIMUM
ENVELOPE
COMPOSITE CURVE
BEAT MAXIMUM
SHORT PERIOD
LONG PERIOD
X
ω1t1 = cos⁻¹ 1/2 = 60°
ω1t2 = cos⁻¹ -1/2 = 120°
ω1 = (ω1t2 - ω1t1)/(t2 - t1) = (120° π)/((t2 - t1) 180°) RAD/SEC
ω2 IS 2π RAD/SEC MORE THAN ω1

FIG. 3. Record of beat with frequency calculations.

example, Fig. 3). It will usually be sufficiently accurate to simplify the calculation by taking the largest peaks as the limits of the interval and calling $\omega_1 t_1 = 0$ and $\omega_1 t_2$ equal to an even multiple of 360° or 2π radians.

Now, to find the frequency of the smaller amplitude component, we note that, when it has a higher frequency than the larger component, A_2 is rotating faster than A_1 (in Fig. 1), and the composite vector B must be rotating faster than A_1 when B is large and slower than A_1 when B is small. In other words, when the peaks are more closely spaced and have a shorter period at the maximum width than they do at the minimum width, as in Fig. 3, we know that $\omega_2 = \omega_1 + \omega_B$. Similarly, if the peaks are less closely spaced at the maximum width than at the minimum, the composite vector B must be rotating more slowly than A_1 when it is large and faster than A_1 when B is small, and A_2 must be rotating more slowly than A_1. Then $\omega_2 = \omega_1 - \omega_B$ if ω_B is considered to be a positive number.

Applications: The writers developed the analysis when numerous problems involving beats presented themselves during the analysis of aircraft vibrations. The more important cases were separating response to a vibrator from "hash" response to engine or propeller excitation near the vibrator frequency and separating normal modes in records of free vibration. In the latter case the measured composite curve is modified by the multiplication by an exponential function of time as the motion decays due to damping; the record could be made into a beat between constant amplitude components by introducing automatic volume control if the damping were the same in the various modes.

C. D. P. PANCU
Curtiss-Wright Research Laboratory
CHARLES C. KENNEDY
Howard University

Dear Sir:

In the paper by J. G. Sawyer, "Design and Application of High-Pressure Coefficient Axial-Flow Fans" (JOURNAL OF THE AERONAUTICAL SCIENCES, Vol. 12, No. 3, p. 281, July, 1945), the following points seem to deserve attention:

(1) Mr. Sawyer's introductory remarks that we now have available design methods that have made possible axial-flow fans with pressure characteristics superior to all other types of fans is certainly not true, unless Mr. Sawyer is thinking of the other fans as being of the centrifugal type, in which case the writer agrees with him. However, exhaustive investigation undertaken during recent years by the writer in collaboration with V. H. Pavlecka, has demonstrated that a certain new type of compressor has superior pressure and also pressure-volume characteristics to the axial-flow, as well as to the centrifugal-flow, compressor.

(2) The writer objects to calling ΔP the fan pressure rise, since, in reality, because of unavoidable friction losses, the true pressure rise is somewhat less than that given by Eq. (3). The true pressure rise can always be obtained by multiplying Eq. (3) by the internal efficiency of the fan.

(3) The writer furthermore objects to the use of inconsistent nomenclature employed in the Eqs. (1) to (4).

(4) Sawyer's Eq. (2) is not a general equation for the pressure rise; the general equation for the pressure rise in terms of the airfoil lift coefficient is

$$(C_L w_\infty l \rho \omega z / 4\pi)(C_m/u) \cot \beta_\infty$$

where $\sin \beta_\infty = C_m/w_\infty$. It is apparent that Sawyer's Eq. (2) represents the special case in which

$$(C_m/u) \cot \beta_\infty = 1.0$$

This expression establishes a fixed relation between the velocity components of the velocity vector diagram, viz.:

$$C_{u1} = -C_{u2}$$

Sawyer does not specify that Eq. (2) holds only for the special case in which $C_{u1} = -C_{u2}$. Sawyer's Eq. (2) is apparently taken from the book by Curt Keller, Eq. (28), page 9, the latter being correct for the conditions that Keller carefully points out, viz., $C_{u2} = 0$ and ΔP_{st} = stage pressure rise—i.e., the total pressure rise over the guide vanes and the fan wheel as well.

(5) Sawyer's Eq. (4) is not the general equation for the fan pressure rise but is true only for the special case in which $C_{u1} = -C_{u2}$, as in Eq. (2). The general equation for the fan pressure rise is

$$\Delta P = \rho u \Delta C_u - (\rho/2) \Delta C_u^2 - \rho C_{u1} \Delta C_u$$

Sawyer's statement, therefore, that the only means of increasing ΔP is to increase ΔC_u is certainly not true, since ΔP may be increased or decreased by decreasing or increasing C_{u1} as well as ΔC_u. In fact, ΔP may even decrease when ΔC_u alone is increased. This will occur when $\Delta C_u > (u - C_{u1})$. It is, therefore, not necessarily true that higher pressures call for highly curved blades, since higher pressures may be obtained by decreasing C_{u1}—i.e., by allowing the blades to operate at smaller pitch angles. Thus, flat blades may develop high pressures, as has been done in a number of machines built and tested in Europe.

(6) According to Fig. 2, $C_{u1} = 0$ and the correct equation for the fan pressure rise becomes

$$\Delta P = \rho u \Delta C_u - (\rho/2) \Delta C_u^2$$

Then, using Sawyer's definition for the pressure coefficient, the correct expression for the pressure coefficient, when $C_{u1} = 0$, is

$$\psi = 2(\Delta C_u/u) - (\Delta C_u/u)^2$$

The maximum pressure coefficient obtainable is $\psi = 1.0$. This result may be obtained by the method generally employed in the elementary calculus for finding the maximum value of a function. The fans that Sawyer claims have developed pressure coefficients greater than 1.0 certainly did not operate with $C_{u1} = 0$ as indicated in Fig. 2.

(7) For the special case when

$$\Delta P = \rho u \Delta C_u$$

it is possible to obtain pressure coefficients greater than 1.0, although the writer doubts that values of $\psi = 3.0$, as indicated on Fig. 7, can be obtained with the airfoil sections described and shown by Sawyer. The following example may help to clarify this statement:

Example: For maximum efficiency, the aerodynamic theory of axial-fan design teaches that β_∞ should be equal to 45°. In the interest of efficiency it is assumed that $\beta_\infty = 45°$. The following expressions for the relative inlet and outlet angles can be derived:

$$\tan \beta_1 = 1/[1 + (\psi/4)]$$

and

$$\tan \beta_2 = 1/[1 - (\psi/4)]$$

For $\psi = 3.0$, $\beta_1 = 29° 45'$ and $\beta_2 = 75° 58'$. The turning angle is

$$\vartheta = \beta_2 - \beta_1 = 46° 13'$$

It has been the writer's experience that turning angles ϑ greater than 20° could not be attained because of flow separation so that values of $\vartheta = 46° 13'$ appear to be outside the range of actual attainment by known means in simple cascades.

(8) In Fig. 3 of the author's paper, the velocity vector diagrams are incorrectly drawn. Fig. 3 shows that $C_{u1} = 0$ and $C_{u2} = 0$. Obviously, therefore, the fan cannot absorb any power (since $\Delta C_u = 0$) and, hence, will produce no flow, since it will not rotate. In the referenced N.A.C.A. publication the velocity vector diagrams for the Schicht fan are shown correctly.

(9) In Fig. 7 Sawyer attempts to show the variation of pressure with flow for various values of ψ. What is actually shown is certainly not clear since all curves for ψ = constant will have a positive slope and not any slope as is indicated. This fact can be shown by the following analysis:

The pressure rise may be expressed by the relationship, Eq. (1)

$$\Delta P = (\rho/2)u^2\psi$$

Upon differentiating and dividing both sides of the resulting equation by the differential change of volume dV, we get

$$\frac{d\Delta P}{dV} = \rho u\psi\frac{du}{dV} + \frac{\rho}{2}u^2\frac{d\psi}{dV}$$

Now for ψ = constant, the above equation reduces to

$$d\Delta P/dV = \rho u\psi(du/dV)$$

This equation shows that for positive values of ψ the slope of the pressure-volume curve $d\Delta P/dV$ is always greater than zero, since for a constant value of ψ the characteristics of all fans are such that $du/dV > 0$—i.e., when the speed increases the volume also increases. All curves shown in Fig. 7 should therefore be drawn with a positive slope.

It is the general practice to represent fan characteristics at constant speed. Thus, for constant speed we have

$$d\Delta P/dV = (\rho/2)u^2(d\psi/dV)$$

The volumetric flow V may be expressed by the relationship

$$V = F\phi u$$

where F = flow area,

$$\phi = C_m/u = \text{flow coefficient}$$

Hence, for u = constant

$$d\Delta P/dV = (\rho u/2F)(d\psi/d\phi)$$

Most fans show a large negative slope of $d\psi/d\phi$ at the design value of ϕ. However, there is a functional relationship between ψ and ϕ which gives $d\psi/d\phi > 0$ at the design value of ϕ. When $C_{u1} < 0$, it can be shown that $d\psi/d\phi > 0$. However, it is important to note that even with $C_{u1} < 0$, $d\psi/d\phi$ may be negative provided C_{u1} is not sufficiently great. This is due to the friction losses that Sawyer chooses to neglect but which, unfortunately, are always present in practice.

Sawyer fails to make clear this well-known fan characteristic, and the presentation of Fig. 7 with the incorrectly shown negative slopes seems only to add to the confusion.

(10) Sawyer correctly indicates and appreciates the design principles as pointed out for the first time in print by Sörensen—viz., that high pressure fans or compressors can be designed rationally only on the basis of the channel theory familiar from the turbine design, instead of on the basis of the airfoil theory of lift. The writer was active in the development of axial compressors before the appearance of Sörensen's paper in this country and recalls the difficulties he had in convincing several eminent aerodynamicists to accept the channel theory in lieu of the airfoil theory for compressor design, a conclusion he had arrived at independently by his own analytical work at that time. Because of the lack of understanding of the subject and insufficient imagination on the part of aerodynamicists into whose hands the development of the axial compressor has been unfortunately entrusted and the confusion contributed by the modern aerodynamic theory by veiling the true nature of the art of compression of gases, the developmental progress of the axial compressors has been substantially delayed in this country—a disadvantage the steam turbine luckily did not suffer from during its formative development some 40 years ago.

FREDERICK DALLENBACH
8918 7th Ave.
Inglewood, Calif.

Aero Medical Aspects of Cabin Pressurization for Military and Commercial Aircraft

W. R. LOVELACE, II,* AND A. P. GAGGE†

Wright Field

SUMMARY

Whenever aircraft fly at high altitudes for long periods of time and over long distances, the foremost design requirement for aircrew efficiency and passenger comfort is cabin pressurization. In military aircraft, cabin pressurization is used to eliminate completely the need for continuous use of oxygen, to prevent aero-embolism only, or simply to reduce the cabin to a level where use of pressure breathing is not required. In commercial aircraft, the health, comfort, and safety of the passengers are of prime consideration. In military aircraft, a significant hazard introduced by cabin pressurization is explosive decompression caused by structural failure of the cabin when under enemy gunfire. Criteria are presented by which safe operating differentials may be chosen to minimize this hazard. The advantages of isobaric cabin altitudes below the now conventional 8,000-ft. level for military aircraft are reviewed as they apply to passengers of commercial aircraft. Finally, emergency procedures necessary for crew and passenger safety in case of failure of the cabin-pressurization system are discussed.

INTRODUCTION

DURING THE PRESENT WAR, technical advances toward realization of high-altitude flight have been many. The three most important on the engineering side are the development of the turbosupercharger and jet propulsion engines and the evolution of the laminar flow wing. Now within reach are flights by military aircraft well above limits tolerated by human beings breathing pure oxygen. Sustained flights at high altitude are also possible for both military and commercial aircraft. Parallel with these rapid engineering advances, methods for maintaining air-crew efficiency and safety as well as passenger comfort must be continually developed. The most logical step taken by the aircraft designers in this direction has been cabin pressurization. It is the purpose of the present paper to present the aero medical requirements for health, comfort, efficiency, and safety of air crews and passengers while flying in pressurized-cabin aircraft.

PHYSIOLOGIC REQUIREMENTS IN FLIGHT

It is a well-accepted fact, based on long flying and operational experience, that optimal efficiency and safety of air crews require the supplementary use of oxygen above 10,000 ft. for daytime flight and above 5,000 ft. for night flight. Flight without oxygen above these levels will result in increasing degrees of anoxia and in progressive loss of judgment and flying efficiency. The demand oxygen system now used by the Army Air Forces is designed to increase automatically the concentration of oxygen from that of pure air at 5,000 ft. to 100 per cent oxygen at 33,000 ft., so that the concentration in the lungs remains equivalent to that at 5,000 ft. or below. Above 33,000 ft. the margin of safety using pure oxygen decreases steadily to 40,000 ft., which is the oxygen altitude equivalent to 10,000 ft. with air. Above 40,000 ft. the 10,000-ft. equivalent can be maintained only by the use of pressure breathing. The top level now recommended for continuous use of pressure breathing is 42,000 ft. with $6\frac{1}{2}$ in. of water positive pressure; this combination corresponds to the 10,000-ft. air equivalent. Under emergency conditions for short periods, pressure breathing may be used to 50,000 ft. with 12 in. of water positive pressure, corresponding to 16,000-ft. air equivalent. For emergencies in flight above 50,000 ft., a lightweight quickly inflatable pressure suit would be required to reduce the equivalent altitude about the flier to 40,000 ft. or below.

Statements similar to those presented in the preceding paragraph apply to the continuous flow type oxygen system. However, where the demand system supplies the necessary supplementary oxygen for all levels of exercise, the level of flow in the former system must be increased as the level of exercise increases in order to maintain a fixed safety level. At altitudes above 25,000 ft. and for the same degree of safety, the demand system is much more economical in the use of oxygen than the continuous flow.

Aero-embolism, which manifests itself in the form of bends, of chokes, and of skin and neurologic symptoms, rarely occurs below 25,000 ft. However, it becomes increasingly significant as the altitude increases above 30,000 ft. For 1 hour's exposure or less at 35,000 ft., one person in ten would be likely to be incapacitated; one in four, at 40,000 ft. Few persons can stay more than 20 min. above 40,000 ft. without suffering from some form of aero-embolism. The incidence of aero-embolism is increased by exercise on the part of air crews. The incidence of aero-embolism can be greatly reduced by prebreathing 100 per cent oxygen for $\frac{1}{2}$ hour before flight and breathing 100 per cent oxygen

Presented at the Los Angeles Meeting, I.A.S., Los Angeles, August 16–17, 1945.

* Colonel, Medical Corps. Chief, Aero Medical Laboratory, Air Technical Service Command. On leave of absence from the Mayo Clinic.

† Lieutenant Colonel, Army Corps. Chief, Biophysics Branch, Aero Medical Laboratory, Air Technical Service Command. Formerly at the John B. Pierce Laboratory, Yale University.

for the entire flight. There is a small percentage of flying personnel for whom oxygen prebreathing gives no protection from aero-embolism, who suffer regularly on flight above 35,000 ft., and who should be disqualified for high-altitude flight.

At altitudes below 10,000 ft., proficiency in night vision and dark adaptation is an extremely important consideration, since it is greatly affected by mild degrees of anoxia. For example, to maintain an equivalent stimulus on, and response from, the retina, the percentage of increase in light intensity for various altitudes is as follows:

Sea level	0 per cent
5,000 ft.	23 per cent
10,000 ft.	59 per cent
12,000 ft.	78 per cent
14,000 ft.	101 per cent
16,000 ft.	140 per cent

Although use of high concentrations of oxygen from sea level up is desirable for the preservation of night vision, the small loss of night visual efficiency at 5,000 ft. is the maximum allowable for effective operational purposes. Above 5,000 ft., use of oxygen is a definite requirement to preserve night vision. A second visual phenomenon associated with mild anoxia is the dimming of peripheral vision, especially when illumination is poor. Both Hecht and Livingston have shown that this effect becomes increasingly serious above 6,000 ft.

Levels of Cabin Pressurization

There are essentially three types of human design requirements for use of cabin pressurization:

First, the cabin shall be maintained at levels where continuous use of oxygen equipment will not be needed.

Second, when oxygen is used continuously, the cabin shall be maintained at a level low enough to prevent incidence of aero-embolism.

Third, for flights above 40,000 ft., sufficient pressurization shall be used to obviate the use of pressure breathing and the risk of mild anoxia above 42,000 ft. with pressure breathing.

To meet these human requirements the engineer must stress his cabin fuselage to take the necessary differential pressure. The maximal required differential pressure is set by the operational ceiling of the aircraft (in contradistinction to the service ceiling).

The first of the foregoing requirements is used by the Army Air Forces in the design of its pressurized bombers. For example, the B-29 is designed for a 6.55 lbs. per sq.in. maximal operating differential, which allows an 8,000-ft. cabin altitude at 30,000 ft. or a 10,000-ft. cabin altitude at 35,000 ft.

The second of the foregoing requirements is followed in the design of pressurized fighters. The differential pressure most frequently chosen by the aircraft designers is 2.75 lbs. per sq.in., which allows a 25,000-ft. cabin altitude at 40,000 ft. or a 30,000-ft. cabin altitude at 50,000 ft.

Choice of any design cabin differentials between the 2.75 lbs. per sq.in. and the 6.55 lbs. per sq.in. value, the aircraft engineer will quickly note, does not increase the tactical efficiency of air crews when flights above 30,000 ft. are possible. A value of 4.0 lbs. per sq.in. at 30,000 ft. would result in a 15,000-ft. cabin altitude, at which level oxygen would have to be used continuously. At 40,000 ft. a 2.75 lbs. per sq.in. differential is adequate for the second requirement; the possible saving in oxygen consumption using a 4.0 lbs. per sq.in. differential instead of a 2.75 lbs. per sq.in. would be balanced by the increased loading of the cabin superchargers and heavier construction of the cabin walls and pressure seals.

The third requirement, listed previously, would be used only under emergency or combat conditions, when other hazards, such as explosive decompression (which will be discussed later), prevent the use of either of the first two requirements.

In Fig. 1, the various factors presented in the two previous sections are outlined to indicate their interrelationship.

Explosive Decompression

The principal hazard to air crews of tactical aircraft, when operating with pressurized cabins, is the possible damage caused by the expansion of internal body gases as a result of explosive or rapid decompression of the cabin itself. The failure of the cabin structure may have been caused by enemy gunfire. The degree of explosive decompression that one can withstand safely is determined by the extent and the rate of expansion of the internal body gases such as are found in the stomach, intestines, and lungs. The experimental studies of Major H. M. Sweeney, of the Aero Medical Laboratory, Wright Field, summarized in detail in the October, 1944, issue of the *Air Surgeon's Bulletin*, have shown that the two most significant factors associated with sudden decompression are the time of decompression (t) and the relative expansion of internal gases (RGE). The latter is evaluated by the following relation:

$$RGE = (P_c - 0.91)/(P_a - 0.91) \qquad (1)$$

where

P_c = cabin pressure before decompression in lbs. per sq.in.

P_a = ambient or final pressure after decompression in lbs. per sq.in.

0.91 = vapor pressure of water at body temperature, 98.6°F. in lbs. per sq.in.

In particular, it was demonstrated in the foregoing series of experiments that for rapid or instantaneous decompressions (approximately 0.01 sec. or less) a relative gas expansion of 2.3 approached the maximum

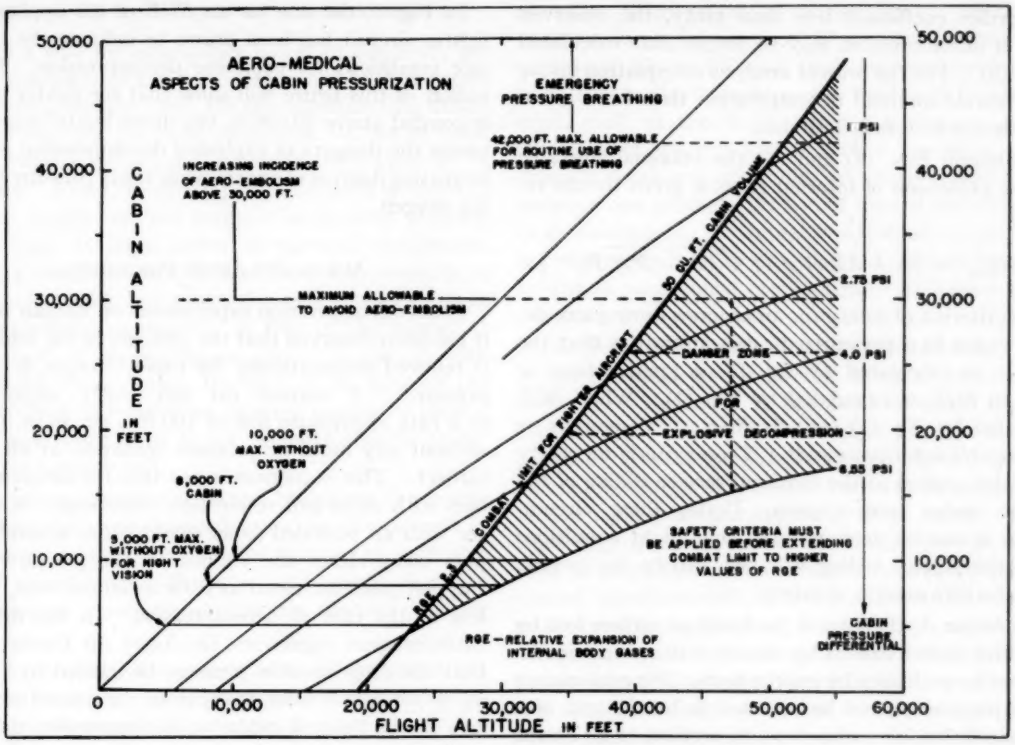

FIG. 1. The aero medical aspects of cabin pressurization.

tolerable. As the time of decompression increases, the increased pressure of expanding gases has time to be absorbed partially by neighboring tissues and the gases can escape from the body; thus the maximal tolerable *RGE* would increase. In Fig. 2, the maximal tolerable decompression conditions, observed for human subjects, have been plotted in terms of *RGE* and the time of decompression, t. A straight line, drawn between the topmost series of experiments, is described by the equation:

$$RGE_{max.} = 2.1 + 17.0t \qquad (2)$$

This line defines the borderline decompression conditions between the zone of safety, determined by adequate laboratory experience, and a zone of uncertainty, in which experimental data either are limited or are unknown. The line described by Eq. (2) can be considered by the aircraft engineer a maximal design limit for tolerable decompression that includes a margin of safety sufficient for military operations. It should be added at this point that it is probable that certain conditions above this line are tolerable; however, the present limit is proposed until new data are available for which a new design line can be drawn.

From Fliegner's equations for the flow of air from an orifice, it can be shown that the time of decompression, t, in seconds, may be described with sufficient accuracy by the equation:

$$t = 0.22\,(V_c/A)\,\sqrt{(P_c - P_a)/P_a} \qquad (3)$$

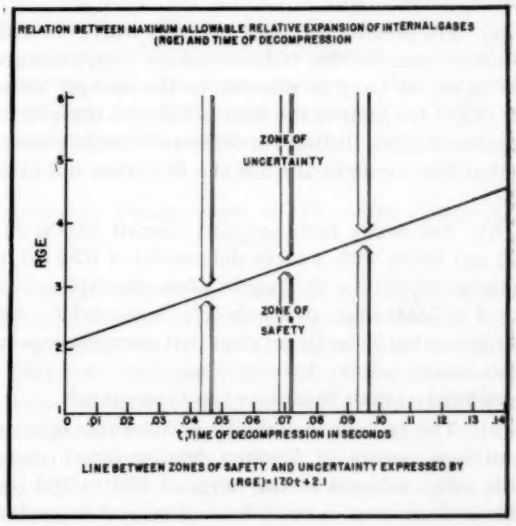
RELATION BETWEEN MAXIMUM ALLOWABLE RELATIVE EXPANSION OF INTERNAL GASES (RGE) AND TIME OF DECOMPRESSION
ZONE OF UNCERTAINTY
ZONE OF SAFETY
RGE
t, TIME OF DECOMPRESSION IN SECONDS
LINE BETWEEN ZONES OF SAFETY AND UNCERTAINTY EXPRESSED BY (RGE)=17.0t+2.1

FIG. 2. Relation between the maximal allowable relative expansion of internal gases (*RGE*) and time of decompression.

where

V_c = volume of pressurized cabin, cu.ft.
A = cross-sectional area of hole caused by structural failure, sq.in.
P_c and P_a as in Eq. (1)

A preliminary test of this equation by an actual decompression in flight indicates that, because of a pos-

sible orifice coefficient less than unity, the observed times of decompression may be longer than calculated in Eq. (3). For the present analysis an equation giving the probable minimal decompression time for a given set of design factors is desirable.

Combining Eqs. (2) and (3) the maximal tolerable relative expansion of internal gases is given by the relation:

$$RGE_{max.} = 2.1 + 3.8\,(V_c/A)\sqrt{(P_c - P_a)/P_a} \quad (4)$$

The criterion of safety for an air crew during any decompression in a pressurized-cabin aircraft is that the $RGE_{max.}$ as calculated by Eq. (4) is greater than or equal to *RGE* as calculated by Eq. (1). When *RGE* calculated by Eq. (1) exceeds $RGE_{max.}$, dangerous or questionable conditions exist. These criteria for safety should be applied at the maximal service ceiling of the aircraft under consideration. Under these circumstances it can be demonstrated that flight conditions below the service ceiling will also satisfy the criteria with a further margin of safety.

The factor A, the area of the fuselage surface lost by structural failure caused by enemy action, must in the long run be evaluated by gunfire tests. For preliminary design purposes it can be assumed to be the area of a jettisonable bubble canopy, a nose section, or an escape hatch door. Practical application of the foregoing criteria shows that:

(a) For pressurized fighter aircraft where the cross-sectional area of the bubble canopy (approximately 600 sq.in.) is large in relation to the cockpit volume (50 cu.ft.) the limit of the zone of safety is described by a choice of cabin altitudes or differential cabin pressures so that for any flight altitude the *RGE* does not exceed 2.3.

(b) For heavy bombardment aircraft (2,000 cu.ft. and up) flying with a cabin differential of 6.55 lbs. per sq.in. at 40,000 ft., the largest allowable explosive orifice A is 7,000 sq.in. or a hole 8 ft. in diameter. Since this hole is ten times larger than that normally expected from enemy action, decompression may, as a rule, be considered a minor hazard for this type aircraft.

(c) The greatest variability in allowable operating conditions occurs in medium bombardment aircraft with cabin volumes in the range of 200 to 400 cu.ft. This is illustrated in the following typical example for an aircraft with a cabin volume of 350 cu.ft. flying at 45,000 ft.

(1) For loss of a jettisonable bubble canopy (2,000 sq.in.), $RGE_{max.}$ is 2.75 and maximal allowable cabin differential is 2.15 lbs. per sq.in.

(2) For loss of a nose section (1,000 sq.in.) $RGE_{max.}$ is 3.85 and allowable differential is 3.5 lbs. per sq.in.

(3) For loss of an escape hatch (600 sq.in.) $RGE_{max.}$ is 5.7 and the allowable differential is 5.7 lbs. per sq.in

In Fig. 1, the line for an *RGE* of 2.3 applicable to fighter aircraft has been drawn to indicate the limit of safe conditions for explosive decompression. Examination of this figure will show that for fighter aircraft in combat above 50,000 ft. the choice has to be made between the dangers of explosive decompression and the increasing degrees of anoxia while using pressure breathing oxygen.

Aural and Sinus Phenomena

From decompression experiments on human subjects it has been observed that the pressure in the middle ear is relieved automatically for rapid changes in outside pressure. A normal ear can easily adjust itself to a rate of pressure loss of 100 lbs. per sq.in. per sec. without any aural or pressure sensation at all to the subject. This statement is not true for air-crew members with colds and respiratory infections. A passenger with an occluded sinus would suffer severely from pain when either the volume or the pressure of the trapped gases increased as little as 30 per cent, regardless of the rate of decompression. In the design of cabin-pressure regulators, the Army Air Forces require that the drop in cabin pressure be limited to 1 lb. per sq.in. per sec., a value that can be considered conservative in the light of explosive decompression data now available.

With a rise in cabin pressure, the negative pressure in the middle ear can be relieved only by a voluntary effort on the part of the air crew. The ability to clear ears varies greatly with the individual and with his flying experience. For military aircraft the rate of rise of cabin pressure is limited by pressure control to 1 lb. per sq.in. per min. (approximately 2,500 ft. per min.), provided the rate of dive of the aircraft itself does not exceed this value. For commercial aircraft, past experience has shown that 0.10 lb. per sq.in. per min. or 300 ft. per min. at sea level is the most comfortable descent rate for the average passenger. Recently, it was shown at the School of Aviation Medicine, Randolph Field, Tex., that, when the cabin is fluctuated between 7,700 and 8,300 ft. at a rate of 600 ft. per min. or 0.25 lb. per sq.in. per min., sensation on the ear drums was so small as not even to disturb sleep. This result will indicate the required constancy in the desired controls.

When the cabin controls are fitted with a rate of climb and descent adjustment, discomfort to the passenger can be reduced to the minimum. This consideration is especially important to engineers designing aircraft for commercial air lines, who must design their pressure cabin controls so that passengers with upper respiratory infections and sinusitis will be comfortable in flight. With such controls it would be possible to maintain in the cabin a rate of descent lower than that of the plane itself, and thus an actual rapid descent to an airport is minimized.

Safety Design of Pressure-Cabin Aircraft

When a side sighting blister is lost in the B-29, the decompression time has been determined by firing tests to be approximately 1 sec. for the full operating differential of 6.55 lbs. per sq.in. and cabin volume of 2,200 cu.ft. During this second, approximately 3,500 hp. is expended. From the safety point of view it is essential that this energy does not reappear in the form of flying debris, such as loose items of personal equipment. During a decompression in the B-29, air velocities as high as 140 m.p.h. have been observed momentarily in the interconnecting tunnel. A flier in the tunnel at the moment of decompression would be ejected with considerable force. Also, the rush of air through the broken blister has sufficient directed energy to blow a gunner overboard if he is not properly secured to his station by a safety belt.

With proper indoctrination and training in the potential hazards of cabin pressurization, accidents such as those described previously for the B-29 are of negligible tactical significance. However, the lessons that can be applied to passenger aircraft are obvious. These are:

(a) Restricted passageways between compartments should be avoided. This precaution is especially important as the size of the aircraft increases.

(b) Regular exits should have safety harnesses or nets across the inner side during flight to prevent passengers and crews from being accidentally blown overboard.

Another important lesson from the operational experiences of the B-29 is that the use of single-layer Plexiglas in pressurized aircraft is an undesirable practice and should be avoided wherever possible. Since the single-layer Plexiglas blisters of the B-29 were replaced by the laminated type about a year ago, there has not been a single report of a blister failure of this type from operational causes. In addition to the use of laminated Plexiglas, another desirable practice is to avoid the use of extremely large Plexiglas sections without segmentation.

The increasing tendency to use formed Plexiglas in the design of nose sections and canopies of pressurized aircraft leads to a word of precaution. Until now, the visual properties of Plexiglas canopies and sections have not been so good as those of grade B plate glass. Where the line of sight is greater than 55° to the normal to the Plexiglas surface, serious errors in depth perception and loss of acuity and of distant vision can be expected. Use of flat laminated plate glass of grade A optical quality is a requirement for crew compartments in passenger aircraft. For tactical aircraft where speed is required, a compromise, using curved plastic, is necessary. However, the plastic industries can well improve the visual properties of viewing sections.

Ideally, all exit hatches should open outward in tactical aircraft. At the present time this is true for fighter aircraft. When space for the air crews is restricted—as it would be, for example, in medium bombardment aircraft of 300 to 400-cu.ft. volume—outward opening of hatches is also desirable. For the heavy bomber aircraft, such as the B-29, and for passenger aircraft, where cabin space is not at such a premium, inward opening doors are allowable. A small residual cabin pressure can preclude the use of inward opening doors in an emergency. In actual practice, all inward opening emergency doors or exits should be able to be opened by simple mechanical means against at least a 0.5 lb. per sq.in. inside pressure.

Escape from high-speed aircraft is becoming of increasing concern to the aircraft designer and to flying personnel. Recently, it has been revealed that the German Air Force has developed an ejection seat propelled by a small gunpowder charge expanding into a piston. This type of seat at the present time appears to be the most practical approach to an escape method from high-speed aircraft. When an ejection seat is used in pressurized-cabin aircraft, the canopy must be ejected simultaneously with the seat causing the pilot or air crew to experience a rapid or even explosive decompression. It is therefore important that a differential pressure in the cabin be so selected by an *RGE* control that the safety criteria for decompression, as outlined previously, always apply. In particular for fighter aircraft, for flight altitudes above 38,000 ft. (Fig. 1), an *RGE* control of 2.3 should override the 2.75 differential control and so keep the cabin safe for rapid escape without risk of unconsciousness for a pilot from a too severe explosive decompression. This statement should apply for all flight conditions and not be limited to combat conditions alone.

Emergency Procedures in Pressure-Cabin Aircraft

There are two critical points in the oxygen altitude scale that require warning for the air crewmen. The first is at 10,000 ft.—a warning to put on oxygen equipment. The second is at 40,000 ft., above which pressure breathing should be used. All tactical pressurized-cabin aircraft use a cabin altitude warning switch to indicate these critical levels by means of a horn or pilot light. At the present time, all fighters and bombers of the Army Air Forces have the demand oxygen system. Those capable of flight above 35,000 ft. are equipped with the pressure-demand system.

A factor that must be given serious consideration while flying in pressure-cabin aircraft is the duration of useful consciousness for a pilot after decompression. Above 30,000 ft. the time of useful consciousness becomes increasingly less. Skill and practice will therefore be required by the pilot to connect his oxygen system. The allowable time for emergency action is illus-

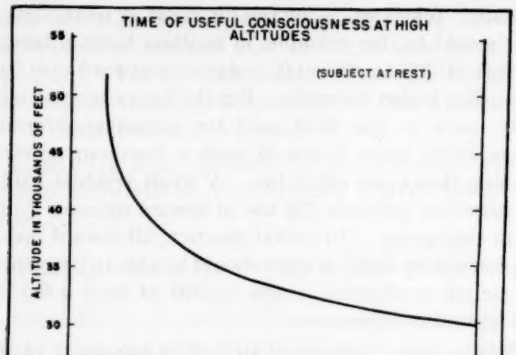

FIG. 3. The time of useful consciousness at high altitudes, based on data presented in Ruff and Strughold.[1]

trated in Fig. 3. On the basis of this chart it may be concluded that all crews of pressure-cabin tactical aircraft in combat areas should wear their oxygen masks for flights above 30,000 ft.

Below 30,000 ft. the loss of flying efficiency as a result of a sudden decompression of the cabin is a matter of minutes rather than seconds. Curves indicating these tolerance limits are presented in Fig. 4. Below 25,000 ft. the limits vary greatly with individual tolerance to anoxia and may be considered in the present chart as indicating a trend rather than a basis for design or operation.

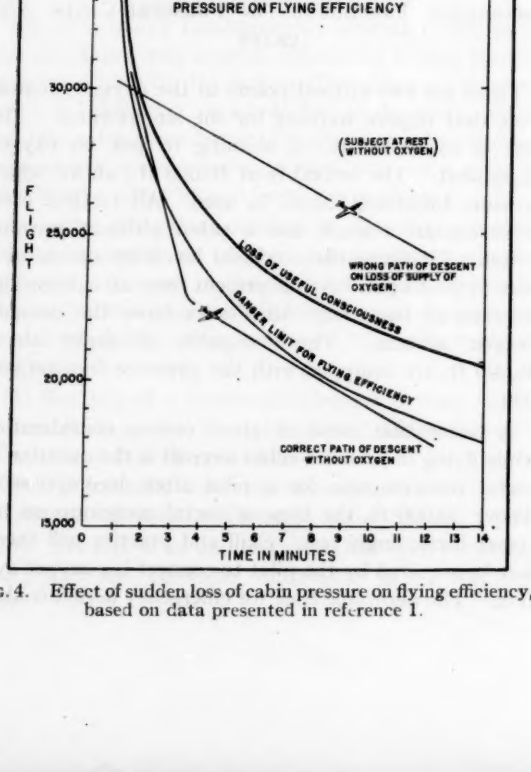

FIG. 4. Effect of sudden loss of cabin pressure on flying efficiency, based on data presented in reference 1.

Use of cabin pressurization serves to reduce the required oxygen capacity rather than to eliminate the need for the system. Cargo and passenger aircraft with pressure cabins, such as the Constellation (C-69) and Strato Cruiser (C-97), have continuous flow systems for both the passengers and the crews.

It would be a fallacious policy for designers and engineers to plan, for postwar commercial use, cabin-pressure aircraft without oxygen systems, when the danger from anoxia to passengers and air crews at altitudes above 10,000 ft. is realized. Although, for the crew, descent from 20,000 ft. to safe altitudes is sometimes possible with safety, occasions may arise when weather conditions preclude sudden lowering of altitude. Under these conditions the danger to crew and passengers is serious. An important safety rule for all pressure-cabin aircraft is that supplementary oxygen must be available at all altitudes when flights above 10,000 ft. are made. Present-type continuous flow oxygen systems, such as used in the Constellation (C-69), weigh only 225 lbs. and cause a weight penalty of approximately $3^1/_2$ lbs. per passenger and crew. This weight penalty may be reduced by use of high-pressure supply oxygen or of liquid supply oxygen. A new type of emergency system that is showing considerable promise experimentally is a chemical oxygen generator using superoxide or perchlorate. Walk-around oxygen bottles for stewardesses and crew members will also be necessary emergency items. Finally, the weight penalty of oxygen equipment for commercial aircraft as safety insurance is small compared with the pay load and certainly small compared with the 1,200 lbs. now required by the Air Transport Command on transoceanic flights for life raft and fire-protection equipment.

Use of oxygen supplied by continuous flow systems below 18,000 ft. does not require any skill or indoctrination of the passenger. Above 18,000 ft. it may be necessary to have an oxygen mask drill for passengers in pressure-cabin aircraft much the same as life-boat drills are held on shipboard. Emergencies, caused by loss of cabin pressure above 25,000 ft., will require quick donning of oxygen equipment by crew and passengers, as the time reserve for useful consciousness is 4 min. or less. An additional emergency consideration above 25,000 ft. is the possibility that aero-embolism may occur in some passenger or crew member. As a general practice, plane crews, including stewardesses, must be thoroughly indoctrinated in low-pressure chambers.

At this point it should be noted that the current Civil Aeronautics Board Regulation (Amendment No. 41.23, dated 27 June, 1945, effective 1 August, 1945) requires an emergency oxygen supply for flight in pressure-cabin aircraft above 18,000 ft. only for the crew but not for the passengers. This regulation would, therefore, fall far short of the safety requirement for care of passengers outlined in the previous sections.

Comfort in Pressure-Cabin Aircraft

At the present time there are few actual flight data on comfort requirements in pressure-cabin aircraft that give a real basis for a clear statement of design requirements. In general, the factors that must be considered are: (a) temperature and humidity; (b) ventilation; (c) sound control; and (d) choice of isobaric.

Fig. 5 illustrates the human comfort zone and the tolerance levels for hot and cold temperature for air crews and passengers dressed in ordinary everyday clothes. The comfort and tolerance levels are defined by the environmental temperature, which may be either the dry bulb temperature or the resultant temperature when radiation effects are considered, and the absolute vapor pressure of the environment. It will be noted that in the warm ranges humidity plays an important role in comfort, while toward the cold range its effect is negligible. The air motion equivalent for this chart is 200 linear ft. per min.

The ventilation requirement in a pressure-cabin aircraft must be sufficient, first, to maintain the necessary cabin temperature when either heating or cooling is required and, second, to remove odors, carbon dioxide, and noxious gases. There are three types of ventilation that may be used in pressure-cabin aircraft. The conventional type, a ram source directed into the cabin from the slipstream, is called the auxiliary ventilation system and would be used only in an emergency or when pressurization is not used. With pressurization, the air from the supercharger acts as the main ventilation source. In bombardment and fighter aircraft this source of ventilation may amount to 70 to 100 cu.ft. per person, which is more than adequate for the removal of obnoxious gases. For passenger aircraft the ventilated air from the superchargers can drop as low as 4 to 6 cu.ft. per person. Although the latter value is sufficient to remove carbon dioxide, it often is insufficient to keep the odor and cigarette smoke level down. Under these circumstances, recirculation of air through air filters and deodorizers may be necessary for comfort. If the experiences of the railroads in conditioning their pullman and dining cars is of any value in aircraft, the total ventilation in aircraft should be at least 10 cu.ft. per person for nonsmoking sections and 20 cu.ft. per person for compartments where smoking is allowed. Deodorization is a specially important consideration if patients are carried for long periods in flight. However, there are no quantitative data available to specify this requirement. For completeness, it should be noted that a part of the ventilated air from the superchargers must be used for defrosting windows and preventing condensation on them. Since with large passenger loads dew points as high as 50°F. can be expected where ventilation is not used, proper insulating methods must be carefully chosen.

Sound control in pressurized-cabin aircraft is no more difficult a problem than for conventional aircraft and in some respects may be easier. Preliminary data to date indicate that pressurization tends to remove noise entirely from the high spectral region and confine the noise level to frequencies below 1,200 cycles.

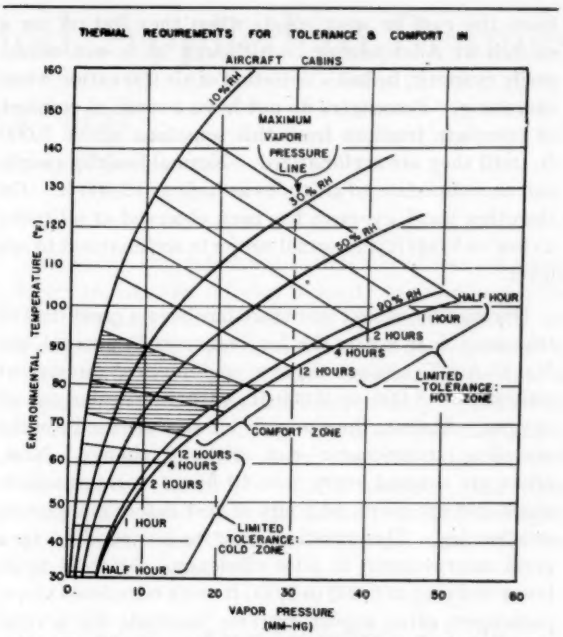

Fig. 5. The above chart, prepared by Capt. Craig L. Taylor, A.C., Chief, Thermal Research Unit, Biophysics Branch, Aero Medical Laboratory, presents the relation between comfort and tolerance to heat and cold in terms of hours, environmental temperatures, and so forth. In this chart environmental temperature is the resultant of air temperature, wall temperature, and effective solar radiant temperature. It is assumed (a) that personnel are sitting and doing no more than light manual work, (b) that standard temperate climate clothing (one clo) is worn, and (c) that air motion is the equivalent of 200 ft. per min. linear velocity. The tolerance lines give the recommended maximum duration of exposure to the stated conditions.

Aside from the effect of altitude on night and peripheral vision noted previously, there are other considerations for maintaining isobaric cabins at the 5,000-ft. level or lower. Comfort may be defined as the state in which one is unconscious of adaptation to his environment. Discomfort, on the other hand, implies consciousness of the accommodative processes that are being made by the body. Discomfort can extend also to a level of pain. From the temperature point of view, a person is comfortable when he feels neither hot nor cold. When he is hot or cold, he can accommodate physiologically to his environment but still be uncomfortable. When acclimatization takes place, he is comfortable since he is no longer conscious of his accommodation. After he is exposed to the environment, permanent physiologic changes take place which are defined as adaptation. Human response to altitude is parallel to the response to heat and cold. When a human being, whose normal environment is sea level, is flown to 8,000 ft., he must accommodate to this level by changes in respiration. He is conscious of an accommodative effort. (This is a common experience of air passengers

from the east or west coasts when they get off for a stretch at Albuquerque.) Although he is not necessarily cyanotic, he has a sensation of air starvation when exercising. Passengers do not have a sense of comfort or complete freedom from this sensation above 5,000 ft. until they are acclimatized. Normal healthy people can accommodate to altitudes as high as 12,000 ft. On the other hand, cyanosis has been observed at altitudes as low as 8,000 ft. in normal subjects acclimatized to sea level.

During the present war there has been a great deal of transoceanic flying by the Air Transport Command, the Naval Air Transport Service, and tactical aircraft at altitudes of 8,000 to 9,000 ft. without regular use of oxygen. At first, the same air crews were used for the complete transoceanic run without change. Now, crews are rotated every 8 to 10 hours at intermediate stops and are given 24 hours of rest before completing another leg. This rotation practice has resulted in a great improvement in pilot efficiency. After 24 to 36 hours of flying at 8,000 to 9,000 ft. with occasional stops, passengers often report extreme lassitude for several days on returning to their businesses.

Although at 8,000 ft. a pilot can act without handicap in an emergency, long exposure of 8 to 12 hours leaves him, as a rule, sleepy, unable to concentrate, and with a general lack of motivation. In reality, the 8,000-ft. isobaric for pressure-cabin aircraft was proposed back in 1934 when flights longer than 4 hours were not contemplated as a routine. The experience of this war at flight levels of 8,000 to 9,000 ft. for 8 to 12 hours has demonstrated that, for pressure-cabin aircraft, comfort of passengers and efficiency of crews demands the use, wherever possible, of isobarics of 5,000 ft. or lower.

In summary, aviation is now long past the pioneering stage in which comfort of passengers and efficiency of crew were minor factors compared to performance and speed and altitude records. Aviation engineering has advanced so far that the price, in weight penalty and performance, for safety and comfort is small. This is especially true when it is realized that speeds of more than 300 m.p.h. and flights of 8 to 12 hours are commonplace. Cabin pressurization is the first step taken by the aviation industry to include in the structural design of an aircraft a factor devoted entirely to the safety and efficiency of air crew and the comfort of the passengers.

Reference

[1] Ruff and Strughold, *Grundriss der Luftfahrtmedizin*, 2nd Ed.; Johann Ambrosius Barth, Verlag, Leipzig, 1944.

The Stress-Area Method Applied to Frames

GILBERT C. BEST*

Consolidated Vultee Aircraft Corporation

SUMMARY

A procedure is worked out to facilitate the design of frames. The necessary alterations in frame section moments of inertia to obtain predetermined stresses at given points are evaluated. The principal saving of labor is due to the use of original frame sections—the added material being considered removed and replaced by loads causing identical stresses throughout the structure. An example problem is given illustrating the method. An appendix gives additional proofs to the relation between section changes and equivalent moments and an extension of the stress-area method applied to beams[1] to include the I_0's of added areas.

INTRODUCTION

IN THE DESIGN OF FRAMES many successive trials are usually required to obtain sections producing satisfactory stresses in extreme fibers. When any alteration is made, a redistribution of moments about the frame occurs which complicates the procedure. It is possible to simplify matters somewhat by considering—after an alteration has been made—that all added material is removed, and, wherever such material was cut away, forces replace the stresses formerly existing across the cut. Stresses throughout the structure remain unchanged by this operation, and it is then possible to work with the original frame sections. The law of superposition of loads also conveniently applies with regard to the new loading. It is obvious that whatever changes in stress occur are then due to such "stress-area" loads. It is also obvious that these loads will depend upon the added area and also upon the moment—and in some cases the axial load—at the section in question.

BASIC EQUATIONS

The energy method will be used,[2] and, as is customary in the analysis of frames, the deflections due to axial loads and shear loads will be neglected. For definiteness assume a single cut. This gives the following equations:

$$\left.\begin{aligned} X_m\int M_m^2\frac{ds}{EI}+X_p\int M_pM_m\frac{ds}{EI}+X_v\int M_vM_m\frac{ds}{EI}&=-\int M_sM_m\frac{ds}{EI}\\ X_m\int M_mM_p\frac{ds}{EI}+X_p\int M_p^2\frac{ds}{EI}+X_v\int M_vM_p\frac{ds}{EI}&=-\int M_sM_p\frac{ds}{EI}\\ X_m\int M_mM_v\frac{ds}{EI}+X_p\int M_pM_v\frac{ds}{EI}+X_p\int M_v^2\frac{ds}{EI}&=-\int M_sM_v\frac{ds}{EI}\end{aligned}\right\}\quad(20)$$

in which X_m, X_p, X_v are the moment, axial load, and shear at the cut, respectively. M_m, M_p, M_v are the moments caused by a unit moment, unit axial load, and unit shear load, respectively, applied at the cut. M_s = static moment.

It is evident that, if an alteration is made and equivalent moments replace added material, the only change will occur in the static moments M_s in the right members of Eqs. (20). Also from consideration of the solution by determinants the above may be solved with only the changes in right members as constants and the resulting values—which will be termed ΔX_m, ΔX_p, ΔX_v—added to the original values for X_m, X_p, X_v to obtain the final solution. Or, if the moment at some section before alterations are made equals M_g

$$M_g = M_s + aX_m + bX_p + cX_v \qquad (21)$$

where a, b, and c are constants depending upon the location of the section.

After alterations are made the moment will be

$$M = M_s + a(X_m + \Delta X_m) + b(X_p + \Delta X_p) + c(X_v + \Delta X_v)$$

or

$$M = M_g + a\Delta X_m + b\Delta X_p + c\Delta X_v \qquad (22)$$

EQUIVALENT MOMENTS

Reducing the frame problem to its essentials, it is sufficient to have given a line in a plane representing

Received June 13, 1945.

* Stress Analyst.

the location of the neutral axis, a value of I at each point on this line, and a loading that is in equilibrium, to determine the distribution of moment about the frame. From the moment and the bending equation My/I the stress at a distance y from the neutral axis can then be determined. In this way a certain "stress field" exists about each point on the neutral axis. The problem in finding a moment equivalent in its effect to material which has been cut away is to find for each removal a moment to apply at the affected portion which will leave the stress field everywhere unchanged. In particular the bending stress at a distance y from the neutral axis at the point being altered must remain unchanged, and when this is the case stresses elsewhere are unaffected, since the equivalent moment replaces the effect of the removed material.

Hence, letting $k = I_{\text{new}}/I_{\text{orig.}}$ and m_a = equivalent moment,

$$f_b = My/kI_{\text{orig.}} = (M + m_a)(y/I_{\text{orig.}}) \qquad (23)$$

or

$$M[(1/k) - 1] = m_a$$

or

$$-[(k-1)/k]M = m_a \qquad (24)$$

Two other proofs of this relation are given in the Appendix.

Approximation of k and m_a

Since it is necessary to know M before k and m_a at a section can be computed and m_a in turn causes changes in the moment M, it is necessary either to use a process of successive approximations or to solve the problem algebraically. In general, an algebraic solution appears unsatisfactory, since it becomes unduly complicated if more than one cut is involved.

Given the moment and axial load at any section after alteration, the stress becomes

$$f_{\text{tot.}} = (My/kI) + [P/A(k)] \qquad (25)$$

where P = axial load and $A(k)$ = a function of k representing the area. Signs are to be determined in this formula by inspection. k is always positive by definition.

Shift of Neutral Axis

Another effect of axial load occurs when a section is altered so as to cause its neutral axis to shift in the plane of the frame by an amount e. In this case an additional moment Pe exists at the altered section. This effect will also put moments upon adjacent sections. All such moments should theoretically be added to M in Eq. (24). Furthermore, to be precise, revision of the dimensions locating the neutral axis would be necessary. Usually it appears satisfactory, however, to neglect such changes, since their effect is small.

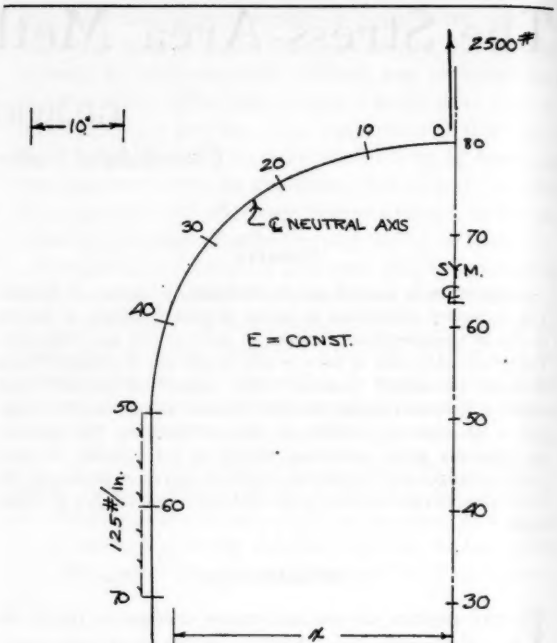

Fig. 1.

From Eq. (25) k can be determined for any selected stress $f_{\text{tot.}}$ once M and P are known. Then from Eq. (24) m_a can be obtained. Substituting m_a for M_s in Eqs. (20) gives ΔX_m, ΔX_p, ΔX_v. Since the left members of the equations are unaltered, this does not involve extensive work. A closer approximation to M may then be obtained from Eq. (22) and the process repeated until convergence is obtained. Substitution of the kI's so obtained for the original I's at each altered section in the recomputation of frame moments produces the desired stresses in extreme fibers. An example problem follows.

Example Problem

The frame of Fig. 1 is loaded as shown. To compute static moments a cut is made at the bottom centerline. Positive moments will be defined as producing compression in the outside fibers. Positive axial loads produce tension. Since the loading is symmetrical, there will be no shear at the cut, and Eqs. (20) become

TABLE 1. Computation of Frame Moments

1	2	3	4	5	6	7	8	9	10	11	12	13	14	15
Sta.	Int. Const.	x Dist. from Centerline	y	z*	I	$\frac{ds}{I} = \frac{②}{⑥}$	$y\frac{ds}{I}$	$y^2\frac{ds}{I}$	M_s	$M_s\frac{ds}{I}\times10^{-3}$	$yM_s\frac{ds}{I}\times10^{-3}$	$-yX_p$	$M_y = ⑩ + ⑬ + X_m$	F_b
0	3.333	0	80.0	1.75	1.5	2.22	178	14,240	−85,000	−188.7	−15,096	+56,680	−53,554	−62,480
10	13.333	10	78.8	1.75	1.12	11.90	938	73,914	−60,000	−714.0	−56,233	+55,830	−29,404	−45,944
20	6.667	19.5	75.8	1.75	0.77	8.66	656	49,725	−36,200	−313.5	−23,763	+53,704	− 7,730	−17,568
30	13.333	27.0	69.5	1.30	0.46	28.98	2,014	139,973	−17,500	−507.2	−35,250	+49,241	+ 6,507	−18,389
40	6.667	31.3	60.5	1.1	0.35	19.05	1,153	69,757	− 6,750	−128.6	− 7,780	+42,864	+10,880	−34,194
50	13.333	33.0	50.5	1.0	0.25	53.33	2,693	135,997	− 2,500	−133.3	− 6,732	+35,779	+ 8,045	−32,180
60	6.667	33.0	40.5	1.0	0.25	26.67	1,080	43,740	− 1,250	− 33.3	− 1,349	+28,694	+ 2,210	− 8,840
70	13.333	33.0	30.5	1.0	0.25	53.33	1,627	49,624	0	0	0	+21,609	− 3,625	−14,500
80	6.667	31.6	20.6	1.0	1.6	4.17	86	1,772				+14,595	−10,639	− 6,649
90	13.333	27.4	11.7	2.0	4.3	3.10	36.3	425				+ 8,289	−16,945	− 7,881
100	8.333	20.2	4.8	5.0	9.5	0.877	4.2	20				+ 3,401	−21,833	−11,491
110	10.5	11.0	1.2	6.0	10.0	1.05	1.26	1.5				+ 850	−24,384	−14,630
121	5.5	0	0	7.0	10.0	0.55	0	0				0	−25,234	−17,664
Σ						213.89	10,467	579,188		$A_1 =$ −2,018.6 × 10^3	$A_2 =$ −146,233 × 10^3			

* Distance from neutral axis to extreme fiber.

$$\left.\begin{aligned} X_m\int\frac{ds}{I} - X_p\int y\frac{ds}{I} &= -\int M_s\frac{ds}{I} \\ X_m\int y\frac{ds}{I} - X_p\int y^2\frac{ds}{I} &= -\int M_s y\frac{ds}{I} \end{aligned}\right\} \quad (26)$$

since $X_s = 0$, $M_m = 1$, $M_p = -y$, and E is constant and may therefore be omitted.

All frame sections are considered to be symmetrical. Frame stations are measured in inches along the neutral axis from the top centerline.

Computation of station moments and extreme fiber stresses is shown in Table 1. A word of explanation may be required regarding the integrating constants shown in Col. 2. These follow Simpson's one-third rule from stations 0 through 100 and the trapezoidal rule thereafter. The constant at station 100 is the sum of both. This was necessary since the evenness of the spacing became interrupted at this station.

It is desired to reduce the stresses at stations 0 and 10 to 38,000 lbs. per sq.in. by alteration of sections just inboard of station 20. To obtain this result sections will be both deepened and increased in moment of inertia. Letting the right members of Eqs. (26) be represented by A_1 and A_2, solutions for X_m and X_p as linear functions of A_1 and A_2 are shown in Eqs. (27).

Computation of Frame Movements

$$\left.\begin{aligned} 213.89X_m - 10{,}467X_p &= -A_1 \\ 10{,}467X_m - 579{,}188X_p &= -A_2 \\ 10^3X_m &= -40.434A_1 + 0.73071A_2 \\ 10^3X_p &= -0.73071A_1 + 0.014932A_2 \end{aligned}\right\} \quad (27)$$

$$X_p = -708.5 \text{ lbs.}$$

$$X_m = -25{,}234 \text{ in. lbs.}$$

This is done to facilitate later work. If, as in the column analogy method, the origin of the x,y axes is chosen at the elastic center of the frame, the terms involving $\int y(ds/I)$ vanish and the solution is thereby simplified. This has not been done in this example, since it was desired to demonstrate a method having a more general application.

The required section change constants k are computed in Table 2, it only being necessary to carry the approximation process through one extra cycle to obtain satisfactory convergence. Lines 7 and 8, etc., may be omitted in an actual computation. They were inserted here only to clarify the example. Table 3 shows a recomputation of section moments and extreme fiber stresses, indicating that the desired results are obtained within the accuracy to which the computations were carried out.

TABLE 2
Computation of k's

		Item	Ref.	0	10	Σ	
	1	I	Col. 6, Table 1	1.5	1.12		
	2	z_{new}		2.5	2.0		
	3	y	Col. 4, Table 1	80.0	78.8		
	4	ds/I	Col. 7, Table 1	2.22	11.90		
	5	M_0	Col. 14, Table 1	−53,554	−29,404		
1st Approx.	6	$k = ② \times ⑤/① \times 38{,}000$	Eq. (25)	2.35	1.38		
	7	$-(k-1)/k$		−0.574	−0.275		
	8	$m_a = ⑤ \times ⑦$	Eq. (24)	+30,740	+8,086		
	9	$m_a(ds/I) = ④ \times ⑧ \times ⑩^{-3}$		68.2	96.2	$A_1 = 164.4$	$\Delta X_p = +75$
	10	$m_a y(ds/I) = ③ \times ⑨ \times 10^{-3}$		5,456	7,581	$A_2 = 13{,}037$	$\Delta X_m = +2{,}879$
	11	$-y \times \Delta X_p$		−6,000	−5,910		Ref. Eq. (27)
	12	$M = ⑤ + ⑪ + \Delta X_m$	Eq. (22)	−56,675	−32,435		
2nd Approx.	13	$k = ② \times ⑫/① \times 38{,}000$	Eq. (25)	2.486	1.524		
	14	$-(k-1)/k$		−0.598	−0.344		
	15	$m_a = ⑫ \times ⑭$	Eq. (24)	+33,892	+11,158		
	16	$m_a(ds/I) = ④ \times ⑮ \times 10^{-3}$		+75.2	+132.8	$A_1 = +208.0$	$\Delta X_p = +94.4$
	17	$m_a y(ds/I) = ③ \times ⑯ \times 10^{-3}$		+6,016	+10,465	$A_2 = 16{,}481$	$\Delta X_m = +3{,}633$
	18	$-y \times \Delta X_p$		−7,552	−7,439		Ref. Eq. (27)
	19	$M = ⑤ + ⑱ + \Delta X_m$	Eq. (22)	−57,473	−33,210		
	20	$k = ② \times ⑲/① \times 38{,}000$		2.52	1.56		
	21	$I_{new} = ① \times ⑳$		3.78	1.75		

Appendix 1

Additional Proofs of Equivalent Moment Formula

Proof A

Consider that a section is so altered as to cause its neutral axis to shift parallel to itself a distance h. Let $I_0 = I_{orig.}$ and $I_n = I_{altered}$; similarly for A_0. Then $-dm_a = f_b dA(y + h) = dA(y + h)(My/I_n)$, where y refers to the neutral axis after alterations have been made and dA = an infinitesimal part of the added area.

Then $-m_a = (M/I_n)[\int y^2 dA + h\int y dA]$, where integrations are to be performed over the added areas only.

Then, since $\int y\, dA = hA_0$ and $I_n = I_0 + h^2A_0 + \int y^2\, dA = I_0 + \Delta I = kI_0$,

$$-m_a = M\Delta I/(I_0 + \Delta I) = M(k-1)/k$$

Proof B

In the column analogy method any change in section corresponds to the addition or subtraction of equivalent area or ds/EI. Any change in section will therefore result in a change in static loading of $M_s(ds/EI)[(1/k)-1]$. Removal of the added "area" working at "stress" M_i and replacing by an equivalent "force" as per the stress area method applied to beams[1] gives a change of $M_i(ds/EI)[(1/k) - 1]$. Since $M = M_s + M_i$, the change in load to be applied to the original section is $M(ds/EI)[(1/k) - 1]$. Proceeding by the method of this article—i.e., dealing with actual areas—the change in loading is given directly as $m_a(ds/EI)$. Comparing with the above shows $m_a = M[(1/k) - 1]$. Since no restrictions were placed upon the section change or M the relation is general. Any frame can be cut into subframes that are capable of analysis by the column analogy method, loads and moments replacing the stresses across the cuts. The above substitution of m_a for material removed can then be made on each subframe without affecting moment distribution thereon, and subframes can then be put back together into the original frame.

Appendix 2

Extension of the Stress-Area Method Applied to Beams to Include I_0's of Added Areas[1]

Since the slope of the stress distribution curve is constant because of the original assumption of simple bending, the slope will be the same for the small added area as for the whole section. Hence it is possible to write

$$\overline{M}_x/I_x = -M_{0x}/I_{0x} \tag{14}$$

where M_{0x}, I_{0x} are the reacting moment and moment of inertia of the small added area about the x axis, and $\overline{M}_x$ = applied moment M_x plus the moment due to the added area. The minus sign is due to the fact that M_{0x} is a reaction and $\overline{M}_x$ an applied moment.

Therefore, when the loads due to the new area at point P_0 working at stress F_0 are considered, the small moment M_{0x} must be added giving—at the c.g. of the original section—

$$\left.\begin{aligned} M_{x_{a_0}} &= a_0F_0y_0 - M_{0x} \\ M_{y_{a_0}} &= a_0F_0x_0 - M_{0y} \\ P_{a_0} &= -a_0F_0 \end{aligned}\right\} \tag{15}$$

TABLE 3. Recomputation of Frame Moments

1	2	3	4	5	6	7	8	9	10	11	12	13	14	15
Sta.	Int. Const.	x	y	z_{new}	I	$\frac{ds}{I} = \frac{②}{⑥}$	$y\frac{ds}{I}$	$y^2\frac{ds}{I}$	M_z	$M_z\frac{ds}{I}\times10^{-3}$	$yM_z\frac{ds}{I}\times10^{-3}$	$-yX_p$	$M_\sigma = ⑩ + ⑬ + X_m$	F_0
0	3.333	0	80.0	2.5	3.78	0.881	70.5	5,640	−85,000	− 74.9	− 5,992	+48,720	−57,671	−38,142
10	13.333	10	78.8	2.0	1.75	7.62	600.5	47,319	−60,000	−457.2	−36,027	+47,989	−33,402	−38,174
20	6.667	19.5	75.8	1.75	0.77	8.66	656	49,725	−36,200	−313.5	−23,763	+46,162	−11,429	−25,975
30	13.333	27.0	69.5	1.3	0.46	28.98	2,014	139,973	−17,500	−507.2	−35,250	+42,326	+ 3,435	− 9,708
40	6.667	31.3	60.5	1.1	0.35	19.05	1,153	69,757	− 6,750	−128.6	− 7,780	+36,845	+ 8,704	−27,355
50	13.333	33.0	50.5	1.0	0.25	53.33	2,693	135,997	− 2,500	−133.3	− 6,732	+30,755	+ 6,864	−27,456
60	6.667	33.0	40.5	1.0	0.25	26.67	1,080	43,740	− 1,250	− 33.3	− 1,349	+24,665	+ 2,024	− 8,096
70	13.333	33.0	30.5	1.0	0.25	53.33	1,627	49,624	0	0	0	+18,575	− 2,816	−11,264
80	6.667	31.6	20.6	1.0	1.6	4.17	86	1,772				+12,545	− 8,846	− 5,529
90	13.333	27.4	11.7	2.0	4.3	3.10	36.3	425				+ 7,125	−14,266	− 6,635
100	8.333	20.2	4.8	5.0	9.5	0.877	4.2	20				+ 2,923	−18,468	− 9,720
110	10.5	11.0	1.2	6.0	10.0	1.05	1.26	1.5				+ + 731	−20,660	−12,396
121	5.5	0	0	7.0	10.0	0.55	0	0				0	−21,391	−14,974
$\sum$						208.27	10,022	543,993		−1,648 $\times 10^3$	−116,893 $\times 10^3$			

$208.27X_m - 10{,}022X_p = +1{,}648{,}000.\quad 10{,}022X_m - 543{,}993X_p = +116{,}893{,}000.\quad X_p = -609$ lbs. $\quad X_m = -21{,}391$ in.lbs.

However $M_{0x} = -\overline{M}_x I_{0x}/I_0$ and $\overline{M}_x = M_x + M_{0x} + a_0F_0y_0$; therefore, letting $I_{0x}/I_x = \iota_{0x}$ gives: $M_{0x} = [-\iota_{0x}/(1 + \iota_{0x})](M_x + a_0F_0y_0)$ and the first of Eqs. (32) becomes

$$M_{x_{a_0}} = a_0F_0y_0 - \frac{\iota_{0x}}{1+\iota_{0x}}M_x - \frac{\iota_{0x}}{1+\iota_{0x}}a_0F_0y_0 = \frac{a_0}{1+\iota_{0x}}F_0y_0 - \frac{\iota_{0x}}{1+\iota_{0x}}M_x \quad (16)$$

Writing the ι_{0x} in the numerator of the second term as

$$\iota_{0x} = I_{0x}/I_x = \beta_{0x}(a_0h_{0x}^2/I_x)$$

where h_{0x} is the length of the added area in a direction perpendicular to the x axis and β_{0x} is a dimensionless constant depending upon the shape of the added area—e.g., if rectangular $\beta_{0x} = {}^1/_{12}$—gives

$$\left.\begin{aligned} M_{x_{a_0}} &= \frac{a_0}{1+\iota_{0x}}\left[F_0y_0 - \beta_{0x}\frac{M_x}{I_x}h_{0x}^2\right] \\ M_{y_{a_0}} &= \frac{a_0}{1+\iota_{0y}}\left[F_0x_0 - \beta_{0y}\frac{M_y}{I_y}h_{0y}^2\right] \\ P_{a_0} &= -a_0F_0 \end{aligned}\right\} \quad (17)$$

Substituting Eqs. (34) into the bending Eq. (1)[1] gives

$$\Delta F_{10} = (-\gamma_{10}'F_0 + \alpha_{10}')a_0 \quad (18)$$

where

$$\gamma_{10}' = +\left(\frac{k_3x_0}{1+\iota_{0y}} - \frac{k_1y_0}{1+\iota_{0x}}\right)x_1 + \left(\frac{k_2y_0}{1+\iota_{0x}} - \frac{k_1x_0}{1+\iota_{0y}}\right)y_1 + \frac{1}{A} \quad (19)$$

and

$$\alpha_{10}' = +\left[\frac{k_3\beta_{0y}M_yh_{0y}^2}{(1+\iota_{0y})I_y} - \frac{k_1\beta_{0x}M_xh_{0x}^2}{(1+\iota_{0x})I_x}\right]x_1 + \left[\frac{k_2\beta_{0x}M_xh_{0x}^2}{(1+\iota_{0x})I_x} - \frac{k_1\beta_{0y}M_yh_{0y}^2}{(1+\iota_{0x})I_y}\right]y_1 \quad (19a)$$

For practical purposes the shape may be assumed rectangular and $1 + \iota_{0x}$ and $1 + \iota_{0y}$ roughly approximated or, if ι is small, set equal to one. If set equal to one, γ_{10}' becomes γ_{10}. It should be noted that α_{10}' does not necessarily equal α_{01}'; nor does γ_{10}' necessarily equal γ_{01}', so symmetry is lost when the effect of the I_0's is considered.

In general, when the effect of the moments of inertia of added areas about their own centroids is considered, terms of the type $(-\gamma_{10}'F_0 + \alpha_{10}')a_0$ replace terms of the type $-\gamma_{10}F_0a_0$ in the general equations.

REFERENCES

[1] Best, G. C., *The Stress-Area Method of Designing Beams*, Journal of the Aeronautical Sciences, Vol. 12, No. 3, pp. 298–304, July, 1945.

[2] Lundquist, E. E., and Burke, W. F., *General Equations for the Stress Analysis of Rings*, N.A.C.A. T.R. No. 509, 1935.

SIXTH INTERNATIONAL CONGRESS FOR APPLIED MECHANICS

At a meeting initiated by Dr. J. C. Hunsaker and Dr. Th. von Kármán, acting as joint secretaries of the Fifth International Congress for Applied Mechanics, a committee was formed for the organization of the Sixth Congress. In line with the decision reached at Cambridge in 1938, it is proposed that the Sixth International Congress for Applied Mechanics be held in Paris, from September 22 to September 29, 1946.

The invitations to the Congress are extended on behalf of l'Académie des Sciences de l'Institut de France, la Direction des Relations culturelles, le Centre national de la Recherche scientifique, l'Institut de Mécanique de la Faculté des Sciences de Paris, la Société française des Mécaniciens, and l'Association technique Maritime et Aéronautique.

The Congress will meet at the Sorbonne.

The Congress will be divided into the following Sections:

I. Structures. Elasticity. Plasticity.
II. Hydro- and Aerodynamics. Hydraulics.
III. Solid Dynamics. Vibration and Sound. Friction and Lubrication.
IV. Thermodynamics. Heat Transfer. Combustion. Fundamentals of Nuclear Energy.

Besides the papers presented in these Sections, a number of General Lectures will be given on subjects of current interest. The titles of these Lectures will be made known in a later notice.

The French Organization Committee of the Congress is composed as follows:

President: Henri VILLAT
Secretary General: Maurice ROY
Members:

Émile BARRILLON
Louis de BROGLIE
Albert CAQUOT
Paul DUMANOIS
Jules DRACH
Frédéric JOLIOT
Henri LAUGIER
Joseph PÉRÈS
Ernest VESSIOT

Those who desire to become members of the Congress are requested to inform the Secretary General as soon as possible of their intention to attend. They should also indicate at the same time whether they wish to present a paper, and in what Section. This is required in order to facilitate the preparation of the program and the issuing of further notices.

Communications are to be addressed to the Secretary General of the Sixth International Congress for Applied Mechanics.

Institut Henri-Poincaré, 11, rue Pierre-Curie, PARIS (V^e^)

Checks or money orders can be made payable to the:

Sixième Congrès International de Mécanique appliquée
Institut Henri-Poincaré, 11, rue Pierre-Curie, PARIS (V^e^)

It is recommended to make payments on the following account: Cheques postaux Paris N° 649 (address given above).

The authors who wish to present papers are requested to submit the titles of their contributions as soon as possible. As at previous Congresses, contributions must be of scientific value and pertinent to the program of the Congress.

The authors are also asked to send to the Secretary General, before July 31, 1946, either the manuscript of their paper (maximum 5,000 words) or a summary of no more than 300 words. It is most desirable to have at least the summaries of all papers available to the members at the time of the Congress, in order to facilitate discussions. The Organization Committee hopes it will be able to have the summaries reproduced at the right time. However, it would be a great help if authors who have facilities to prepare a sufficient number of copies of their summaries, or manuscripts, would do so and send such copies to the Secretary or bring them to the meeting.

The Proceedings of the Congress, containing the minutes of the sessions, the texts of the General Lectures, and the papers presented in the Sections, will be published with the least possible delay. The members of the Congress will have the right to buy these volumes by subscription. The surplus copies will be sold later on at a higher price.

Adequate facilities will be provided for the members for their stay in Paris. Arrangements will be made known in due time. As at the previous Congresses, excursions and visits to various institutions, places of scientific, historic, and artistic interest will be arranged.

The payment of an inscription fee of 300 francs is required from the members of the Congress; this fee can be paid immediately or not later than on the opening day of the Congress. Ladies accompanying members will not be required to pay such fee, except those who wish to address the meetings or to submit papers.

INSTITUTE of the AERONAUTICAL SCIENCES

President
ARTHUR E. RAYMOND

Vice-Presidents
P. R. BASSETT
J. H. KINDELBERGER
JOHN C. LESLIE
BURDETTE S. WRIGHT

Director
S. PAUL JOHNSTON

Executive Vice-President
BENNETT H. HORCHLER

Past-Presidents
J. C. HUNSAKER
CHARLES L. LAWRANCE
DONALD W. DOUGLAS
GLENN L. MARTIN
CLARK B. MILLIKAN
T. P. WRIGHT
GEORGE W. LEWIS
JAMES H. DOOLITTLE
FRANK W. CALDWELL
HALL L. HIBBARD
HUGH L. DRYDEN
R. H. FLEET
CHARLES H. COLVIN

Assistant to the President
GEORGE R. FORMAN

Secretary
ROBERT R. DEXTER

Treasurer
C. S. JONES

Controller
JOSEPH J. MAITAN

COUNCIL

LESTER D. GARDNER, *Chairman*

E. E. ALDRIN
PETER ALTMAN
REX B. BEISEL
LAWRENCE D. BELL
GEORGE W. BRADY
W. A. M. BURDEN
CHARLES H. COLVIN
JAMES H. DOOLITTLE
WILLIAM K. EBEL
SHERMAN M. FAIRCHILD
DONALD W. FINLAY
CHARLES FROESCH
LEROY R. GRUMMAN
R. PAUL HARRINGTON
W. WALLACE KELLETT
OTTO E. KIRCHNER
JEROME LEDERER
ROBERT J. MINSHALL
EARL D. OSBORN
ELMER A. SPERRY, JR.
ERNEST G. STOUT
FRED E. WEICK

ADVISORY COMMITTEE

W. M. ALLEN
WALTER BEECH
ERNEST R. BREECH
RALPH S. DAMON
DONALD W. DOUGLAS
R. H. FLEET
JACK FRYE
ROBERT E. GROSS
R. M. HAZEN
H. MANSFIELD HORNER
J. C. HUNSAKER
CROIL HUNTER
TH. VON KÁRMÁN
I. M. LADDON
P. W. LITCHFIELD
F. W. MAGIN
ALFRED MARCHEV
GLENN L. MARTIN
THOMAS A. MORGAN
R. C. MUIR
JOHN K. NORTHROP
W. A. PATTERSON
E. T. PRICE
F. W. REICHELDERFER
LAURANCE S. ROCKEFELLER
FRED H. ROHR
T. CLAUDE RYAN
GUY W. VAUGHAN
EDWARD P. WARNER

HONORARY MEMBERS

JOHN C. ADAMS
GRIFFITH BREWER
W. A. M. BURDEN
E. U. CONDON
L. C. CRAIGIE
IRA C. EAKER
HARRY F. GUGGENHEIM
HENRY G. HOUGHTON
GEORGE B. PEGRAM
L. WELCH POGUE
J. LAURENCE PRITCHARD
ARTHUR W. RADFORD
F. W. REICHELDERFER
H. B. SALLADA
CARL SPAATZ
L. C. STEVENS
NATHAN F. TWINING

HONORARY FELLOWS

H. H. ARNOLD
DONALD W. DOUGLAS
HUGH L. DRYDEN
W. F. DURAND
SIR RICHARD FAIREY
SIR ROY FEDDEN
J. C. HUNSAKER
SIR MELVILL JONES
GEORGE W. LEWIS
GLENN L. MARTIN
GEORGE J. MEAD
SIR FREDERICK HANDLEY PAGE
D. R. PYE
IGOR I. SIKORSKY
G. I. TAYLOR
TH. VON KÁRMÁN
EDWARD P. WARNER
ORVILLE WRIGHT
T. P. WRIGHT

BENEFACTORS

E. E. ALDRIN
HART O. BERG (Deceased)
W. A. M. BURDEN
E. L. CORD
DONALD W. DOUGLAS
SHERMAN M. FAIRCHILD
SIR RICHARD FAIREY
R. H. FLEET
FLORENCE GUGGENHEIM (Deceased)
C. D. HANSCOM
JOHN P. V. HEINMULLER
ALEXANDER KLEMIN
PAUL KOLLSMAN
BELLA C. LANDAUER
WILLIAM LANDAUER
GROVER LOENING
EDMUND C. LYNCH (Deceased)
F. W. MAGIN
GLENN L. MARTIN
GEORGE J. MEAD
S. A. REED (Deceased)
LAURANCE S. ROCKEFELLER
EDWARD P. WARNER

AMERICAN FELLOWS

JOHN D. AKERMAN
EDWIN E. ALDRIN
HARRY G. ARMSTRONG
KARL ARNSTEIN
J. L. ATWOOD
PAUL S. BAKER
RALPH S. BARNABY
P. R. BASSETT
WELLWOOD E. BEALL
REX B. BEISEL
G. M. BELLANCA
DON R. BERLIN
HENRY A. BERLINER
WILLIAM BOLLAY
B. C. BOULTON
GEORGE W. BRADY
LYMAN J. BRIGGS
W. G. BROMBACHER
CHARLES P. BURGESS
FRANK W. CALDWELL
KENNETH CAMPBELL
CHARLES H. CHATFIELD
ALLAN CHILTON
V. E. CLARK
FRANKLIN R. COLLBOHM
CHARLES H. COLVIN
KARL T. COMPTON
JOHN W. CROWLEY, JR.
RALPH S. DAMON
LUIS DE FLOREZ
SMITH J. DE FRANCE
J. P. DEN HARTOG
WALTER S. DIEHL
JAMES H. DOOLITTLE
C. S. DRAPER
IVAN H. DRIGGS
WILLIAM K. EBEL
C. L. EGTVEDT
FREDERIC FLADER
CHARLES FROESCH
JACK FRYE
GARLAND FULTON
LESTER D. GARDNER
RICHARD C. GAZLEY
MICHAEL E. GLUHAREFF
MELVIN N. GOUGH
LEROY R. GRUMMAN
HAROLD R. HARRIS
R. M. HAZEN
ALBERT F. HEGENBERGER
EDWARD H. HEINEMANN
S. D. HERON
HALL L. HIBBARD
L. S. HOBBS
PAUL E. HOVGAARD
WILLIAM HOVGAARD
ROBERT INSLEY
EASTMAN N. JACOBS
CLARENCE L. JOHNSON
ALEXANDER KARTVELI
PAUL H. KEMMER
J. H. KINDELBERGER
OTTO E. KIRCHNER
ARTHUR L. KLEIN
ALEXANDER KLEMIN
W. B. KLEMPERER
PAUL KOLLSMAN
OTTO C. KOPPEN
B. V. KORVIN-KROUKOVSKY
S. M. KRAUS
I. M. LADDON
E. S. LAND
CHARLES L. LAWRANCE
JOHN G. LEE
JOHN C. LESLIE
CHARLES A. LINDBERGH
WILLIAM LITTLEWOOD
GROVER LOENING
W. RANDOLPH LOVELACE, II
EUGENE E. LUNDQUIST
R. D. MACCART
JOHN R. MARKHAM
ERLE MARTIN
WM. H. MCAVOY
C. J. MCCARTHY
CLARK B. MILLIKAN
ROBERT J. MINSHALL
SANFORD A. MOSS
JOSEPH S. NEWELL
ALFRED S. NILES
JOHN K. NORTHROP
ARTHUR NUTT
SHATSWELL OBER
ROBERT R. OSBORN
W. BAILEY OSWALD
GEORGE A. PAGE, JR.
F. W. PAWLOWSKI
F. W. PENNOYER, JR.
A. A. PRIESTER
ARTHUR E. RAYMOND
F. W. REICHELDERFER
ELLIOTT G. REID
H. J. E. REID
H. C. RICHARDSON
LEONARD E. ROOT
C. E. ROSENDAHL
WILLIAM T. SCHWENDLER
JAMES M. SHOEMAKER
MAC SHORT
IGOR ALEXIS SIKORSKY
SELDEN B. SPANGLER
ELMER A. SPERRY, JR.
JOHN STACK
WILLIAM B. STOUT
HARRY A. SUTTON
C. FAYETTE TAYLOR
EDWARD S. TAYLOR
PHILIP B. TAYLOR
TH. THEODORSEN
T. E. TILLINGHAST
S. TIMOSHENKO
STARR TRUSCOTT
L. B. TUCKERMAN
RALPH H. UPSON
J. G. VINCENT
RICHARD VON MISES
FRANK L. WATTENDORF
P. V. H. WEEMS
FRED E. WEICK
R. D. WEYERBACHER
JOHN B. WHEATLEY
ANDREW V. WILLGOOS
DONALD H. WOOD
ROBERT J. WOODS
JOHN E. YOUNGER
ALBERT F. ZAHM
STEPHEN J. ZAND

An Appreciation
To Corporate Members of the Institute of the Aeronautical Sciences

Listed below are the leading aeronautical and industrial companies that make possible the publication of the *Journal of the Aeronautical Sciences*.

They enable the Institute to publish scientific and technical papers in the *Journal* and to devote its pages exclusively to editorial material.

Dues from individual members which would normally be used to publish this scientific and engineering monthly are thus released for additional services to the profession and industry.

The *Aeronautical Engineering Review* and the *Aeronautical Engineering Catalog*, together with the JOURNAL, provide a comprehensive technical information service for the benefit of the aircraft and related industries.

Academy of Aeronautics
Aero Insurance Underwriters
Aerojet Engineering Corporation
Aeroquip Corporation
Agawam Aircraft Products, Inc.
Airchox Company Division, Joyce Aviation, Inc.
Aircraft Radio Corporation
Aireon Manufacturing Corporation
AiResearch Manufacturing Company
  AiResearch Manufacturing Company of Arizona, Inc.
Airex Manufacturing Company, Inc.
Allis-Chalmers Manufacturing Company
Allison Division, General Motors Corporation
Aluminum Company of America
American Airlines System
  American Overseas Airlines, Inc.
American Bosch Corporation
American Phenolic Corporation
Associated Aviation Underwriters
Associated Foundries & Manufacturers, Inc.
Atlas Supply Company
Baker Steel & Tube Company
Beech Aircraft Corporation
Bell Aircraft Corporation
Bendix Aviation Corporation
  Bendix Products Division
  Bendix Radio Corporation
  Eclipse-Pioneer Division
  Export Division
  Friez Instrument Division
  Pacific Division
  Scintilla Magneto Company
The BG Corporation
Boeing Aircraft Company
Boeing School of Aeronautics
Breeze Corporations, Inc.
  Essex Tool & Die Company
  Federal Laboratories, Inc.
Cal-Aero Technical Institute, A Division of Grand Central Airport Company
Carrier Corporation
Cessna Aircraft Company
Chandler-Evans Corporation
Chase National Bank of the City of New York
The Cleveland Graphite Bronze Company
The Cleveland Pneumatic Tool Company
  Automotive-Aircraft Division
Clifford Manufacturing Company
Consolidated Vultee Aircraft Corporation
  Nashville Division
  Stinson Aircraft Division
Continental Motors Corporation
Cox and Stevens Aircraft Corporation
Culver Aircraft Corporation
Curtiss-Wright Corporation
  Airplane Division
  Development Division
  Propeller Division
  Wright Aeronautical Corporation
Doak Aircraft Company, Inc.
Douglas Aircraft Company, Inc.
  El Segundo Plant
  Long Beach Plant
The Dow Chemical Company
Dzus Fastener Company, Inc.
Eastern Air Lines, Inc.
Eaton Manufacturing Company
Thomas A. Edison, Incorporated, Instrument Division
Edo Aircraft Corporation
The Electric Auto-Lite Company
Electrol Incorporated
Engineering and Research Corporation
Ethyl Corporation
The Fafnir Bearing Company
Fairchild Camera & Instrument Corporation
  Fairchild Aerial Surveys, Inc.
Fairchild Engine and Airplane Corporation
  Duramold Division
  Fairchild Aircraft Division
  Ranger Aircraft Engines Division
Federal Telephone and Radio Corporation
Firestone Aircraft Company
Fleetwings Division, Kaiser Cargo, Inc.

Fletcher Aviation Corporation
G & A Aircraft, Inc.
General Aircraft Equipment, Inc.
General Aviation Equipment Company, Inc.
General Electric Company
General Instrument Corporation
General Motors Corporation
  AC Spark Plug Division
  Aeroproducts Division
  Buick Motor Division
  Cadillac Motor Car Division
  Chevrolet Motor Division
  Delco Products Division
  Delco-Remy Division
  Eastern Aircraft Division
  Fisher Body Division
  Frigidaire Division
  Harrison Radiator Division
  Research Laboratories Division
  Rochester Products Division
The B. F. Goodrich Company
The Goodyear Tire & Rubber Company
The Gray Manufacturing Company
Grumman Aircraft Engineering Corporation
Guiberson Diesel Engine Company
W. & L. E. Gurley
Hanna Engineering Works
Haskelite Manufacturing Corporation
Hawaiian Airlines Limited
The Hilliard Corporation
The International Nickel Company
Jack & Heintz, Inc.
Jacobs Aircraft Engine Company
Johns-Manville Sales Corporation
Casey Jones School of Aeronautics, Inc.
Kellett Aircraft Corporation
Kenyon Instrument Company, Inc.
Walter Kidde & Company, Inc.
Kollsman Instrument Division, Square D Company
Langley Corporation
Lavelle Aircraft Corporation
Lear Incorporated
Liberty Aircraft Products Corporation
Link Aviation Devices, Inc.
The Liquidometer Corporation
Lockheed Aircraft Corporation
Longines-Wittnauer Watch Company, Inc.
Magnaflux Corporation
The Marquette Metal Products Company
The Glenn L. Martin Company
The W. L. Maxson Corporation
Warren McArthur Corporation
McDonnell Aircraft Corporation
Menasco Manufacturing Company
Micromatic Hone Corporation
Minneapolis-Honeywell Regulator Company
Moore Drop Forging Company
National City Bank of New York
National Credit Office, Inc.
The New York Air Brake Company
Norma-Hoffmann Bearings Corporation
North American Aviation, Inc.
  North American Aviation, Inc., of Texas
Northrop Aircraft, Inc.
Northwest Airlines, Inc.
Otto Aviation Corporation
Owens-Corning Fiberglas Corporation
Pan American World Airways System
The Parker Appliance Company
Pennsylvania-Central Airlines Corporation
Pesco Products Company Division, Borg-Warner Corporation
Phillips Petroleum Company
Pioneer Parachute Company, Inc.
The Pure Oil Company
Republic Aviation Corporation
J. P. Riddle Company
A. V. Roe Canada Limited
John A. Roebling's Sons Company
Rohr Aircraft Corporation
Roosevelt Field, Inc.
The Ryan Aeronautical Company
Sciaky Brothers
Scott Aviation Corporation
Shell Oil Company, Inc.
Simmonds Aerocessories, Inc.
Skydyne, Inc.
Socony-Vacuum Oil Company
Solar Aircraft Company
Sperry Gyroscope Company, Inc.
Square D Company
Standard Oil Company of California
Standard Oil Company (Indiana)
Standard Oil Company of New Jersey
Swedlow Aeroplastics Corporation
Teleflex Limited
The Texas Company
Thompson Products, Inc.
Tinnerman Products, Inc.
Titeflex, Inc.
Transcontinental & Western Air, Inc.
Triplett & Barton, Inc.
Union Carbide and Carbon Corporation
  Bakelite Corporation
  Haynes Stellite Company
  Linde Air Products Company
  National Carbon Company
United Aircraft Corporation
  Chance Vought Aircraft Division
  Hamilton Standard Propellers Division
  Pratt & Whitney Aircraft Division
  Pratt & Whitney Aircraft Corporation of Missouri
  Sikorsky Aircraft Division
United Air Lines, Inc.
United States Aviation Underwriters, Inc.
United States Rubber Company
  Dominion Rubber Company, Ltd.
The Variety Aircraft Corporation
Vickers, Inc.
Vidal Corporation
The Waco Aircraft Company
Warner Aircraft Corporation
The Weatherhead Company
Western Air Lines, Inc.
Westinghouse Electric Corporation
Weston Electrical Instrument Corporation
Wyman-Gordon Company
Young Radiator Company

Services of the Aeronautical Archives of the Institute of the Aeronautical Sciences

The services of the Aeronautical Archives are available to all members of the Institute, to Corporate Members, to advertisers in the AERONAUTICAL ENGINEERING REVIEW and, under usual library limitations, to the public. Four specialized services are available.

The Paul Kollsman Lending Library

This lending library service makes available, ***without charge***, the latest and more important aeronautical books.

Members may request the loan of any aeronautical or technical book they wish to borrow. Through an exchange agreement with the Engineering Societies Library, any book on general engineering may be borrowed from its great collection of over 160,000 volumes.

A photostating service is available at usual library rates.

Applications for membership in the library and further information will be sent on request.

The W. A. M. Burden Reference Library

This reference library contains over 12,000 aeronautical books, magazines, pamphlets, and reports gathered from world-wide sources and is one of the most complete aeronautical libraries in the world. Material from this library is not available for loan but may be used for reference purposes at the Aeronautical Archives.

The Pacific Aeronautical Library

6715 Hollywood Boulevard
Hollywood 28, California

Established in cooperation with the aircraft companies the library serves. The leading aircraft companies in or near Los Angeles participate in its support and operation.

This service library for aeronautical research is available to the public for reading privileges. Source material includes aerodynamic and structural research reports, as well as books on drafting, production methods, history, and allied sciences. It furnishes books, periodicals, and pamphlet material to the participating aircraft companies to supplement their engineering libraries.

Technical Information Service

This service has experienced personnel under the supervision of trained aeronautical engineers to compile any information desired. The services range from listing specialized reference books to the preparation of exhaustive bibliographies, digesting of reports, and general surveys of any aeronautical subject. Some of the available services are:

Bibliographies on any aeronautical subject.
Reports on any aeronautical subject.
Digests of aeronautical books, papers, periodicals, and references.
Translations.
Engineering investigations of special aeronautical subjects.
Biographies of individuals engaged in aeronautics.
Photostats of any aeronautical or general engineering material.
Microfilms made on special order.
Photographs made from the Institute's photographic collection.
Drawings and tracings made.

In addition to the services mentioned any commission which comes within the scope of the Service will be accepted. Special arrangements may be made for work requiring several weeks or months.

Translators are available for accurate transcriptions of all foreign language data. Translations are carefully edited by trained engineers.

Reproductions of any material in the Aeronautical Archives of the Institute may be ordered at standard photostat rates.

INSTITUTE OF THE AERONAUTICAL SCIENCES, INC.
2 EAST 64th STREET, NEW YORK 21, N.Y.